ICE WEAR AND ABRASION OF MARINE CONCRETE:

Design of Experimental Apparatus and Procedures

By Amanda Ryan

A thesis submitted to the School of Graduate Studies in partial fulfillment of the requirements for the degree of Master of Engineering

Faculty of Engineering and Applied Science
Memorial University of Newfoundland

May 2018

St. John's, Newfoundland and Labrador

Abstract

Abrasion of marine concrete structures from passing ice is an ongoing problem that leads to loss of structural integrity over time. The purpose of this study is to develop new experimental approaches and apparatus that would allow long term testing of ice wear on concrete samples as a prelude to a larger study that will investigate the wear of concrete by ice.

This thesis has drawn on the experiences of previous work to identify the important issues, including those areas where different approaches may be beneficial. A review has been completed of previously used tests setups, contributing factors and areas of uncertainty. This has resulted in two conceptual designs that approach the problem from slightly different angles. The first is a lab scale apparatus that aims to standardize the testing methods for concrete wear due to ice. The conceptual design of a new apparatus will allow wide ranging load applications, long test durations and the inclusion of surrounding water. The second is an in-situ apparatus that has been developed to allow direct comparison between concrete mixtures in terms of wear resistance under realistic but uncontrolled ice conditions.

Pilot experiments have been completed and reviewed to refine the initial concept and to determine effective means of abrasion measurement. These experiments provided insight into important features of the designed apparatus, trial results from measurements of ice-induced wear on concrete and useful information on concrete wear experiments in general.

Acknowledgements

Thanks to Memorial University, Kvaerner Canada Ltd., the Research and Development Corporation of Newfoundland and Labrador (RDC) and the Natural Sciences and Engineering Research Council (NSERC) for monetary support of the project.

This study and paper would not have been possible without the continued support from my supervisors at Memorial University, Dr. Steve Bruneau and Dr. Bruce Colbourne. Their discussions, guidance and knowledge were essential in the completion of the research and experiments outlined in my thesis. Additional thanks are conveyed for their contributions to my paper submitted to the ISOPE'17 conference.

Endless appreciation to those who helped with the preparation and completion of the pilot experiments, especially Craig Mitchell, Matt Curtis, Jerry Smith, Shawn Organ, Billy Bidgood and Matthew Fudge. Every day was a learning experience and their knowledge and willingness to help was invaluable.

A special thanks to Darlene Spracklin-Reid for her advice, perspective, and, pep talks. To Reta, for the daily smiles and coffee refills. To my m5 team/soulmates who are a constant reminder of strength, leadership, the power of education, and more importantly, the power of women supporting women. To my family, friends, and Kyle, for being there for me. Finally to my parents, for their support; even though there is no thank you in this world big enough to do it justice.

Table of Contents

List of Tables

List of Figures

Chapter 1 Introduction

1.1 Background of Study

Marine concrete structures in harsh, ice prone environments can be subject to seasonal wear due to high-intensity and prolonged interactions with the ice. The result is gradual loss of material and degradation of the concrete over the years, thereby reducing the life span of the structure, and increasing inspection time and maintenance. Ice friction and ice sliding remains a subject of debate; the addition of concrete further complicates the interactions. Increased knowledge of ice-concrete interactions and the wear process will provide insight into concrete design and loss of structural integrity.

1.2 Objectives of Study

The overarching objective of the larger project is to gain knowledge on ice-concrete friction and its effect on physical concrete abrasion and material loss. This requires further insight into the surface characteristics of both the ice and concrete throughout the interaction. The proposed research program on ice-concrete friction, abrasion and wear will be centred on conventional marine grade concrete mixtures and will seek to build on prior work to improve both understanding and modeling of the interface processes; and to improve the ability to predict wear and possibly to identify mitigation strategies or protection methods. The purpose is to determine the response of the concrete, and the individual components of the mixture, to the ice interaction. Finally, the work will seek to improve wear prediction methods, possibly by incorporating additional dimensions such

as concrete characteristics, ice pressures or other aspects of the problem into existing prediction models based on duration of interaction.

The goal of this portion of the study is to develop a detailed design concept for a laboratory scale experimental apparatus and procedure that addresses issues of test duration, realistic pressures and larger contact areas than previous approaches. The apparatus should allow close monitoring and control of concrete and ice properties, their interaction and provide the opportunity for wet and dry experiments.

A secondary goal is to develop a design concept for in-situ testing that would allow higher pressures and simple field deployment for use in comparative concrete evaluation with some limitations on the control of ice properties and measurement of concrete wear.

The first stage of the research project is an evaluation of the current state of the art in the physical testing of ice wear and abrasion on concrete at laboratory and full scale. This review identifies methods of testing, methods of measurement, current apparatus designs and the range of test parameters identified as relevant to the problem. The review supports the development of the basic design and experimental procedure concepts presented.

In further support of the research objectives, a set of pilot long-duration ice wear on concrete tests with rotational samples was conducted on a smaller scale to determine if the two developed apparatus concept designs are practical, and to explore wear rates in both the concrete and ice samples. These tests allowed preliminary trials and evaluation of possible procedures for measuring the wear in the concrete samples. Further, these

tests provided some specific design criteria including ice wear under various pressures, the expected rate of concrete abrasion and some insights into appropriate loading methods and speeds.

1.3 Thesis Methodology

Figure 1-1 displays a flowchart of the methodology and describes a new approach for investigating concrete degradation due to ice abrasion in marine environments, as presented in this thesis.

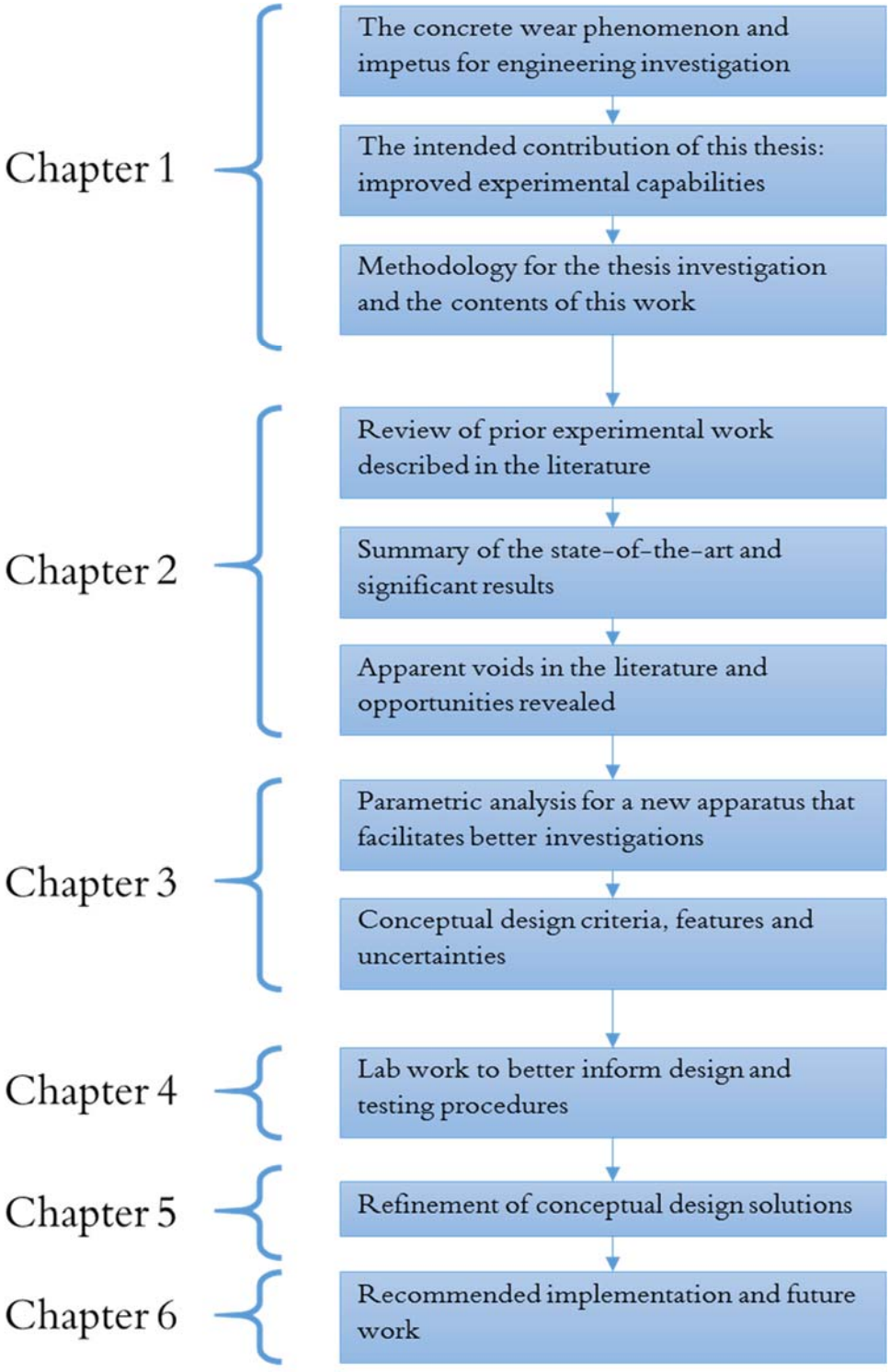

Figure 1-1: Flowchart of Research Approach

Incorporated in this thesis is a review of past and current literature pertaining to the topic, including laboratory investigations and results, and full scale data collection and validation. An overview of the problem statement, design criteria and constraints, and design concept of the laboratory scale apparatus is detailed. These factors were subsequently incorporated into a secondary field apparatus design. Learnings and design refinement are provided by the completion and analysis of a pilot laboratory testing program. This program provided validation of the proposed approaches and some data that could be used in further development of the apparatus. To conclude the thesis, two refined conceptual designs including setup sketches, for laboratory and field, are provided with final design details and recommendations for future research.

Chapter 2 Review of Literature

This chapter summarizes a review of literature on ice wear and abrasion of offshore concrete structures. Prior work will serve as a foundation for moving forward with the experimental apparatus designs. The primary objective of the overall project is to improve efficiency and performance of concrete subject to harsh environmental conditions, specifically the wear resistance of concrete under ice abrasion. Particular attention will be paid to loss of concrete due to simulated pack-ice interaction situations. Pack-ice interactions with structures are characterized by long duration loading that can be applied as normal forces, shear forces or a combination of the two. This is in contrast to studying other forms of ice interaction such as infrequent iceberg loadings that exhibit brief, but high-intensity interactions. Concrete surfaces are porous, rough and non-uniform, therefore characterizing the interaction between ice and concrete poses a challenge.

The objective of the research in this study, as an element of the larger project was to develop new experimental approaches and apparatus that would allow long term testing of ice wear on concrete samples. The literature review was focused on previous work on experimental analysis of ice wear and on the various testing machinery that has been used.

A review of previous articles, papers and conference proceedings has been completed to obtain background information and to take note of gaps in knowledge at this point in time. The literature under review for this work begins in 1990 and extends to present day, concentrating on a comparison of methodologies and test setups, a summary of common

concepts and trends in research, as well as test results. Additionally, full-scale ice load data on commonly studied marine structures has been summarized in order to compare laboratory values to full-scale. The objective of this review is to summarize the state of the art and identify promising areas of further study and experimentation.

2.1 Laboratory Investigations

Investigation into the effects of ice abrasion on concrete structures has increasingly become an area of study for researchers. Prominent early research focused on the wear effects of moving ice floes on concrete at the waterline of marine structures, as discussed by Huovinen (1990). Laboratory tests, icebreaker tests, analysis of Finnish lighthouses and computer models were used to complete the evaluation of concrete abrasion. Arrangements of the laboratory and icebreaker setups can be seen in Figure 2-1 and Figure 2-2. The laboratory test used a loaded rotary cutter to abrade concrete samples that had been previously exposed to a varying number of freeze-thaw cycles. For the icebreaker experiments, a 30-60 MPa concrete specimen was attached at the waterline of the icebreakers' bow using fixing plates and run through ice for a distance of 40 km, abrasion was measured between a range of 2 and 15 mm (Huovinen, 1990).

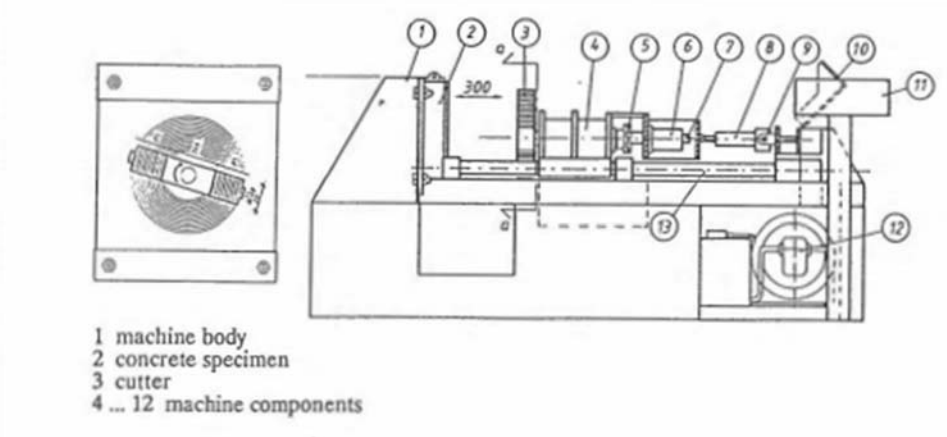

Figure 2-1: Laboratory Test Setup (Huovinen, 1990)

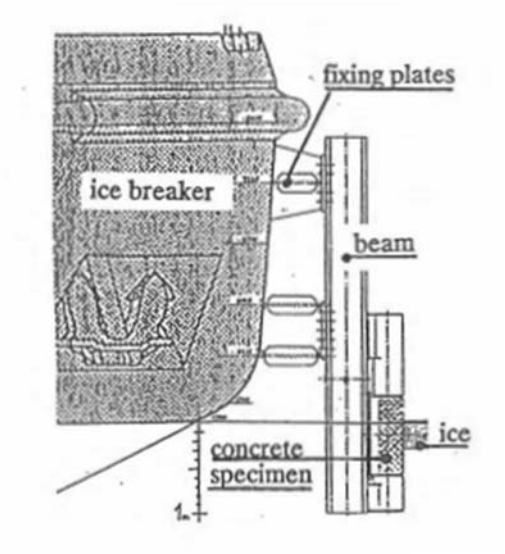

Figure 2-2: Icebreaker Test Setup (Huovinen, 1990)

The abrading concept adopted for this research and the resulting calculation models saw ice loads that were produced by both normal and shear components.

It is acknowledged by Itoh et al (1994) that there are several different abrasion test setups, ie. relative wear, revolving disc, tumbler abrasion, sliding wear (Hoff, 1989), and that there are conflicting results in ice abrasion depending on which test is used. Itoh et al

(1994) stated that ice abrasion is a complicated process and cannot be uniquely measured by simple abrasion tests.

The setup Itoh et al (1994) used in the research, as seen in Figure 2-3, performed more complex tests which can simulate both static and kinetic friction with adjustable speeds. The contact pressure applied by the hydraulic ram can be changed and additionally, blowing air, with the same temperature as the ice block, onto the contact area removes abrasives and dissipates frictional heating (Itoh et al, 1988). Previously, Itoh et al (1988) completed testing with contact pressures ranging between 5 and 30 kgf/cm^2, sliding velocities between 1 and 20 cm/s and ice temperatures between -5 °C and -20 °C. For the overview in this research, there was a focus on the data collected when the temperature of the ice sample was held at -20 °C, the sliding velocity was 5.0 cm/s and the applied pressure was 10 kgf/cm^2 or 0.98 MPa (Itoh et al, 1994). Transverse profile measurements were taken along five lines of the concrete surface.

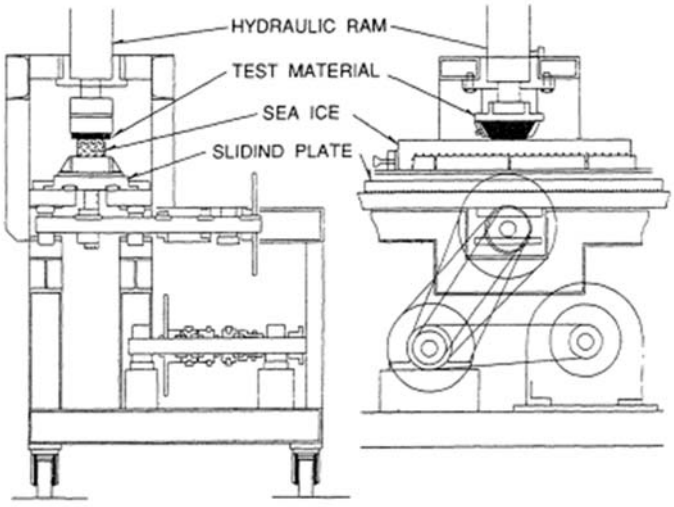

Figure 2-3: Laboratory Test Setup (Itoh et al, 1994)

An abrasion estimation model was developed based on the results of the testing. To benchmark the model, a field investigation was completed on the Sydostbrotten lighthouse in Bothnia Bay that was showing signs of ice wear. It was confirmed that the estimation method accurately predicted the amount of abrasion that had occurred.

Continued research on this topic was carried out by Fiorio et al (2002) and Fiorio (2005). Informative papers were published that focused on ice friction coefficients and small-scale testing.

Fiorio et al (2002) recognized that in order to better predict the abrasion process, further understanding of ice friction during the ice and concrete interaction was needed. The interaction is a very complex process and so certain simplifications were made in the small-scale experiments to maintain the focus on friction. First, the temperature was maintained at a constant value of -10 °C and second, two different tests, constant load and level load, were performed (Fiorio et al, 2002). The freshwater ice used was grown in a laboratory as it was assumed that brine pockets would have a negligible effect on ice friction (Jones et al, 1991). The concrete mix that was tested aimed to represent a more realistic small-scale concrete surface with fewer large aggregates.

The tests were carried out using a direct shear box machine, as seen in Figure 2-4. The concrete sample was fixed to a platform that moved back and forth in one plane, while the cylindrical ice sample was placed above the plate and subjected to an applied normal force. During the constant load test, the normal stress was held at a constant value for the duration of the experiment. In comparison, the level load test initially applied a constant

normal stress of 500 kPa to reach a stable friction and then the normal stress followed an increasing and decreasing loading pattern ranging from 25 to 800 kPa (Fiorio et al, 2002). The average roughness of each concrete plate's topography was taken before and after each test using optical microscopy techniques. However, upon completion of the tests the researchers noted that plates with the same average roughness yielded small variations in frictional behaviour. This indicates that using the average roughness does not completely capture the topography of the concrete samples.

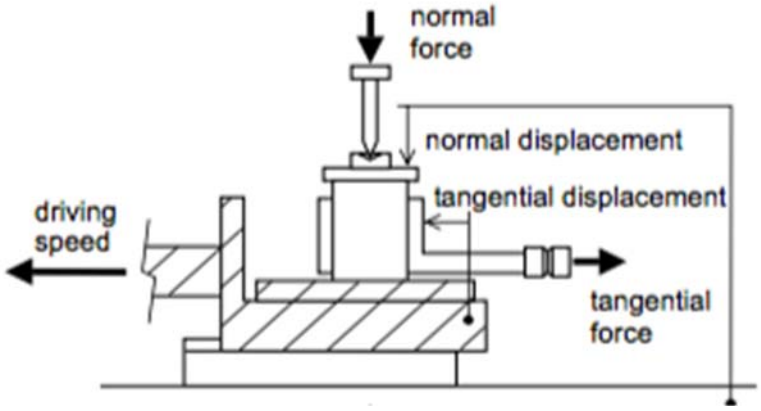

Figure 2-4: Laboratory Test Setup (Fiorio et al, 2002)

The friction coefficient was calculated by determining the ratio of tangential stress to normal stress. The coefficients were averaged from the first and tenth cycle to describe an initial and final value. However, due to the procedure followed for the level load tests, they did not provide an initial friction coefficient.

Fiorio (2005) is an extension of the previous research by Fiorio et al (2002). Similarly, small-scale tests were completed using a direct shear box machine. The goal was to further investigate the friction parameters and active friction mechanisms.

As before, the micro-concrete samples were formed into plates and the freshwater ice was grown in the laboratory. However, for these tests there were two different concrete surface types molded, rough and smooth. The direct shear box machine was the same as seen in Figure 2-4. The freshwater ice and micro-concrete mixture, although simplifying the complex interaction, allowed for a well-controlled testing setup. Constant load tests were completed with the applied normal stress ranging from 25 to 800 kPa, as performed by Fiorio et al (2002). The sliding velocity was held steady at a variety of speeds ranging from 0.1 to 10 mm/min and a cold room was used to maintain the atmospheric temperature stable, within allowable error, at -10 °C (Fiorio et al, 2002).

Before the experiments, optical microscopy was used to record the topographical features including maximum height and mean height. Following the testing, maximum and mean abrasion values were evaluated. The results of this research provide more insight into the small-scale friction mechanisms in ice-concrete interactions. However, Fiorio (2005) acknowledges that more investigation into different concrete mixtures and contact conditions would be advantageous.

Fosså (2007) noted the need to improve performance of the ice zone on offshore concrete structures. He states the need to develop an established program to better understand ice abrasion and also to test alternative solutions. At present, there is a general consensus that ice abrasion causes serious damage to the cementitious material within a concrete mixture.

Further testing and improvement of testing methods would provide additional insight and improvement in this area of research. Field-testing and exposure to actual conditions would provide the most valuable information. However, laboratory testing is more controllable and less expensive. While progress has been made with laboratory testing of ice wear on concrete, Fosså (2007) states that at this point in time, there is no standardized test to determine the abrasive effects on concrete due to ice.

Moving forward, a standardized testing process would allow enhanced prediction of the amount of abrasion during a structure's service life. The procedure must be able to allow varying factors of both the ice and concrete properties. Concurrently, more field studies would allow beneficial benchmarking to the laboratory experiments (Fosså, 2007). The ultimate goal is to enhance the performance of concrete in the abrasion zone as well as to further evaluate alternative methods to reduce abrasion.

More recently, Bekker et al (2011) developed an experimental setup to estimate the intensity of ice abrasion on concrete. Not only is the abrasion damaging to the concrete of the structure, but also as a direct consequence, exposure of reinforcement and enhanced corrosion damage can occur. The determination of the wear induced by drifting ice remains a top-level concern for offshore structures in ice prone waters (Bekker et al, 2011). With their testing results and this paper, Bekker et al (2011) propose an empirical model of the abrasion mechanism that can then be applied to estimate the expected yearly abrasion on a concrete structure.

The laboratory room and testing equipment were specially designed to accommodate this type of experiment, allowing control of the temperature. The researchers examined ice and air temperature as well as the applied pressure. The temperature varied within a range of -5 to -20 °C while the pressure was applied at 0.5, 1.5 and 3.0 MPa (Bekker et al, 2011). It is stated in the paper that the ice samples to be used were similar to natural grown ice. However, no further information regarding the ice samples is provided in this report. The only provided information on the concrete mixture is that there were two types of mixes tested, shaft mix and ice zone mix. The testing arrangement that was used in the ice laboratory can be seen in Figure 2-5.

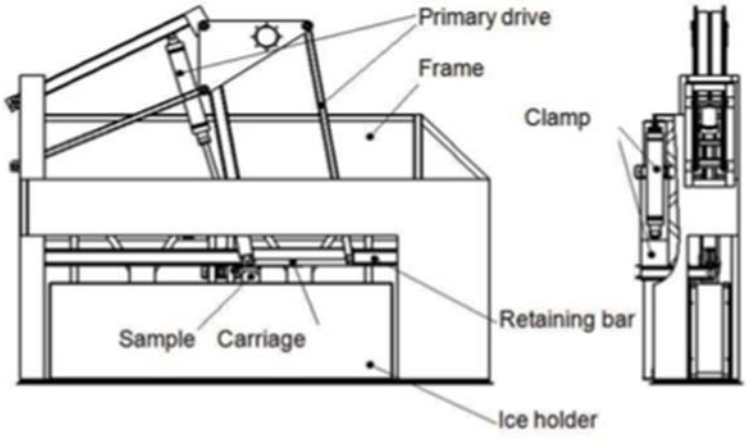

Figure 2-5: Laboratory Test Setup (Bekker et al, 2011)

Prior to testing, a micrometer device was used to measure the concrete samples. The samples were exposed to varying freeze-thaw cycles and each test was replicated for differing combinations of pressure and temperature. Post-abrasion, 168 points on the sample surfaces were re-measured to assess the amount of abrasion (Bekker et al, 2011).

The researchers observed depth of abrasion as well as length of the abrasive path. Computer software was used to create visual models of the abrasive effects.

Bekker et al (2011) notes that to improve the accuracy of the results, the tests should be run until there exists a more uniform area of abrasion formed along the entirety of the concrete sample. The abrasion measurement should then be taken from these grooves.

Due to the findings that ice sliding had more abrasive effects than ice crushing (Janson, 1988), Møen et al (2015) conducted laboratory sliding tests. The focus of that study was to determine the effect of specific factors including the compressive strength of concrete, the applied ice pressure and the temperature of the ice sample. Previous research (Huovinen, 1990) showed that the abrasion process occurs by first wearing away the cementitious material of the concrete which leads to aggregate exposure and loosening. In an effort to observe the abrasive effects on both the outer cementitious material and directly on the aggregate, tests were completed on outer concrete surfaces as well as on samples that were sawn in half (Møen et al, 2015). Even further, both laboratory-made and field-cored concrete samples were tested.

The testing machine, shown in Figure 2-6, used to complete these series of tests was similar to that used by Fiorio (2005). The concrete sample was held stationary while a prepared freshwater ice sample slid back and forth at a specified sliding velocity and normal load. In comparison, the setup used in this research was capable of applying higher loads and velocities than previously used setups (Møen et al, 2015). An average sliding velocity of 0.2 m/s was set and applied pressures ranged between 0.5 and 1.5

MPa. The atmospheric and ice sample temperatures remained between -5 and -20 °C. Tests were completed in a temperature-controlled setting that could be decreased to -20 °C. However, a heated copper plate was placed below the concrete to ensure the moist surface, resulting from frictional heating, didn't form an ice layer and disrupt the interface between the ice and concrete samples (Møen et al, 2015).

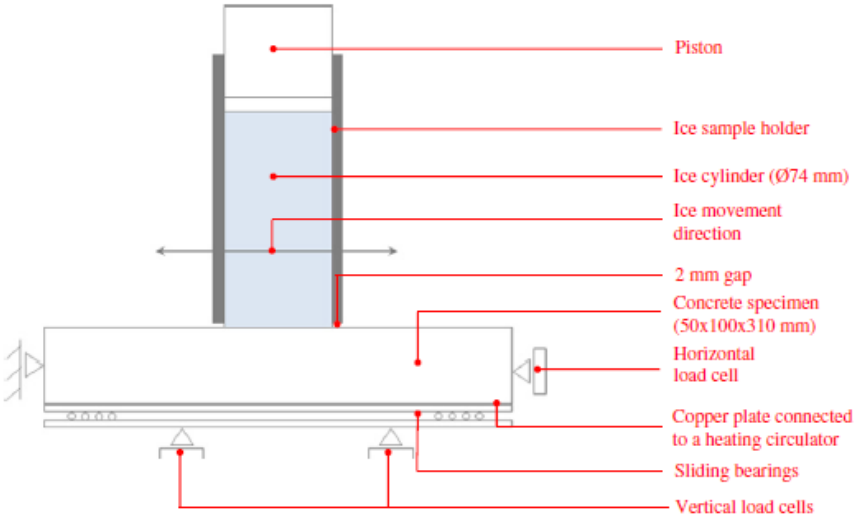

Figure 2-6: Laboratory Test Setup (Møen et al, 2015)

Møen et al (2015) divided the research into two different series. In series 1, there were no alterations made to the testing surface of the laboratory made concrete. In comparison, series 2 contained both laboratory and field-cored concrete samples that were cut in half to expose the inner aggregate. Series 2 tests were all completed with an applied pressure of 1.5 MPa. The laboratory-made concrete samples were exposed to freeze-thaw temperatures prior to testing. The field-cored samples were taken from the Raahe lighthouse, found in the Gulf of Bothnia (Møen et al, 2015).

The surface of the concrete samples was recorded by Møen et al (2015) before any testing took place, after a cumulative 1 km of abrasion testing and again after another 4 km of testing was complete. In total 5 km of testing was completed and a micrometer was used to measure the depth of abrasion for each recording.

Jacobsen et al (2015) provides an in depth analysis of ice-concrete wear theories, previous testing and results. Analysis of existing concrete structures that have experienced abrasion agree with the previously reviewed papers; the abrading process wears the cement paste first which then exposes the aggregate beneath. Inspection of the Confederation Bridge in Atlantic Canada, as seen in Figure 2-7, provides visual proof of this process. Clearly, there are differences between field tests and laboratory testing. Jacobsen et al (2015) stress the need to simulate real exposure conditions so that accurate service life estimations can be made. Currently the main laboratory setups for measuring the amount of concrete wear are sliding machines. Differences in laboratory and field tests lead to differing results from researcher to researcher.

Figure 2-7: Confederation Bridge Abrasion Damage (Newhook & McGuinn, 2007)

Tijsen et al (2015) continued with more abrasion testing and also began looking into the difference between abrasive ice loading versus a decrease in abrasion resistance of the

concrete surface. Abrasion for this particular research is defined as loss of surface concrete material measured by decrease in mass. The concept for the test setup is based on three separate regions of interaction between the ice and concrete, resulting in varying angles of contact (Tijsen et al, 2015), denoted α in Figure 2-8.

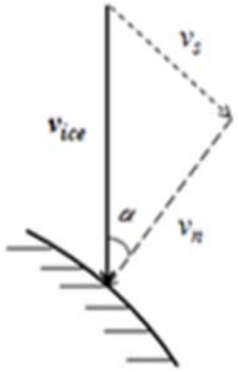

Figure 2-8: Contact Zone of Approaching Ice (Tijsen et al, 2015)

The ice samples prepared for testing for this paper were conical shaped (Tijsen et al, 2015); this is different in comparison to the cylindrical samples that were typically used up until this point in time. There were two types of concrete mixes to be tested; a high performance mix with high compressive strength and a smooth surface and a lower performance mix with low compressive strength and rougher surface. The laboratory test setup, Figure 2-9, performed three different tests, normal force only, sliding only and a combination of both (Tijsen et al, 2015). These tests represent the three interaction regions and therefore were completed at three varying angles of contact. The normal force test sequence, dictated by crushing, ran at 0.1, 1.0 and 10 mm/s. In comparison, the sliding tests were performed with a 10 kN normal force at 1.8 and 180 mm/s. All tests were performed in a cold room with a constant temperature of -10°C (Tijsen et al, 2015).

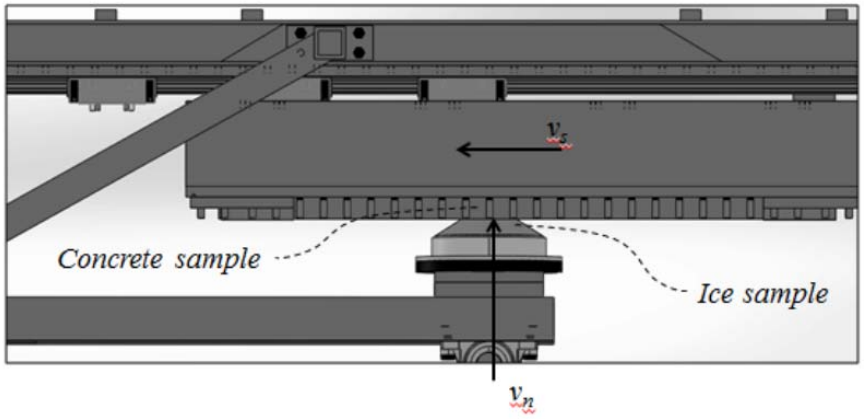

Figure 2-9: Laboratory Test Setup (Tijsen et al, 2015)

The test setup carried out by Tijsen et al (2015) allowed for three different types of testing at various angles of contact. However, it is noted that testing longer sliding distances is not easily completed.

2.2 Comparison of Experimental Methods

There are obvious trends to take note of when reading the research papers by Huovinen (1990) and Itoh et al (1994). Primarily the focus of the research is on waterline ice abrasion on offshore concrete structures. The attention is placed on sustained ice floe and pack ice situations as opposed to brief, high-intensity ice loads. The importance of field investigation is noted (Bjerkås, 2007). Particularly, the analysis of Finnish lighthouses in Bothnia Bay has been important in verifying abrasion estimation models.

It is important to consider gaps in knowledge in early investigation in order to advance continuing research. Huovinen (1990) carried out many different tests including icebreaker, laboratory and computer models. However, there is limited information provided about his laboratory experiments and the ice conditions surrounding the

icebreakers. Itoh et al (1994) used a more realistic testing setup with clearly defined controls, yet they recognize that the resulting model may not have accurate predictions in situations where there is higher ice temperature in combination with high contact pressure. At this point in time there are conflicting results with no reliable prediction method.

There are many trends and common concepts between the tests completed by Fiorio et al (2002) and Fiorio (2005). Both experiments were completed using a direct shear box machine to measure concrete abrasion on the small scale. The goal output from the testing was to develop models of the coefficient of friction for ice. In both papers, the coefficient was calculated by taking the ratio of tangential stress to normal stress.

The tests performed by Fiorio (2005), though similar in many ways to Fiorio et al (2002), had some small setup differences. Two types of concrete surfaces were tested, those with a smooth surface and those with a rough surface. However, the sliding velocity range, normal stress range and room temperature were the same. From these tests, Fiorio (2005) broke down the ice wear into two types, general and catastrophic and further broke down general wear into two stages, initial and permanent.

In a paper for the conference held by The Nordic Concrete Federation, Fosså (2007) acknowledged the need to further investigate ice-concrete abrasion, but also noted alternative resistance strategies and solutions. The main takeaway from this paper is that while valuable progress has continued in this field of research, it is evident from the various laboratory test setups used to date that standardized friction tests are needed.

Further efforts to carry out tests and investigation into wear theories have produced more literature on this topic. The testing and results from Bekker et al (2011) have provided researchers with an empirical model for ice abrasion that according to Jacobsen et al (2015) is the most complete model at this time. It is important to note however, that the researchers state if testing reproducibility was more feasible the accuracy of the model would be higher. This would provide more uniform areas of abrasion and more precise measurements.

Further sliding tests by Møen et al (2015) provided a look into both laboratory prepared and field-cored concrete samples. Cumulatively, 5 km of testing was completed however direction changes were still required as with previous experimental setups.

Experimentation into angle of contact and conical ice samples by Tijsen et al (2015) provided insight on stick-slip action and alternative test setups. Again, it is noted that reproducibility and the ability to test long distances are a challenge. The extensive research by Jacobsen et al (2015) has given a detailed look at related and applicable wear theories. The overarching point of the paper is the necessity of producing realistic exposure in a laboratory environment.

The sliding test setup is the current standard for abrasion testing on concrete due to passing ice. Valuable information has been recorded and advancements have been made in this area. However, there are drawbacks to this particular setup, including reproducibility, long duration ability and directional changes. As well, all tests have been completed under dry conditions. Typically the applied loads range between 0.025-0.8

MPa and 0.5-3.0 MPa for small scale and large scale tests, respectively. Abrasion measurement data and surface roughness has commonly been recorded by using optical microscopy, micrometres and visual data (photos and videos).

A summary of applied loading from the previous research can be seen in Table 2-1. Similar magnitudes of pressure application are clear between Itoh et al (1994), Bekker et al (2011) and Møen et al (2015). While the pressures applied by Fiorio et al (2002) and Fiorio (2005) are much smaller, this can be attributed to the small-scale form of testing that was completed for the scope of that work. Some setups varied the applied pressure throughout testing (Fiorio et al, 2002) and (Fiorio, 2005), while other tests were held constant for the duration (Bekker et al, 2011). Tijsen et al (2015) completed testing using cone shaped ice samples therefore the applied load is provided as a force value, rather than as a pressure.

Table 2-1: Laboratory Scale Ice Load Data Summary

Research	Applied Load	Applied Load (MPa)
Itoh et al (1994)	10 kgf/cm^2	0.98
Fiorio et al (2002) (small scale)	25-800 kPa	0.025-0.8
Fiorio (2005) (small scale)	25-800 kPa	0.025-0.8
Bekker et al (2011)	0.5, 1.5, 3.0 MPa	0.5, 1.5, 3.0
Møen et al (2014)	0.5 - 1.5 MPa	0.5 - 1.5
Tijsen et al (2015)	10 kN	10 kN

An expanded summary of previous testing can be seen in Table 2-2. This provides a high level overview of parameters and types of tests that have been completed and discussed in

this literature review. Blank spaces in the table are due to absence of information on the specific parameters provided in the corresponding papers.

Table 2-2: Comparison of Test Parameters, with contributions from Barker *(2016)*

Reference	Type of Test	Ice Type	Friction or abrasion	Material	Material Sample Size	Contact Pressure	Velocity	Distance	Temperature	Ice Removal	Dry/Wet	Measurement System
Nawwar and and Malhotra (1988)	Rotating	Lab grown saline ice	Abrasion	Concrete	Cylindrical (300 mm diameter, 500 mm long)	6000 kPa	1 m/s		-10 °C air temperature	1/3 submerged in water (1-5 °C)	Wet	
Huovinen (1990) Lab	Sliding		Abrasion	Concrete						None stated	Dry	
Huovinen (1990) Field			Abrasion	Concrete		30-60 MPa		40 km		None stated	Wet	
Itoh et al (1988)/(1994)	Sliding	Sea ice blocks (8 cm wide, 5-10 cm thick, 70 cm high	Abrasion	Concrete	10 cmx10 cm	5, 10, 15, 20, 30 kgf/cm2	1, 5, 20 cm/s	10 km total	Ice Sample -5 °C, -10 °C, -20 °C	Blowing air, same temperature as ice block	Dry	Surface profile measured along 5 traverse lines
Fiorio et al (2002)	Sliding	Columnar freshwater (60 mm diameter, 60 mm high)	Friction	Micro-Concrete	175x150 mm flat plates	25 - 800 kPa (constant and varying)	1.67x10-6 to 1.67x10-4 m/s	30 mm stroke (4m total)	-10 °C	None stated	Dry	Avg roughness, optical microscopy techniques
Fiorio (2005)	Sliding	Columnar freshwater (60 mm diameter, 90 mm high)	Friction	Micro-Concrete	175x150 mm flat plates	26 - 800 kPa (constant and varying)	1.67x10-6 to 1.67x10-4 m/s (0.1-10 mm/min)	30 mm stroke (15m total)	-10 °C	None stated	Dry	Avg roughness, optical microscopy techniques
Bekker et al (2011)	Sliding		Abrasion	Concrete	70 mm long	1-10 kN (0.5-3.0 MPa)	0.2-1.0 m/s	2 km total (20x30 mm sample space)	-5 to -20 °C	None stated	Dry	Micrometre
Bøhn (2012)	Sliding	Freshwater cylinders 74 mm diameter	Abrasion	Concrete	310x100x50 mm	1 MPa	0.1m/s	1350m total	-10 °C	Temperature control of concrete	Dry	Advanced camera/laser scanner, digital indicator
Møen et al (2014)	Sliding	Freshwater cylinders 70 mm diameter, 180 mm high	Abrasion	Lab cast and field cored concrete	50x100x310 mm moulds 100 mm diameter, 250 mm long cores	0.5-1.5 MPa	<0.4 m/s	200 mm stroke (5 total)	-5 to -20 °C	Copper plate temperature control	Dry	Micrometre for abrasion depth
Tijsen et al (2015)	Sliding	Cones	Abrasion	Concrete	1495Lx195Wx207H	10 kN	1.8 and 180 mm/s	<900 mm	-10 °C	Heat gun between each run	Dry	Visual data (video and photo), surface roughness measurement

2.3 Previously Determined Significant Factors

It is noted in the research by Huovinen (1990) that there are many effects that contribute to the wear of concrete in seawater including chemical reactions with the saline environment and concrete shrinkage. However, this particular study of wear focuses on the mechanical loading of moving ice and the concrete freeze-thaw effect (Huovinen, 1990).

As a result, Huovinen (1990) developed abrasion diagrams that estimated abrasion depth depending on ice movement and the compressive strength of concrete. It was concluded that concrete samples used in the abrasion machine should be subject to 50 freeze-thaw cycles in seawater to be conservative. However, concrete that has limited exposure to freeze-thaw action is less susceptible to wear. To achieve good abrasion resistance, concrete should have a minimum compressive strength of 70 MPa and should use large aggregates in a uniform concrete mix. The large aggregates can help break the ice before the ice can abrade the cement and a uniform surface will promote even abrasion, which can reduce the number of loosening stones (Huovinen, 1990).

The abrasion process concept assumed in the paper by Itoh et al (1994) is to consider three different layers in the concrete during abrasion, the surface region, transition region and the stable region. The abrasion rate decreases as the concrete surface is abraded from the surface layer, to the transition and finally becomes constant in the stable region. This is especially seen when there is a rough concrete finish (Itoh et al, 1994). Primary focus in this article was placed on the stable region, as it is considered to be more independent of

ice sliding distance. The main factors considered in the abrasion process during these tests were ice temperature, fine sand concentration and the contact pressure. It was previously determined by these researchers that sliding velocity had a negligible effect on the abrasion rate.

Ignoring sand concentration for the time being, the researchers looked at the effects of ice temperature and contact pressure. From their research, it can be seen that ice that has a temperature less than -10°C has a higher abrasion rate (Itoh et al, 1994). It is explained that as ice temperature decreases the brine crystallizes, these salt crystals can increase wear on the concrete and the formation of brine pockets can render a rougher ice surface. When looking at contact, it is easy to understand that abrasion rate increases proportionally to contact pressure; this seems to indicate that shear stress increases with a higher contact pressure. These results are summarized in Figure 2-10. The researchers also look at sand concentration within the ice and its abrasive effect on concrete. Sand concentration is not a prominent factor in ocean environment ice, therefore this will not be a consideration for this specific research and will not be further elaborated on.

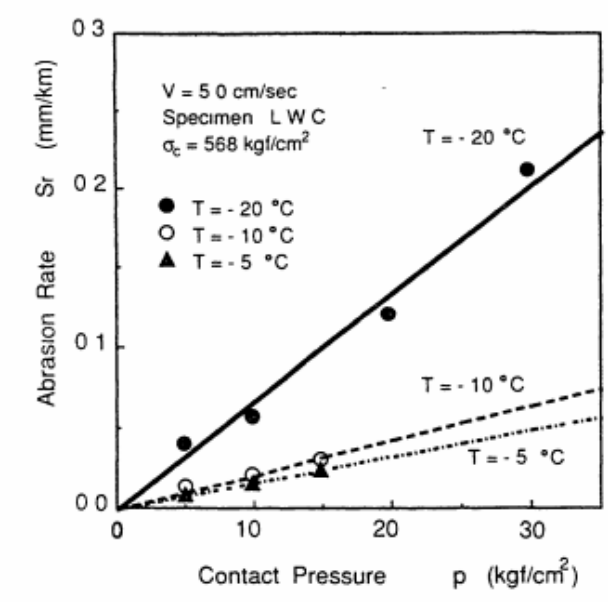

Figure 2-10: Contact Pressure and Abrasion Rate Relationship (Itoh et al, 1994)

From Itoh et al (1994), it can be concluded that ice temperature and contact pressure have a significant influence on the abrasion rate. Additionally, decreasing the interaction surface roughness plays an important role in reducing the amount of abrasion. However, according to this study, factors including sliding velocity, compressive strength of concrete and type of aggregate play a negligible role in the abrading process. Itoh et al (1994) also determined that the majority of abrasion damage occurred as a result of ice sliding as opposed to ice impact.

The results of the small scale testing completed by Fiorio et al (2002) show that friction evolves as the experiments progressed from the initial cycle to the tenth cycle. The final and more stable friction coefficients were higher than the initial friction coefficients. The researchers also found a spike in friction when there was a stop in motion, either at the beginning of the test or when the sliding changed direction. This is indicative of adhesion

between the ice and concrete. It is described as stick-slip action where the adhesive bond needs to be broken, therefore increasing the tangential stress. The analysis led to a predictive ice friction model that was a function of contact conditions including sliding velocity, normal stress and average roughness of the concrete. A sample of the model can be seen in Figure 2-11. The friction coefficient seen in this model is higher than typically recorded in other studies. The average friction coefficient for sea ice on concrete has been recorded to range between 0.1 and 0.2 (Frederking & Barker, 2002).

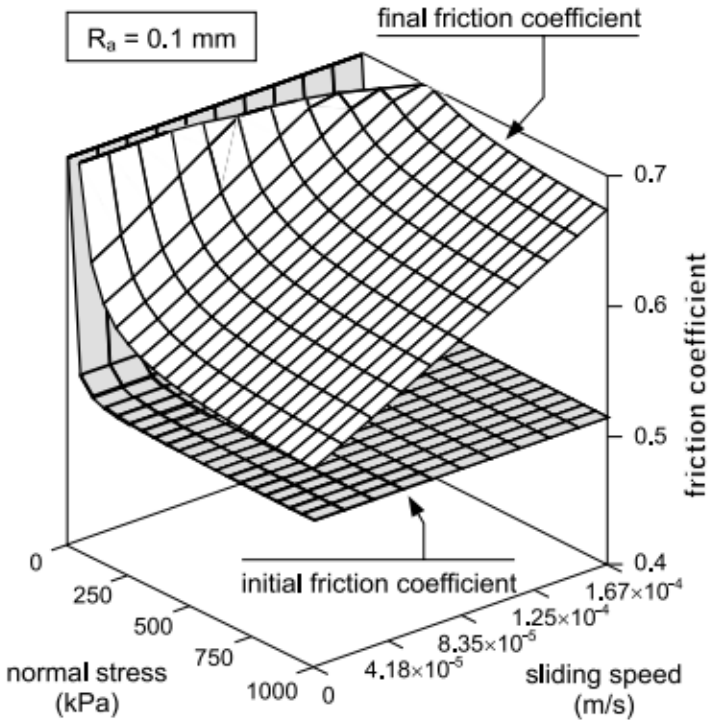

Figure 2-11: Friction Model (Fiorio et al, 2002)

Stemming from these results, Fiorio et al (2002) suggest viscoplastic behaviour in the ice to explain the effects of surface roughness and sliding velocity. A higher sliding velocity directly produces higher strain rates against the raised portions of the concrete surface,

this increases tangential stress and therefore produces higher friction. It is also clear from the results that adhesion is present between the ice and concrete and acts as the main friction factor at low normal stresses (Fiorio et al, 2002). Bearing in mind the two mechanisms for ice friction, viscoplastic behaviour of ice and ice adhesion, the researchers developed a contact model with some simplifications. In this model, the concrete is assumed to be rigid while the ice is viscoplastic, the contact geometry is two-dimensional and protruding aggregates are semi-circular.

From the experiments, the coefficient of friction for ice increased from an initial value to a stable, final value. The predictive model for friction coefficients is based on contact conditions and is a useful output from this research, however it does not describe the physical mechanisms. The contact model based on its simplifying assumptions cannot be used for accurate coefficient calculations, but it does show evidence of ice viscoplasticity.

From continued research by Fiorio (2005), observations of the abraded concrete and ice samples post-testing showed that there was a layer of fine sand and cement that had been removed from the concrete sample and remained in the contact space. It could be determined from the tests that the ice induced friction abraded grooves in the concrete and wore away the cement and fine sands, gradually exposing the larger aggregates (Fiorio, 2005). Fiorio (2005) has divided the abrasion process into two forms of wear, general and catastrophic. The term general wear refers to the even and gradual wearing of cementitious material. In contrast, as a result of general wear and exposure of the coarse aggregates, catastrophic wear refers to loosening and pulling out of these larger particles.

Catastrophic wear occurs at a contained space and time. Depictions of general and catastrophic wear can be seen in Figure 2-12.

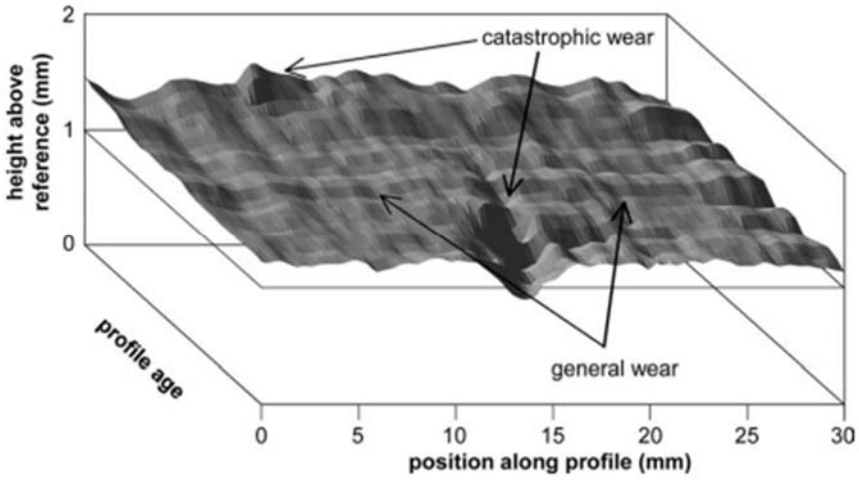

Figure 2-12: Tested Profile Showing General and Catastrophic Wear (Fiorio, 2005)

In paying closer attention to the general wear, Fiorio (2005) found two different stages. By plotting the mean and maximum abrasion for both smooth and rough plates against the sliding distance, it could be seen that there was an initial and permanent stage of general wear, Figure 2-13. During the initial stage, up to a sliding distance of 5000 mm, the abrasion rate is high and dependent on the concrete surface roughness. After a sliding distance greater than 5000 mm has passed, the abrasion rate decreases and no longer depends on the concrete surface roughness. Fiorio (2005) attributes the lower abrasion rate to the protrusion of larger aggregates protecting the cement particles.

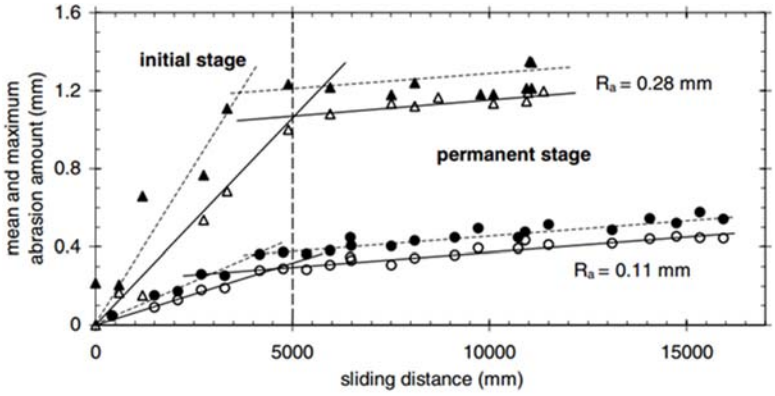

Figure 2-13: Evolution of Friction (Fiorio, 2005)

Fosså (2007) suggests that concrete with a higher tensile strength would aid in reducing the abrasion mechanism. As an example of the use of alternative solutions, in 2004 and 2005 in Sakhalin, steel shields were attached to two offshore concrete structures at their waterline level.

Steel is a useful and well-known material. Currently, it is accepted as a useful technique to protect concrete in high abrasion zones. The downside is that it is a costly method that is complex to put to use. Other alternatives noted by Fosså (2007) include high strength concrete, concrete sealants and ultra-high strength concrete. The advantages and disadvantages of these alternatives can be seen in Figure 2-14. The main drawbacks of these alternative solutions are the lack of standardized testing and lack of documented use (Fosså, 2007).

Material in the splash zone	Advantage / disadvantage	Comments
Steel shield on concrete	Expensive and complicated method.	Acceptable method (steel quality and thickness need to be determined in each case).
High strength concrete	Cost and schedule attractive method.	Not a documented alternative.
Sealing of the concrete surface	Applied during slipforming. Cost and schedule attractive method.	Require inspection and maintenance. Not a documented alternative.
Ultra-high strength concrete/mortar	Applied during slipforming? Cost and schedule attractive method.	Not a documented alternative.

Figure 2-14: Alternative Material Summary (Fosså, 2007)

Test setups for ice and concrete should become standardized and must be able be able to observe the effect of factors including ice composition, ice temperature and hardness, contact force and speed as well as the duration of the interaction. Fosså (2007) notes that there is still insufficient experience on the abrasion effect of ice on concrete.

To better prepare the Arctic concrete for an extended service life, Sistonen & Jacobsen (2007) suggest increased concrete compressive strength and a strong bond between the cementitious material and hard aggregate. A sacrificial concrete layer at the waterline could be an option for structural protection. It is evident from this paper that more research on predictive service life models would increase the reliability of concrete structures in harsh Arctic environments.

The results of the testing completed by Bekker et al (2011) were analyzed and empirical models of the ice abrasion were produced. One model represents the concrete in the shaft

mix while the other is representative of the ice zone mix. The formulas calculate abrasion as a result of the temperature to pressure ratio. These results, when combined with other models, can be used as an initial abrasion estimate for concrete structures subject to drifting ice (Bekker et al, 2011).

However, there are still some uncertainties within the testing and hence, the resulting models. Factors including concrete properties, ice properties as well as the interface between the concrete and ice are still not fully understood.

The results of all the testing completed by Møen et al (2015) for each series were statistically analyzed to determine the significance of the varying experimental factors. For series 1, it was seen that a higher compressive strength of concrete resulted in a lower kinetic coefficient of friction and a lower abrasion rate. Møen et al (2015) explain the findings by assuming the higher compressive strength in the concrete helps to maintain a smoother surface.

As seen in previous studies, abrasion rates were noted to become higher as the applied ice pressure increased (Itoh et al, 1994). However, there was no conclusive evidence of a significant statistical effect from varying the temperature of the ice (Møen et al, 2015). Previously, the researchers made note of an experimental uncertainty regarding this factor. Due to the temperature control of the concrete sample surface, the ice in contact with the surface may not have been completely maintained. On the other hand, the ice was worn away relatively quick which continuously exposed new ice.

The resulting abrasion rates for an applied pressure of 0.5 MPa and a compressive strength ranging from 60.4-72.8 MPa were 0.002-0.018 ± 0.006 mm/km. For an applied pressure of 1.5 MPa and compressive strength ranging from 60.4-147.8 MPa, the rates ranged from 0.004-0.021 ± 0.007 mm/km (Møen et al, 2015).

In series 2, the applied ice pressure was not a changing factor and was held constant at 1.5 MPa. Overall, Møen et al (2015) found the cored field samples from the Raahe lighthouse were more susceptible to abrasion than the laboratory prepared samples. As in series 1, higher compressive concrete strength resulted in lower abrasion rates, however there was no statistical significance of the effect. In general, a higher ice temperature was found to decrease the abrasion rate, however this was inconsistent (Møen et al, 2015).

Resulting abrasion rates from the tests completed by Møen et al (2015) ranged from 0.004-0.018 ± 0.010 mm/km for an applied pressure of 1.5 MPa and compressive strengths from 45-85.9 MPa.

Jacobsen et al (2015) provided an in depth analysis of ice-concrete wear theories, previous testing and results. Three separate contact regions during pack ice interactions with an offshore concrete structure. Region 1 is the main contact zone where there exist high normal loads and Region 2 experiences lower normal forces but has high shear forces from ice rubble being dragged along the surface. Region 2 generally experiences the largest amount of abrasion. Finally, Region 3 experiences small amounts of force but has accumulated debris.

Analysis of existing concrete structures that have experienced abrasion agree with the previously reviewed papers; the abrading process wears the cement paste first which then exposes the aggregate beneath. The researchers note that the main factors that differ from the field to the laboratory include contact pressure, temperature, wetness of the concrete and the application of the load.

To highlight these differences, in the paper Jacobsen et al (2015) compare the results from Bekker et al (2011) and Itoh et al (1994). Both studies found that increasing the normal pressure resulted in an increase in abrasion. Yet, while Bekker et al (2011) found that lower temperatures reduced the abrasion, Itoh et al (1994) had contrasting results. Jacobsen et al (2015) guess that the differences could be due to variances in sliding speed between the two tests.

Regardless, Jacobsen et al (2015) note that the empirical model developed by Bekker et al (2011) is the best estimate at this point in time. In this paper they further investigate wear theories to try and understand the physical mechanisms that result in concrete abrasion. There are many details covered in the paper, however, this literature review will only provide a high-level overview of the main theories.

In reviewing Archard's Law, which describes the contact between two flat surfaces with asperities, and previous studies, it can be determined that the depth of abrasion increases with exposure time, amount of ice movement and increased pressure. Another mechanism under review is the fatigue property of concrete. As both the concrete and ice are not smooth surfaces, there could be alternating dynamic loads when asperities from the two

surfaces contact each other. This is a different approach than considering a more static interaction between the two surfaces. Eventually, it will lead to fatigue wear in the concrete surface (Jacobsen et al, 2015).

In looking at contact mechanics, the researchers suggest that Hertzian contact theory could be applied to describe the interaction of short duration loading on a rough surface. Previous studies show that ice is a harder material when the loading time is short and the temperatures are low (Jacobsen et al, 2015). At a low strain-rate, creep is expected in the ice and is more representative of actual ice behaviour. During the slow loading at the contact zone between the ice and concrete, it is expected the concrete surface will be wet as it occurs at the waterline. This fluid in the contact zone can actually increase the amount of abrasion (Jacobsen et al, 2015). The liquid can be highly pressurized and can be forced into cracks and breaks in the concrete surface as depicted in Figure 2-15. Additionally, previous tests have shown that wet concrete has a lower strength than when it is dry (Jacobsen et al, 2015). From this paper, it is important to note that broken off debris from the abrasion process can remain in the contact zone and add to the abrasion mechanism.

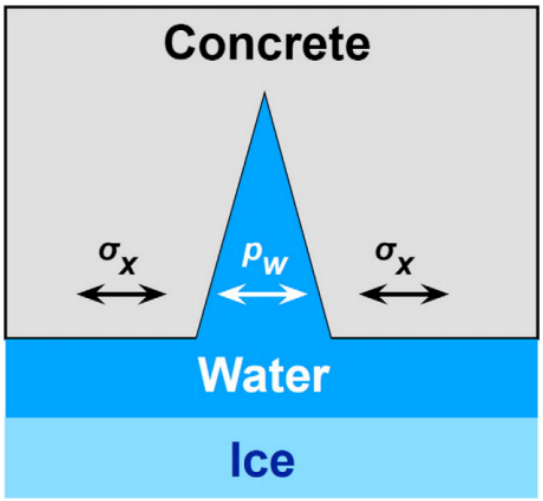

Figure 2-15: Pressurized Liquid in the Contact Zone (Jacobsen et al, 2015)

Jacobsen et al (2015) list three possible mechanisms that could all contribute to the abrasion of concrete from ice floes. These include pressurized water in the pores at the contact zone, residual debris enhancing abrasion in the contact zone and stress in the concrete from ice friction. Tensile stresses caused by the friction will cause more cracks and pore space in the concrete. This in turn allows more water within the contact zone to be pushed in these resulting cracks. Finally, abraded concrete particles can remain as debris that contributes to the friction between the ice and concrete (Jacobsen et al, 2015). Moving forward with laboratory sliding tests, the researchers suggest that intermittent pauses in the sliding should be scheduled to observe crack formation and analysis of debris. They also suggest further investigation into pressurized water in concrete cracks.

Another suggestion pertains to the actual concrete mixture, fibers and silica fume could help in retaining the concrete surface and decreasing the amount of debris (Jacobsen et al, 2015). Additionally, using smoother aggregate, rather than jagged, in the mixture will reduce the abrasive effects if they are loosened and removed from the concrete.

Figure 2-16 depicts the 3 regions of interaction that are discussed by Tijsen et al (2015), similar to those explained by Jacobsen et al (2015). Region 1 in this paper is governed by crushing. The large normal and shear forces exerted on the concrete in this region directly causes abrasion. The stresses exceed the resistance of the concrete, resulting in damage. Tijsen et al (2015) refer to this as primary order of loading. The crushing only test was indicative of the abrasion process in this area and resulted in scour and exposure of aggregate (Tijsen et al, 2015). According to the researchers, Region 2 is characterized by stick-slip behaviour that results in a reduced abrasion resistance of the concrete over time. They have termed this secondary order of loading. The researchers determined the stick-slip cycles were dependent on the velocity of the ice, the angle of contact as well as the type of concrete. The adhesion depended on contact area and therefore was more sensitive on the smoother concrete. Region 3 has low stresses and is considered more of a slip region however in some conditions, abrasion can occur.

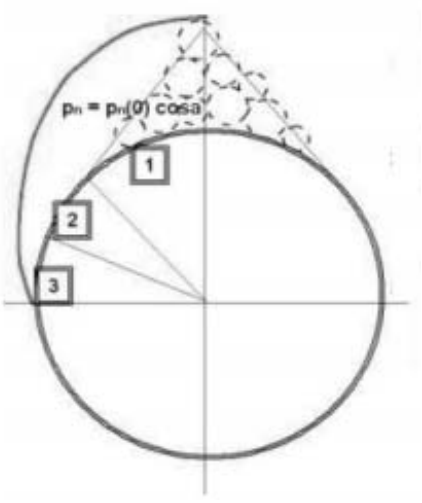

Figure 2-16: Regions of Ice-Structure Interactions (Area [1]: Crushing, Area [2]: Stick-slip, Area [3]: Lower stress abrasion) (Tijsen et al, 2015)

The breakdown between primary order and secondary order of loading is useful in better characterizing abrasion effects. Regions 1, 2 and 3 have been broken down to specify the type of loading typically seen. Additionally, Tijsen et al (2015) observed concrete particles transferred to the oncoming ice sample that increases the ice roughness. As well, frictional heating between the two surfaces caused localized stresses and act as another form of secondary order of loading (Tijsen et al, 2015). In general, the high performance concrete mix demonstrated a better resistance to the abrasion processes.

2.4 Comparison of Significant Factors

A significant trend to acknowledge is the impact of freeze-thaw cycles. There is a general agreement that reducing freeze-thaw action by keeping concrete permanently frozen or permanently unfrozen will reduce the abrasion process. However, Huovinen (1990) followed a conservative approach by incorporating freeze-thaw into his experimental concrete samples. In contrast, it is noted by Itoh et al (1994) that advancement in high strength concrete design has increased the durability of concrete when subject to these conditions. In the testing completed by Bekker et al (2011), the concrete samples were subject to varying freeze-thaw cycles. This is similar to the prepared samples by Huovinen (1990). However, Jacobsen et al (2015) remark that abrasion occurs even if there is no freeze-thaw action. This is proved by the Huovinen (1990) icebreaker tests. Perhaps freeze-thaw is best explained by Tijsen et al (2015), a secondary order of loading. In other words, freeze-thaw may not directly abrade the concrete, however it can lower the abrasion resistance of the concrete.

There are also some contrasting results that should be summarized in order to compare with the progress in more recent research. The most significant difference is that Itoh et al (1994) found that the compressive strength of the concrete didn't have a significant effect on the abrasion rate. This disagrees with the previous model by Huovinen (1990) and later testing results from Møen et al (2015). Itoh et al (1994) also determined that the type of concrete aggregate was not significant, but Huovinen (1990) stated that larger aggregates could actually reduce abrasion. However, stemming from this difference, there is a common ground. Both papers acknowledge that a more even and smoother surface will result in a reduced abrasion rate. Itoh et al (1994) breaks the process down further and names regions of varying abrasion rate; the lowest being in the stable region.

Reviewing the literature by Jacobsen et al (2015) and Tijsen et al (2015) shows tendencies towards many similar concepts with respect to ice abrasion. They are in agreement with previous research that during the abrasion process, the cement paste is most susceptible to wear and consequently exposes the underlying aggregate. Similarly, they are in agreement regarding the three interaction regions and the type of loading that characterizes each. Both papers acknowledge that as the concrete abrades, debris can remain in the contact zone or become embedded in the ice. This debris increases the roughness in the interface, which can enhance the abrasion rate. Both Jacobsen et al (2015) and Itoh et al (1994) observed frictional heat that is the result of fast moving ice and can result in local thermal stresses that affect the concrete strength. Finally, both papers conclude that the addition of silica fume to the concrete mixture increases the abrasion resistance of the concrete.

Primarily, there is a general agreement that the abrasion process wears away the cementitious material that in turn exposes and loosens the coarse aggregates. The ice samples used in both tests by Fiorio et al (2002) and Fiorio (2005) were laboratory grown freshwater ice as it was determined that the brine pockets in the ice had a negligible effect on the abrasion rate. This contradicts the findings of Itoh et al (1994) which stated that the brine pockets added roughness to the ice surface which could enhance abrasion.

Early studies by Itoh et al (1994) showed that sliding velocity has a negligible effect on abrasion rate. However, the model friction coefficient developed by Fiorio et al (2002) was a function of sliding velocity, normal stress and average roughness. Recent studies prove that sliding velocity plays a significant role in the abrasion process, specifically regarding the coefficient of friction of ice during ice-concrete interactions (Schulson, 2015). A higher sliding velocity can produce higher friction due to the increase in strain rates and tangential stress against raised concrete asperities (Fiorio et al, 2002). Schulson (2015) studied ice on ice friction; nonetheless the results are also relevant for ice on concrete friction. Slow sliding velocities which are considered less than 10^{-5} m/s results in ductile creep of the ice asperities that risks adhesion to the concrete sample (Schulson, 2015). Conversely, higher sliding velocities can produce frictional heating and create a wet interface between the two surfaces. Figure 2-17 provides an overview of the findings (Schulson, 2015). It can be seen that at higher velocities, there is a wetted portion between the asperities of the two contacting surfaces.

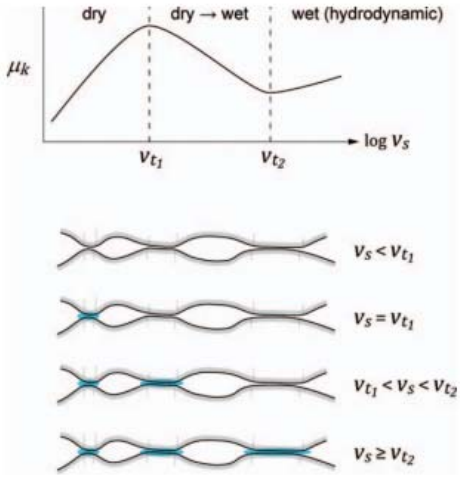

μ_k – Friction coefficient, v_{t1} – Velocity limit for dry sliding
v_{t2} – Velocity limit for dry/wet sliding, v_S – Sliding velocity

Figure 2-17: Effect of Sliding Velocity on μ_k of Ice (Schulson, 2015)

Observations showed that friction evolved over time, the coefficient increased from initial values to final values, and secondly, there was evidence of viscoplastic behaviour of ice (Fiorio et al, 2002). In comparison, it was found that the abrasion rate decreases from the initial stage to the permanent stage (Fiorio, 2005). An explanation for this is that the coefficient of friction increases as the coarse aggregate is exposed and the concrete surface becomes rougher. However, the aggregate is more resistant to abrasion than the cement and therefore reduces the abrasion rate.

As with Fosså (2007), Bekker et al (2011) reiterate the appeal for standardized testing and specified requirements for concrete existing in Arctic conditions.

2.5 Full Scale Ice Load Data Collection

Comparison of laboratory scale data to full scale data is important in test setup design to ensure adequate loads can be applied and supported. Historically, the Confederation

Bridge has been a valuable project for investigating concrete abrasion due to passing ice. Tibbo et al (2009) provide a 12-year overview of an ice monitoring system installed on the Confederation Bridge since it opened in 1997. This study has allowed surveillance of ice-structure loads, corresponding visuals and environmental data which has been used to determine the validity of the bridge design. The two main goals for this program were to gather records of ice conditions in this area and to determine the difference between the design and actual ice loads (Tibbo et al, 2009). The Confederation Bridge piers can usually see around 4000 km of ice floes during the typical ice season of January to late April or early May (Brown T. , 2001). Typical ice seen in the Northumberland Strait consists of broken first year ice floes and consolidated ridges (Brown T. , 1997).

Equipment placed on two neighboring bridge piers allowed monitoring of the structures reaction to ice loads and wind loads. The strain gauge panels placed on the pier to measure sheet ice loads had an area of 0.25 m^2 (Cheung et al, 1997). Additionally, there were cameras installed which allowed visual images of the physical interactions. Data was continuously recorded every 17 s, however, if the limit of a predetermined load was reached indicating a significant loading event, recordings began collecting information every 0.034 s (Tibbo et al, 2009).

At the time this paper was written, the ice monitoring program had been ongoing for twelve years, from 1997 to 2009. The year 2008 was noted as a distinct year that had abnormalities in temperature which resulted in a more extreme and lengthy ice season (Tibbo et al, 2009). For this study, the predetermined load for the 1400 ice events that occurred was considered when loads were greater than 0.75 MN, or 3 MPa for the 0.25m^2

load panels. Seven percent of these were significant events with a load greater than 2 MN (Tibbo et al, 2009). The piers also experienced two major loading events in the 2008 season which reached a maximum of 6.06 MN and 4.81 MN (Tibbo et al, 2009). Unfortunately, due to issues with the monitoring equipment, a portion of the ice season logging time was missed.

Due to the sloped design of the Confederation Bridge piers, the majority of the ice load data that is gathered arises from the ice floes failing in flexure as they ride up the concrete structure. Even though loads less than 0.75 MN were not considered significant, they continually apply load and would contribute to the abrasion of the piers for the duration of the ice season. Typically, the higher event loads are only sustained for short periods of 15 minutes or less (Tibbo et al, 2009).

Full scale ice loads on offshore structures, primarily lighthouses and channel markers, in the Baltic Sea also have been monitored for many years. The locations of the structures are as seen in Figure 2-18. The ice conditions in the Baltic Sea, especially in the more northern Bay of Bothnia, provide a harsh and costly environment for fixed structures. The Norströmsgrund lighthouse was built in 1971 and since then has been continuously studied for ice-induced damage (Fransson & Lundqvist, 2006).

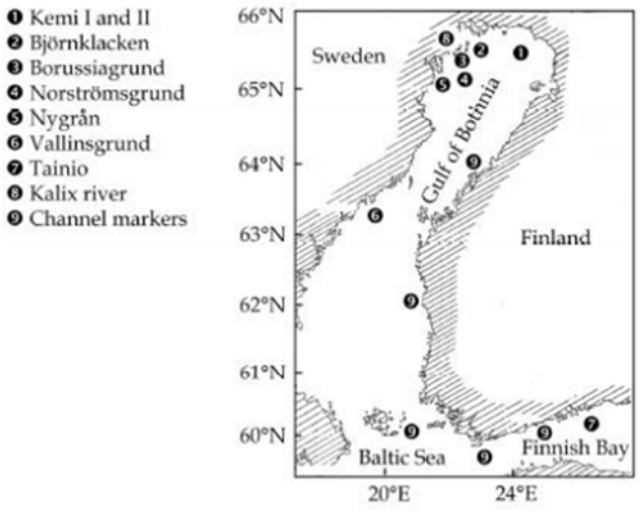

Figure 2-18: Baltic Sea Lighthouse Locations (Bjerkås, 2006)

Ice formation normally begins in December and eventually consolidated ice floes up to 40 cm thick can be seen (Fransson & Lundqvist, 2006). The full sea area in the Bay remains ice covered through February and March and northerly drift can result in thick ridges in the North or in reconsolidated icebreaker channels. The concentration and thickness of ice is greater in the North, while in the South the ice is slightly thinner and open water areas can be seen. Large floes continue to inhabit the area until the end of May (Fransson & Lundqvist, 2006). A study conducted at Norströmsgrund, as part of the late '90s Low Level Ice Forces (LOLEIF) research project, collected ice load data that was broken down into static ice loads, brittle ice crushing and phase locked ice loads. Nine load panels were installed on the lighthouse with the goal of collecting full scale data (Fransson & Lundqvist, 2006).

The largest static loads were recorded under two similar scenarios, one being a sustained load due to a lack of driving force. The second showed a positive correlation between load and driving force that peaked just before movement (Fransson & Lundqvist, 2006).

Additionally, the structure diameter in comparison to the ice sheet thickness shows a strong influence on the ice load. Maximum pressures were seen to be between 1.0 and 1.5 MPa. However, it is noted that if the ice in this environment was more confined, these values could be higher.

During the LOLEIF project, it was recorded that as ice velocities reached 0.1 to 0.6m/s, failure in the ice would occur by brittle crushing at the interface with the lighthouse. Maximum ice pressures of 1.5 MPa when altered for the length and height structure ratio were assumed to be 2.2 MPa. The researchers found that the total travel length during crushing has an increasing effect on the maximum pressures experienced by the structure (Fransson & Lundqvist, 2006). It is expected that as an interaction continues, the initially recorded measurements could be surpassed.

Supplementary to the focused research on the Confederation Bridge and LOLEIF project, a compilation of full scale structures that have been analyzed for significant ice forces over the years has been completed. Specifically recorded are highlights of the maximum global load, in terms of pressure, for each structure. The global pressure is calculated by dividing the global load by the structure diameter multiplied by the ice thickness (Bjerkås, 2007). The structures under investigation are located in Russia, Europe, Canada, the United States and Asia as shown in Figure 2-19. The loads have been determined from one of four different measurement techniques including load cell readings, structural response analysis, application of Newton's Second Law and hindcast back calculations.

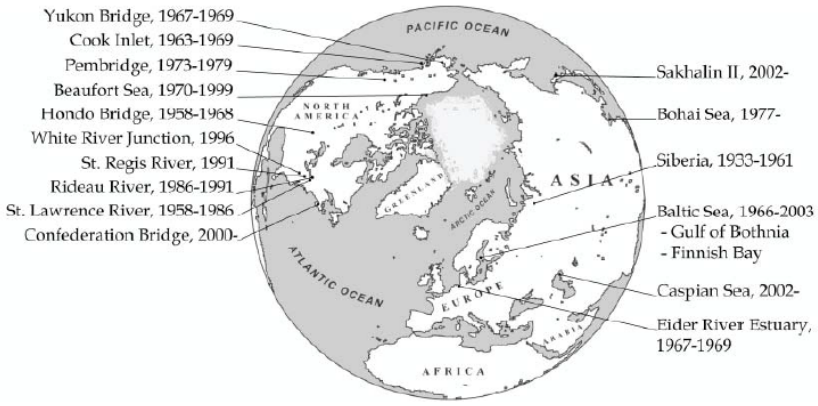

Figure 2-19: Studied Structure Locations (Bjerkås, 2007)

Primarily since the late 1960s, offshore lighthouses have been the main source for ice load data in Europe. From the observations, the highest ice pressure of 4.3 MPa, or a local load of 3.9 MN, was seen at the Kemi-2 lighthouse located along the Finnish Coast. Other notable pressure maximums include 3.4 MPa at the Vallinsgrund lighthouse and 3.0 MPa at a bridge pier in the Kalix River. In comparison, the lowest observed ice pressure of 0.3 MPa was experienced at the Kemi-I lighthouse once the lighthouse had been modified into a cone following previous damage. From the presented data presented by Bjerkås (2007), 2.2 MPa is the average peak global ice pressure that a studied structure has been subject to in Europe.

Structures studied in the Bohai Sea, China have shown lower static ice loads due to the formation of thinner ice in this region. The highest recording reported by Bjerkås (2007) is 1.8 MPa.

In North America there are a variety of marine structures that have been studied; primarily being bridge piers and oil and gas platforms. The highest recorded pressure of

2.7 MPa was seen at Pembridge during the 1970s. Commonly, global pressures typically are seen in the range of 0.7 – 1.5 MPa. These values were obtained and studied at structures in the St. Lawrence River, the Confederation Bridge and Cook Inlet (Bjerkås, 2007).

Bjerkås (2007) has divided the summarized loads into 6 different categories based on the size and shape of the structures, location and measurement method. From five of these groups, a curve can be seen in Figure 2-20 that serves as an upper limit of static global pressures for vertical structures with a diameter between 5 m and 162 m. The upper limit based on the previously studied structures is around 2 MPa. It should be noted that predictive models will differ when analyzing local instead of global loads. Generally speaking, local loads will have a higher value than global loads as they will develop as peaks in high pressure zones from the drifting ice.

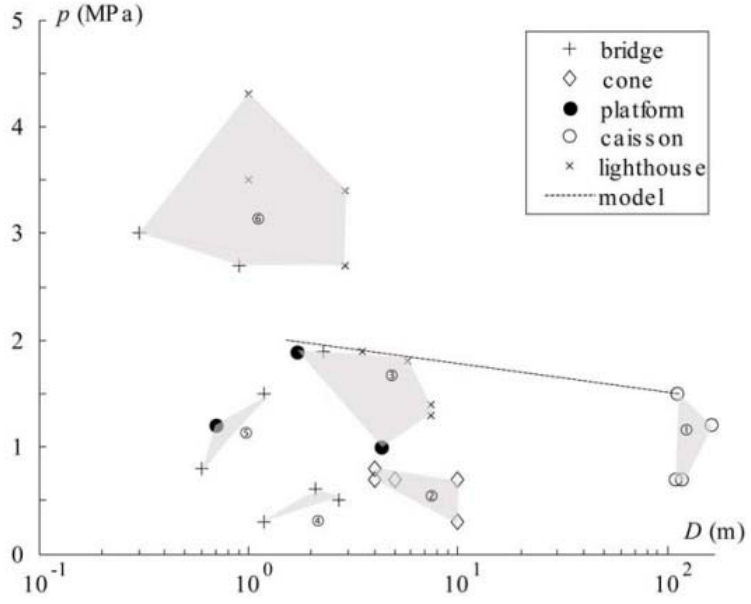

Figure 2-20: Effective Ice Pressures (Bjerkås, 2007)

In reviewing the presented full scale data, lower loads experienced by some structures in North America ranged from 0.7 – 1.5 MPa. However, pressures around 3 MPa and higher have been recorded by the Confederation Bridge piers. European lighthouses have recorded some higher loads around 3.4 and 4.3 MPa. Keeping consistent with full scale and previous laboratory scale loads is important for obtaining realistic testing scenarios. These values will be used in the design to determine the minimum and maximum loads the proposed experimental apparatus will be capable of producing.

2.6 Research Expansion Opportunities

Considering the information provided in the previous sections of the literature review, there are some modifications to laboratory testing procedures that would improve the understanding of ice and concrete interactions. These are expanded upon and investigated in the following two chapters. Results from the investigation will also be used to develop the field testing apparatus concept design.

Chapter 3 Problem Definition, Criteria & Conceptual Features

This chapter provides the design rationale and a laboratory experimental apparatus conceptual design to allow study of the effects of ice wear and abrasion on marine concrete. Some design criteria that are identified in this section are further refined in the next chapter where a series of trial experiments were conducted to determine answers to questions raised in this exercise.

3.1 Development of Design Criteria

Concrete wear from ice contact requires standardized examination. The overall project focus is on loss of concrete material in environments prone to pack-ice conditions. Pack-ice interactions with marine structures are characterized by long duration loading that can be applied by normal forces, shear forces or a combination of the two. The continuous frictional interaction between the ice and the structure results in gradual abrasion of the concrete. This is in contrast to other forms of ice interaction such as infrequent iceberg loadings that exhibit brief, but high-impact, interactions.

Existing experimental equipment and procedures are most often borrowed from other disciplines in material testing (Fosså, 2007). However, due to the non-uniformity of concrete surfaces, ice-concrete interactions pose a greater challenge than many other commonly studied materials. In order to make progress with this problem, testing must be completed to specifically isolate the abrasive effects of ice.

There are few tools in existence that effect and measure concrete wear from long term ice contact. The opportunity therefore exists to build upon previous research and to develop a standardized laboratory testing environment and apparatus that accurately simulates, monitors and measures prolonged realistic ice-concrete friction interactions.

Ultimately, the objective is to develop an improved understanding of the abrasive effects of pack-ice on marine concrete. This will help develop abrasion resistance strategies and enhance the performance of concrete subject to harsh ice abrasion conditions. The following sections provide a discussion of issues that inform the design criteria and design process for a new apparatus to measure ice-concrete friction and abrasion.

Based on the state of the art review, the following factors or features have been identified as important in guiding the design of the ice-concrete abrasion apparatus: relative wear rates, motion mode, applied pressure, wet or dry testing, ice sample type, relative velocity range, temperature control and range, waste ice removal, measurement of abrasion/material loss, applied and resultant force measurements. Each of these factors is discussed in detail in the following sections.

3.1.1 Relative Wear Rates

Pack-ice interactions with marine concrete, resulting in significant material loss, are not a short duration process. Throughout the course of a winter season, thousands of kilometers of pack-ice can continuously wear away the cementitious material and underlying aggregate. This can either be new pack-ice that continuously passes a structure, or broken up floes that pass back and forth throughout the season (Tibbo et al, 2009).

Wear rates in the ice are orders of magnitude higher than wear rates in the concrete so an experimental design will have to contemplate a high feed rate for ice but a negligible requirement to replace concrete samples. This also points to the need to achieve many thousands of meters of relative motion in order to achieve measurable wear in concrete samples.

As the abrasion process progresses there is a change in the friction and wear rate between the ice and concrete. It was shown that friction evolves over time, with a more permanent stage of abrasion noted after 5000 mm of testing, Figure 2-13 (Fiorio, 2005). However, there is a significant difference between a laboratory test that runs for 15000 mm and a full winter season with thousands of kilometers of pack-ice that is contributing to concrete wear. Performing longer duration testing would better simulate full scale interactions and achieve a more constant and measurable abrasion rate. This would decrease the amount of error and uncertainty that arises from data extrapolation.

Bekker et al (2011) recommends continued testing to obtain a uniform area of abrasion along the concrete surface. This will help in obtaining accurate results in the lab that can then be extended to more realistic scenarios.

3.1.2 Motion Mode – Testing Speed, Start-stop, Adhesion

Previous research shows a spike in friction during the interaction at the start of a test, during a stop in movement, and during a direction change in sliding mechanisms. This indicates adhesion between the ice and concrete samples (Fiorio et al, 2002). Typical test setups that have been used previously slide the ice specimen back and forth on the

concrete surface; this motion promotes this form of adhesion and interrupts, or possibly augments, the concrete wear. A different approach was taken by Nawwar & Malhotra (1988) where continual abrasion was achieved using cylindrical concrete samples. This indicates that two forms of experimentation might be considered, one in which start-stop motions that assess the effects of adhesion are considered, and a second type of experiment in which continuous motion is induced without a requirement for starting and stopping. In the immediate case, the design concept will focus on the second type in which start-stop motions are undesirable.

3.1.3 Applied Abrasion Pressures and Forces

In dense ice floe environments, structures are subject to significant loading. Pressurized forces cause ice crushing against fixed structures. As well, applied tangential sliding forces from currents, wind and surrounding ice, continually cause wear to the exposed concrete. Previous studies confirm that there is a positive relationship between contact pressure and the amount of material loss (Itoh et al, 1988). It is important to be able to generate forces and speeds that could be expected in realistic environments where ice abrasion is a recurring issue. Figure 3-1 shows a commonly seen buildup of ice on the bridge piers.

Figure 3-1: Ice Buildup on Confederation Bridge Piers (Newhook & McGuinn, 2007)

Realistic forces and pressures have been derived based on the highest reported normal pressures identified from full scale trials and laboratory tests.

Considering the presented full scale data, it is reasonable to design the proposed laboratory test setup to sustain a maximum applied pressure of 2 MPa. This is consistent with full scale loading scenarios while remaining feasible for testing purposes. This is selected as the design criteria for normal ice sample sizes (which are defined later). Pressures can be applied to replicate higher loading patterns which can be seen in the laboratory scale experiments, as shown in Figure 3-2, by reducing the ice sample cross sectional areas for cases where higher pressures are desired.

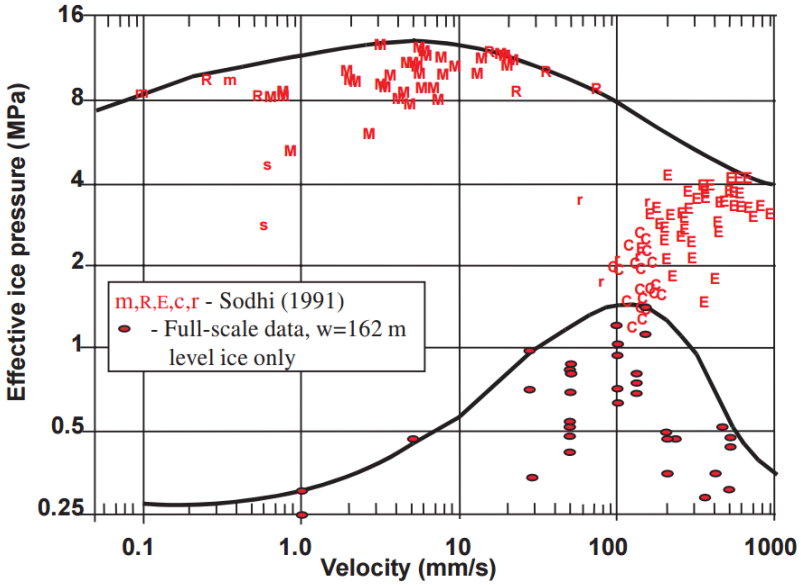

Figure 3-2: Effective Ice Pressure Data (Blanchet, 1998)

3.1.4 Wet-Dry Testing

Although many previous studies have been performed with dry contact between ice and concrete it is recognized in most of the literature that most marine interactions take place in the presence of seawater or freshwater. The presence of fluid at the interface has been identified as an important factor. There are conflicting reports on whether the water promotes grit removal and thereby slowing the wear process, or debris retention, accelerating concrete abrasion (Jacobsen et al, 2015). The theory that pressurized fluid can be forced into concrete cracks and flaws, (Jacobsen et al, 2015), has not been thoroughly investigated as the majority of previous research has been completed in dry environments. Creating a testing environment that allows liquid in the interface zone would provide improved insight into the real abrasion process.

3.1.5 Ice Type

Despite previous comments by Itoh et al (1994) that brine pockets in saline ice would increase surface roughness and consequently abrasion rates, the majority of experiments have been completed using laboratory grown freshwater ice (Fiorio et al, 2002), (Fiorio, 2005), (Møen et al, 2015), and (Schulson, 2015). In general, freshwater ice is considered to have higher strength than saline ice and is consequently the worst-case scenario for abrasion. A further benefit is the ease of reproducibility and consistent ice material. For the purposes of initial testing, freshwater ice samples and water will be used. As testing continues, experiments can begin to incorporate runs using varying degrees of ice and water salinity to answer questions and definitively determine the statistical significance of this factor. The criteria for sample size and shape will allow for either ice type and will be able to accommodate saline samples.

3.1.6 Relative Velocity

Sliding velocity is identified as another important factor. Previous studies have shown that slow ice velocities give rise to viscoelastic deformation and failure properties of ice resulting in high global pressures (Tijsen, 2015). It is also essential that the sliding velocity between the ice and concrete samples is slow enough to avoid melting of the ice sample but fast enough to model realistic interaction scenarios.

The concept apparatus will have the capability of producing a range of abrasion speeds that reflect ice passing rates seen by existing structures. The maximum sea current seen by the Kemi-I lighthouse is 0.1 m/s, while the Confederation Bridge can be subject to currents greater than 1.5 m/s (Brown & Määttänen, 2009). Ice passing rate is generally

linked to water current velocity and unlikely to exceed measured current velocity maxima. Conducting experiments with a range of velocities will determine significance of current on the abrasion process. An additional desirable feature would be the capability to start and stop the abrasion at planned times. This will allow the introduction and control of stick-slip action and adhesion processes.

3.1.7 Testing Temperature and Temperature Control

Many previous researchers made use of a cold room to control the atmospheric temperature with a range varying within -5°C and -20°C (Itoh et al, 1994, Fiorio et al, 2002, Fiorio, 2005, Bekker et al, 2011, Møen et al, 2015 and Tijsen et al, 2015). It is important to note however, that wet sample testing was not used for these experiments. Use of a cold room that is set for sub-zero testing temperatures would freeze any water and prove detrimental to the results.

The proposed solution for wet testing would be a test environment with a temperature around 0 °C. This is in agreement with Sodhi (2001), who noted that pack-ice which floats at the waterline typically exists at a temperature near the melting point. This feature may require that the ice samples be locally cooled in order to prevent sample degradation.

3.1.8 Ice Waste Buildup

Given that the wear of ice and removal of ice during abrasion testing will occur at relatively high rates it has been observed that worn ice can form a protective layer over the concrete and should be removed from the interface for the purposes of long term wear testing. As an example, Møen et al (2015) achieved this by attaching a heated plate to the

concrete sample and making use of the thermal conductivity of the concrete to control the surface temperature and ensure worn ice did not build up. According to Nawwar & Malhotra (1988), submerged and wet concrete and ice interactions prohibit ice layer formation. For that reason, it is expected that there will be negligible amounts of worn ice during the wet experiments. In the case of the dry experimental setup, brushing and air blowing techniques will be evaluated for ice removal options.

3.1.9 Measurements of Abrasion and Material Loss

In previous studies, abrasion has been measured using laser scanning, optical microscopy, and linear variable differential transformers (LVDTs). Advances in optical technology to measure material loss and determine abrasion rates are thought to offer improved options for measuring both the wear and the nature of the interaction. A second approach may be to collect wear material as an indication of material loss. As there was relatively little literature on either of these approaches as applied to concrete wear measurement, these ideas were evaluated as part of the experimental program detailed in the following chapter.

3.1.10 Force Measurements at Abrasive Interface

The issues of friction and wear are commonly dealt with simultaneously and it is generally believed that higher friction forces lead to higher wear (Itoh et al, 1994). For this reason it would be desirable to incorporate the ability to measure both normal force/pressure and the tangential force during testing. This would provide the ability to measure friction force and to calculate the friction coefficient as experimentation proceeded.

3.2 Summary of Design Criteria

Table 3-1 provides a summary of desired design outcomes of the apparatus. These factors are identified in the preceding discussion and are summarized here for convenience. The development of the concept design and the features of that concept are presented in the section following with each aspect of the design tied back to the criteria identified in this table.

Table 3-1: Design Factors

Identified Design Issue	Design Criteria
1. Relative wear rates	Ability to provide a relatively high ice feed rate. Required rate to be determined by subsequent experimentation.
2. Motion mode	Continual movement with minimal start-stop and no reversal of motion.
3. Applied pressure	Applied loads that are consistent with full scale data with a maximum 2 MPa at nominal sample size. Higher pressures available for reduced sample sizes.
4. Wet or dry testing	Wet and dry testing conditions to be accommodated within the design.
5. Ice sample type	Design to be able to accommodate samples of a uniform size/shape but with differing ice types in terms of saline content, grain structure or samples cut from in-situ locations.
6. Relative velocity	Control of sliding velocity within the range of 0-2 m/s.
7. Temperature control	Control of atmospheric temperature.
8. Waste ice interfering with testing	Removal of worn ice from concrete surface to be incorporated into design.
9. Accurate measurement of abrasion/material loss	Collection of wear material to be incorporated into design.
10. Load measurements	Ability to measure normal and tangential forces at the wear interface to be incorporated into the design.

3.3 Concept Design

Based on the criteria developed in the previous section, a number of preliminary concepts were developed to incorporate the desired features and assessed for operational

practicality and ease of use in laboratory and full scale settings. The apparatus finally selected as the preferred option for laboratory testing, makes use of a rotary machine that will continuously revolve a formed concrete sample. A pre-made ice sample will be normally loaded to the side of the concrete sample as it spins. The only necessary pause in testing will be to replace the ice samples as they continue to be worn away. This avoids the issues with direction change and satisfies the second design criteria.

Generating the concrete sample shape required consideration of several factors. The concrete sample must be of circular shape to accommodate the continuously revolving testing concept as used by Nawwar & Malhotra (1988). Additional concerns include adequate aggregate distribution, robustness and portability. To increase the ease of concrete pouring and removal from forms, a truncated cone is proposed. This solution will satisfy the design criteria. As part of design optimization the size and forming may be modified to reduce the material used in the center of the concrete samples, thereby reducing the weight. While dimensions may be further refined, the sample will remain within a size limit that allows easy handling and transportation. Nominal values for the concept design are a 1m bottom diameter with a 45° angle. This was chosen in consideration of overall sample size and positioning of the loading application tools. Figure 3-3 depicts the concept of the preliminary concrete sample shape.

Laboratory grown cylindrical ice samples, with a diameter of approximately 150 mm, will be used to induce wear and should withstand the applied crushing loads.

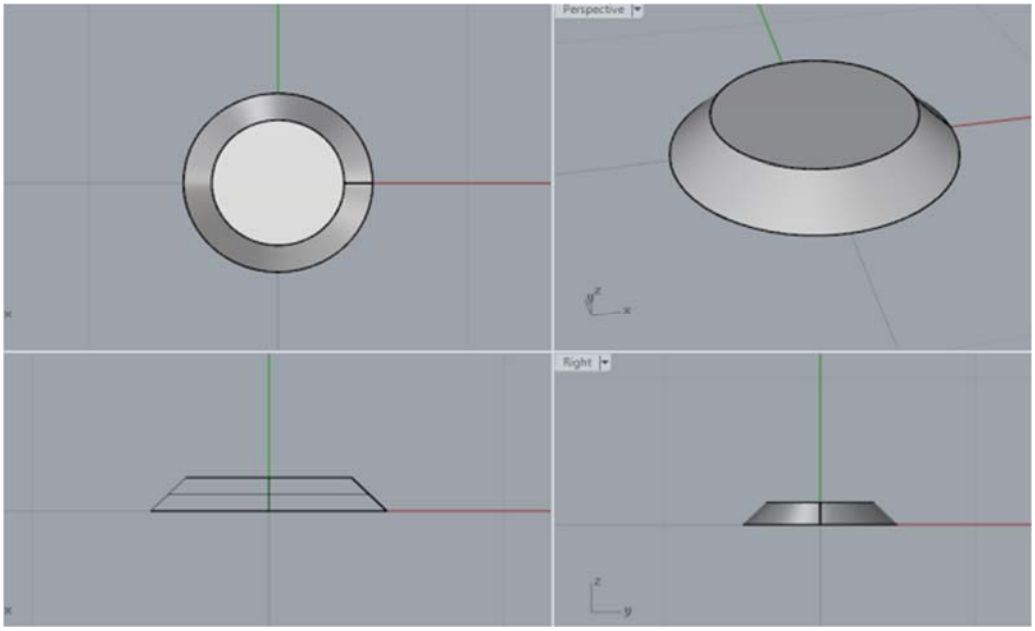

Figure 3-3: Proposed Concrete Sample Shape

In order to satisfy the requirement to allow the experiments to be conducted in an environment where the concrete sample could be dry, semi-submerged or completely submerged in water, a water bath, in which the water level can be easily controlled, is incorporated into the design. Figure 3-4 shows the concept design for positioning of the concrete sample, water bath and supporting frame. This allows testing while varying the depth of submergence of the concrete test samples resulting in a more accurate simulation of full scale interactions. The partial submergence of the concrete will allow the ice load to be applied directly at the waterline level.

A water bath has not previously been used when testing concrete for ice abrasion. Dry testing can also be achieved by simply emptying the water bath. The use of a bath also allows the abraded ice and concrete material to be collected either after or during a test to allow analysis of the rates of material loss in either ice or concrete.

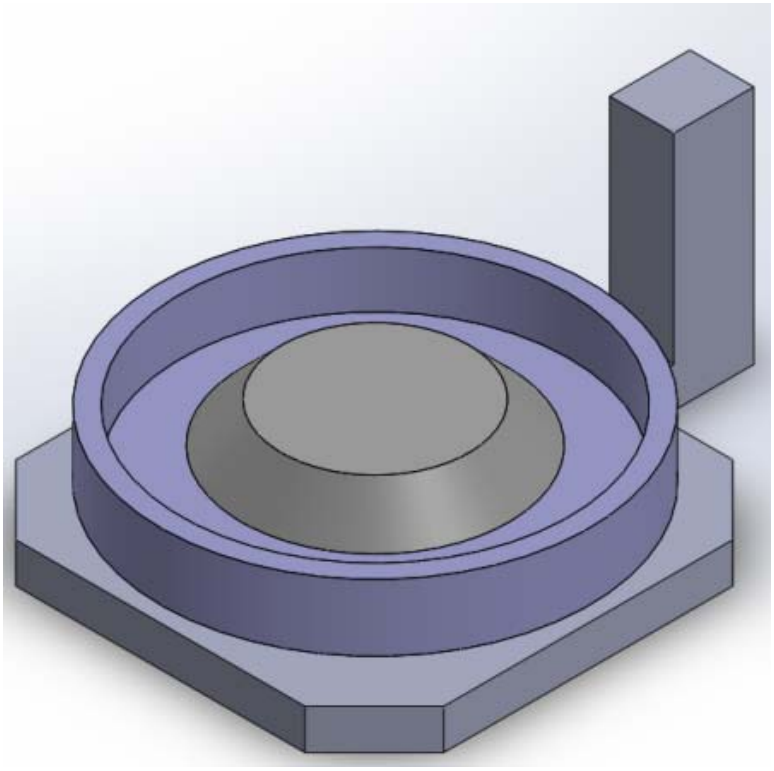

Figure 3-4: Preliminary Setup Layout

In order to develop the required forces applied at the abrasion interface an analysis of the contact and friction forces was carried out based on nominal figures. Figure 3-5 depicts a simplified free body diagram of the dual directional applied forces from the ice floes with respect to the direction the ice is moving. The force is applied as an orthogonal load to the concrete surface; the shear force is taken as a parallel sliding force that acts on the sample. Also shown, are the normal and frictional forces resulting from the ice-concrete interaction.

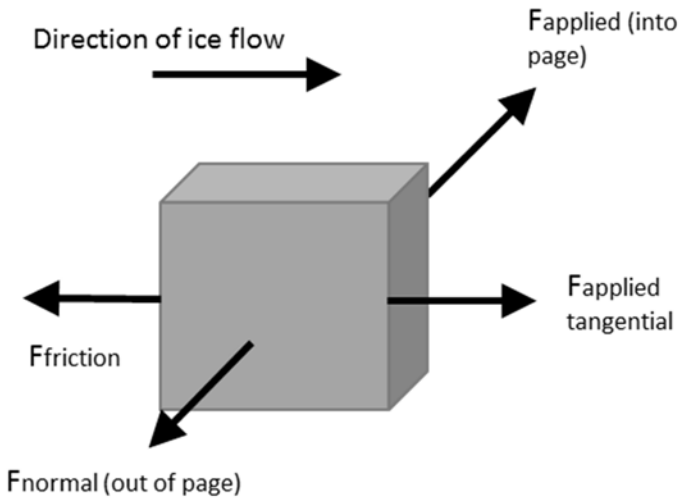

Figure 3-5: Free Body Diagram of Applied Loads

During testing and ice load application, the experimental apparatus must have the capacity to produce sufficient torque to overcome the frictional forces and turn the concrete sample. Furthermore, components, bearings and structure must have sufficient strength to withstand the applied and resultant forces. As can be seen from equations (1) through (4), the required torque (τ) is a function of the concrete sample radius (r_{con}), the frictional coefficient (μ), the applied pressure (P) and the cross-sectional area of the ice sample (A_{ice}). An increase in either of these factors will result in a higher required torque.

$$P = \frac{F_N}{A_{ice}} \therefore F_N = P \cdot A_{ice} \qquad (1)$$

$$F_f = \mu \cdot F_N \qquad (2)$$

$$\tau = r_{con} \cdot F_f \qquad (3)$$

$$\tau = r_{con} \cdot \mu \cdot F_N = r_{con} \cdot \mu \cdot P \cdot A_{ice} \qquad (4)$$

These equations lead to the following design forces at the abrasion interface which are used to size the motors, bearings and structure of the experimental apparatus. This will also determine the required measuring range for the apparatus implemented to measure the applied and frictional forces.

Maximum Normal Force based on 150 mm diameter ice sample:

$$F_N = P \cdot A = 2\ \text{MPa} \cdot \pi \cdot 75\ \text{mm}^2 = 35.3\ \text{kN}$$

Maximum Tangential Force based on a friction coefficient of 0.1:

$$F_f = \mu \cdot F_N = 0.1 \cdot 35.3\ \text{kN} = 3.53\ \text{kN}$$

One of the most important considerations for the proposed experimental setup is the abrasion measurement technique. In the past, abrasion has been measured using laser scanning, optical microscopy, and linear variable differential transformers (LVDTs). The proposed plan, at this point in time, is to make use of optical technology to measure material loss and determine abrasion rates. This aspect is covered further in the experimental section following.

In addition, as shown in Figure 3-6, the ice sample diameter will be smaller than the concrete sample side surface. During testing, the centre area will be abraded while the outer edges can be used as reference points as they will not experience abrasion.

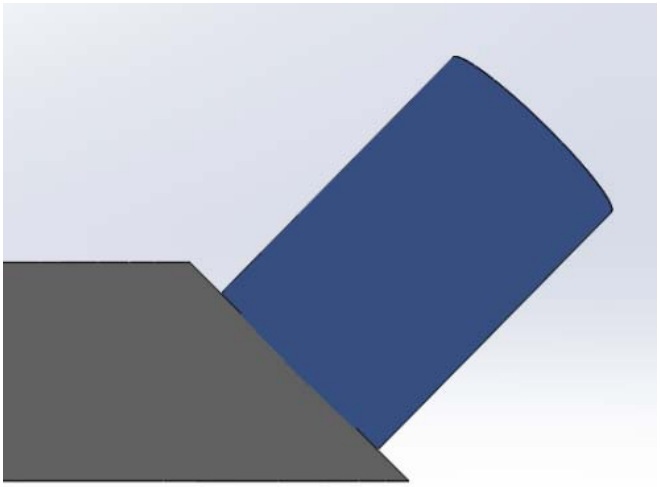

Figure 3-6: Proposed Ice-Concrete Sample Interaction Layout

The testing process for the concept design would proceed as follows: the circular concrete sample will be placed in the water bath and slowly revolve. Laboratory-made ice samples will be formed into cylinders that can be placed and piston loaded onto the side of the concrete. The ice sample will wear away and therefore must be changed periodically. This changing process represents the only break in the continuous loading and the goal will be to minimize the amount of necessary changes.

Concrete abrasion will be induced along the circumference of the concrete samples and the testing will be run for an adequate length of time, such that uniform and consistent results will be attained.

It is expected that as results are obtained, the opportunity will exist to further determine the significance of additional factors that are thought to contribute to abrasion. The water bath will allow further investigation into observing differences between freshwater or saline baths by varying levels of salt concentration in the water, as well as different

temperatures of the setup materials. The tests can be carried out on different mixtures of concrete and with various ice samples. The desired outcomes are to provide more cohesive and complete findings.

Table 3-2 provides a summary of features incorporated into the concept apparatus, with reference to the original design criteria. Additionally, issues that were identified during the concept development that could not be adequately determined from the literature are identified to be evaluated in a series of pilot experiments that are detailed in the following section.

Table 3-2: Design Features and Uncertainties

Identified Design Issue	Design Criteria	Concept Design Features	Issues to be determined in experiments or detailed design stage
1. Relative wear rates	Ability to provide ice at relatively high rates. Required rate to be determined by subsequent experimentation	Pre-made ice sample refills will be readily available	Preliminary experiments to determine rate of ice wear under various pressures
2. Motion mode	Continual movement with minimal start-stop and no reversal of motion	Rotary table and motor with the ability to apply sufficient torque	
3. Applied pressure	Applied loads that are consistent with full scale data with a minimum 2 MPa at nominal sample size and higher pressures available for reduced sample sizes	Hydraulic ram to induce 2 MPa pressure Normal F_{Max} = 35.3 kN* Tangential F_{Max} = 3.53 kN* *based on nominal 150 mm diameter ice samples	
4. Wet or Dry testing	Wet and dry testing conditions to be accommodated within the design	Stainless steel water bath allowing dry, submerged and semi-submerged conditions	
5.Ice sample type	Design to be able to accommodate samples of a uniform size/shape but with differing ice types in terms of saline content, grain structure or samples cut from in-situ locations	Nominal ice sample dimension: 150 mm diameter cylinder	Appropriate lengths to be determined based on experimental program
6. Relative velocity	Control of sliding velocity within the range of 0 to 2 m/s to be translated into a rotary velocity of 0 to 40 RPM	Achieved with off-the-shelf variable speed drive to be sourced as part of detail design	
7. Temperature control	Control of atmospheric temperature	Apparatus to be used in available cold room	Possible consideration of incorporating ice sample cooling into apparatus at detail design stage
8. Waste Ice interfering with testing	Removal of worn ice from concrete surface to be incorporated into design	Modular system, ability to brush away waste ice	Preliminary experiments to determine amount of worn ice to be removed
9. Accurate measurement of abrasion/material loss	Collection of wear material to be incorporated into design	Worn concrete collection incorporated into water bath tray	Preliminary experiments to determine amount of worn concrete produced
10. Load measurements	Ability to measure normal and tangential forces at the wear interface to be incorporated into the design	Normal and tangential load range determined	

Chapter 4 Pilot Experiments for Design Refinement

In order to investigate some of the assumptions made in developing the apparatus and process, and refine the conceptual design, pilot experiments were conducted in the laboratory to gain insight on the ice-concrete interactions. It was desired to conduct experiments that were of similar nature to the concept testing machine. Primarily, the experiments remained consistent with rotating concrete samples and the ability to perform both wet and dry concrete surface testing.

Specific interest was paid to the abrasion process, abraded material from the ice and concrete samples, adhesion of worn ice to the concrete and duration of each ice block during testing, as well as measurement techniques. From conducting the pilot experiments, modifications were made to the conceptual design on the basis of results from the pilot experiments. This will decrease technical uncertainties in the concept design.

The pilot experiments made use of a metal lathe located in the prepping area of the cold room at Memorial University in an effort to use readily available resources in the laboratory. Standard sized 100 x 200 mm concrete cylinders were formed and placed in the lathe chuck for rotation while ice samples were loaded from the top on the rounded concrete side. Figure 4-1 shows the setup of the lathe during testing.

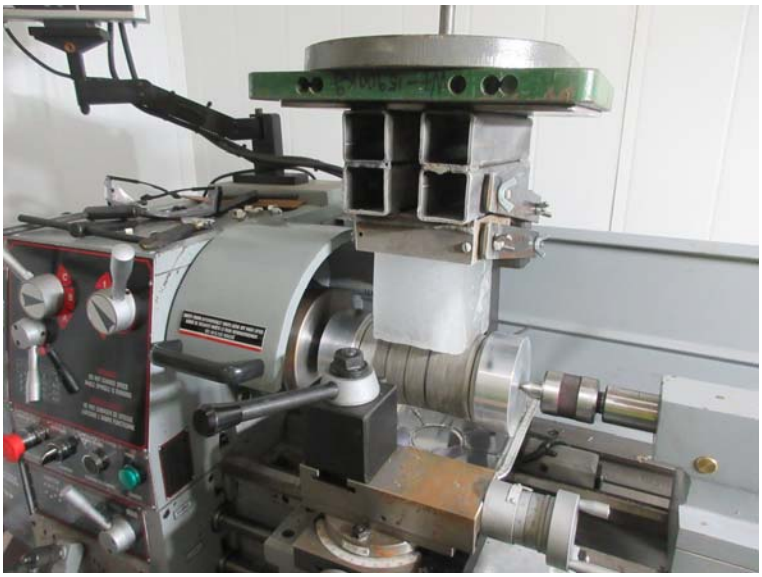

Figure 4-1: Pilot Experiment Setup

4.1 Theory

4.1.1 Rotating Samples

The desired outcome in the conceptual design was to create an experimental setting that allowed long duration and uninterrupted movement between ice and concrete. The solution was to develop a design that allowed continual rotation. Similar outcomes were desired for the pilot experiments. On a smaller scale, rotating a concrete sample interacting with a fixed ice sample would provide valuable information in moving forward and refining the conceptual design. This was achieved by employing the rotary device in a lathe to spin the concrete sample.

With a 100 mm nominal diameter cylinder, a distance of 314.16 mm will be covered with each rotation of the sample.

$$\text{Diameter} = 100 \text{ mm}$$

$$\text{Circumference} = \pi \cdot 100 \text{ mm} = 314.16 \text{ mm}$$

A realistic and achievable testing distance of 10 km is the goal of the experiments. This would require approximately 318301 rotations of the concrete cylinder. The amount of time required to obtain this distance is dependent on the rotational speed of the lathe.

$$\frac{10000 \text{ m}}{0.31416 \text{ m}} \cong 318301 \text{ rotations}$$

4.1.2 Surface Interaction

For the pilot experiments, there will be a continual interaction between a cylindrical concrete sample and an ice sample block. This represents a cylinder-flat plate interaction. However, as time progresses during the tests, the ice will wear away faster than the concrete and the interaction of the two surfaces will change. Theoretically, the initial interaction during the time of minimum surface interaction will produce a line load. Gradually, the interaction area will increase until the point where 50 mm of ice has worn away, see Figure 4-2. At this point, it will have reached a depth equal to the radius of the cylinder.

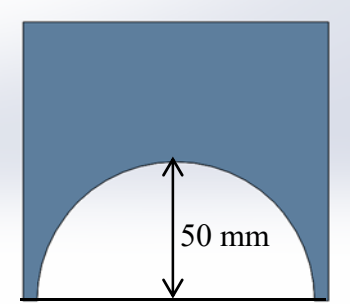

Figure 4-2: Worn Ice Sample

Bottom views of the ice block show the theoretical wearing process of the ice and changing surface interaction with the concrete. Each test will continue until such time that the ice has been worn away and the holder arm risks interfering with the rotating concrete cylinder.

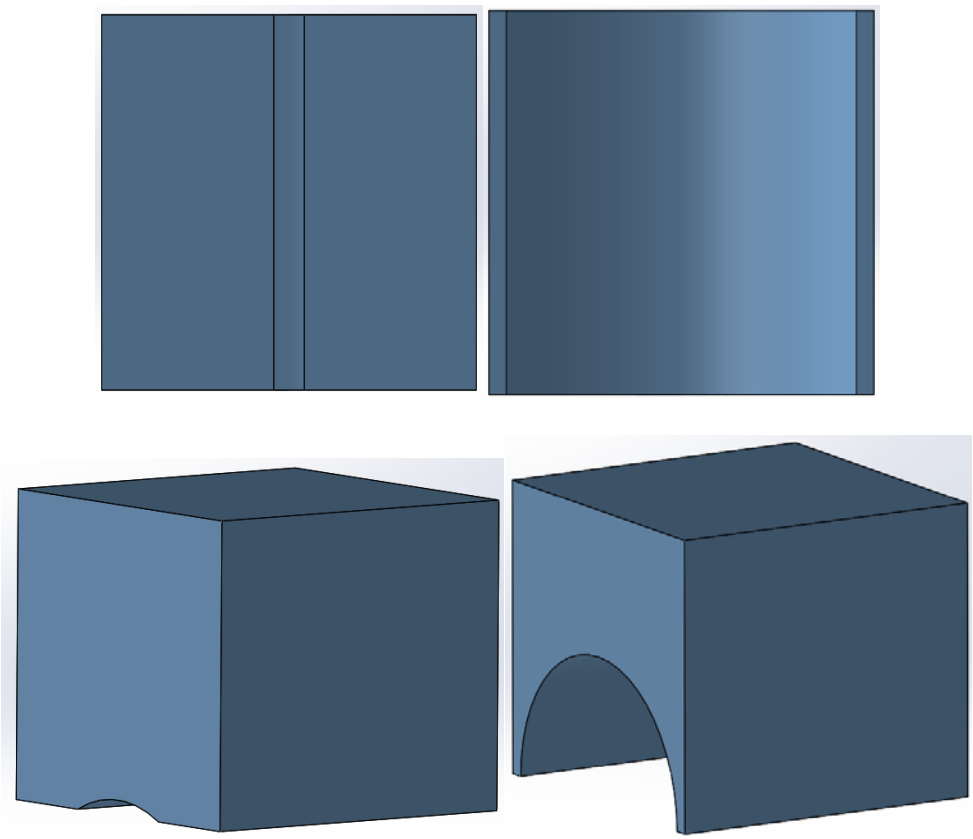

Figure 4-3: Gradual Wear of Ice Sample

4.2 Test Apparatus

The lathe, shown in Figure 4-4, used for the pilot experiments was a King Industrial capable of nine rotation speeds, the lowest being 60 RPM or one rotation per second.

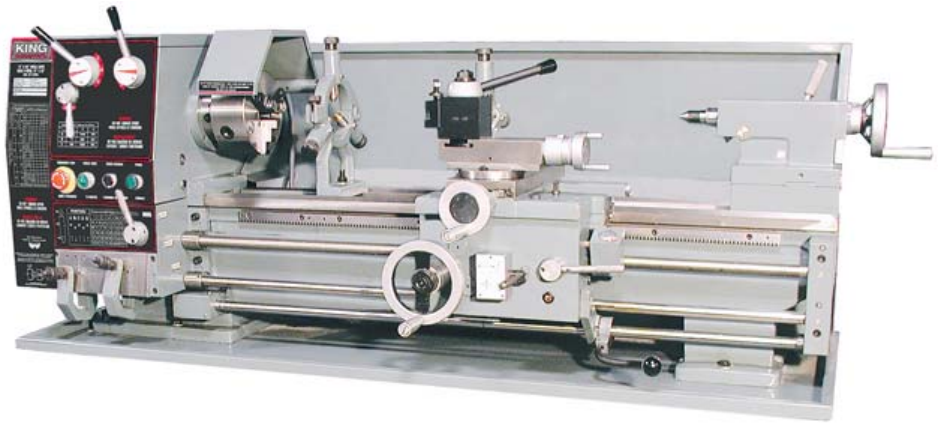

Figure 4-4: King Industrial Lathe (BlackRockTools, 2016)

As is, the lathe was the appropriate size, capable of holding the 100 mm diameter concrete sample in the chuck. Special design and modifications were required to ensure stability and safety during testing and to hold a loaded ice sample in place. Two end caps were machined for the concrete sample and secured on each end of the concrete cylinder using set screws. One cap fit into the chuck of the lathe allowing the teeth to be tightened without the risk of crushing the concrete. The other cap fit into the lathes' centre at the free end of the concrete sample allowing the cylinder to be supported on both ends. Figure 4-5 shows the concrete cylinder with the two endcaps, as well as the loading and supporting forces.

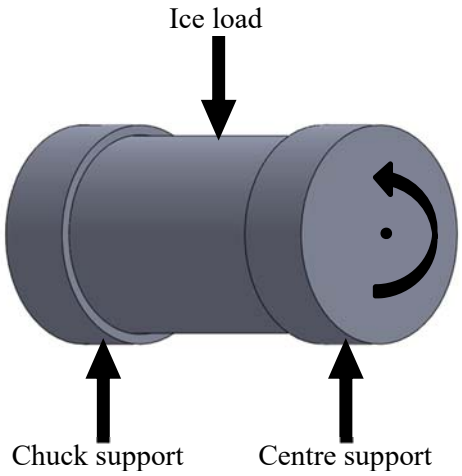

Figure 4-5: End Cap Placements and Supports

An ‘ice holding arm’ was designed to attach to an existing plate that was located on the tool carriage of the lathe, Figure 4-6. This would hold and vertically load a block of ice on to the rotating concrete below.

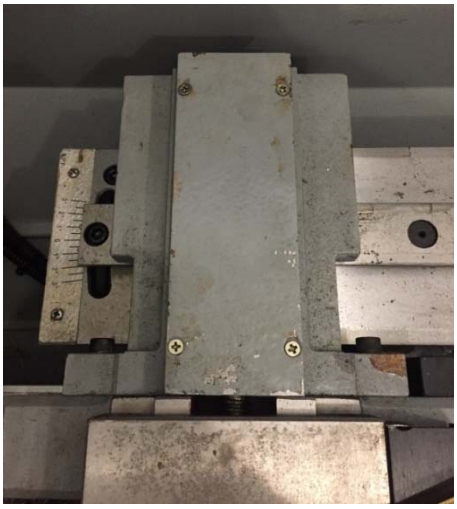

Figure 4-6: Existing Tool Carriage Plate

The design of the arm, shown in Figure 4-7, was an important piece of the experimental setup and involved several considerations as it influenced the ice-concrete interaction.

Special attention was paid to the size and application of load to the concrete. The base plate was designed be able to mate with the existing platform on the lathe. The setup was held in place by using two C-clamps to secure the arm. Weight of the arm was not an issue; it simply added to the constant load that was applied during the experiment.

The design allowed set weights to be placed on top of the arm for the duration of a test, thereby eliminating the need for load cells during testing. The extended section of the arm was capable of holding a 110 mm x 110 mm ice block in place. The arm allowed sufficient swing to accommodate a maximum ice block height up to 150 mm and ranged down to contact with the concrete cylinder positioned in the lathe. The arm was held together using bolts and wing nuts; plastic washers were used to decrease friction in the setup. The wing nuts provided easy adjustment to loosen the crews, allowing the full load to be applied to the concrete.

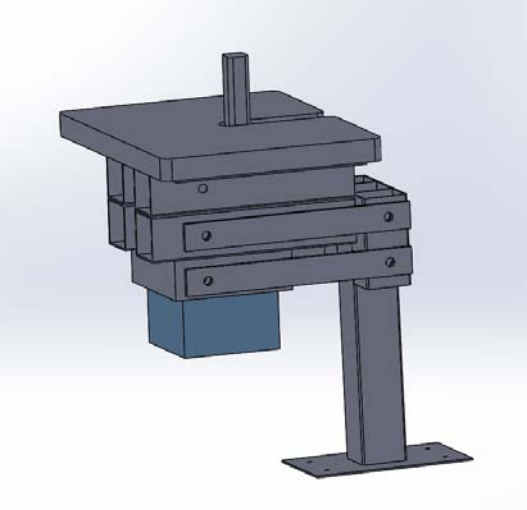

Figure 4-7: Ice Holding Arm Design

4.3 Parameter Validation

4.3.1 Weight Recordings

For the course of this testing program, four weights were used to apply load to the concrete cylinders. These included two rectangular weights (G1 & G2) with a nominal weight of 16 kg and two circular weights (C1 & C2) with a nominal weight of 10 kg. Each exact weight was measured, see Figure 4-8, and summarized in Table 4-1. The weight of the entire arm was also measured for load validation recordings. The weight of the ice was negligible in comparison to the applied load and was consistent for each test.

Figure 4-8: Weight Recording of C2

Table 4-1: Weight Measurements

Green Weight 1 (G1)	15.900 kg
Green Weight 2 (G2)	16.140 kg
Circle Weight 1 (C1)	10.050 kg
Circle Weight 2 (C2)	10.085 kg
Arm Total	15.603 kg

4.3.2 Load Test

Prior to commencing the test programs, load validation tests were completed to determine the applied forces (N) from the ice block to the rotating concrete samples. Tests were completed using a load cell placed at the centre of the arm beneath the weights, see Figure 4-9. Theoretically, a small percentage of the applied load would transfer into the supporting arm, attached to the lathe. The load validation tests provided a value to the load lost to the arm.

A series of load tests were performed at three different arm positions with three different weight combinations: no weight, G1&G2, and all weights. The low position was taken as the lowest possible arm setting before interference with the concrete cylinder. The mid position was taken when the arm was in a horizontal position and the high position was taken as the initial starting height with a fresh ice sample in place.

The readings from the load cell were live recorded using Signal Express software and Data Acquisition (DAQ) system from National Instruments, the data was further analyzed using Excel. A compilation of parameter validation data can be seen in Appendix A: Parameter Validation Data.

Figure 4-9: Load Cell Placement

Each recording for the applied load can be seen at low, mid and high position. Averages of these recordings were taken and a percent difference was calculated to ensure values were consistent. The actual total applied load was then determined so that the average load taken by the supporting arm could be given a value. A sample calculation of the No Weight condition is detailed as follows:

Recorded Average Load:

$$\frac{112.050 + 113.674 + 111.068}{3} = 112.264 \text{ N}$$

Largest Difference:

$$\text{Max} \begin{cases} 112.264 - 112.050 \\ 113.674 - 112.264 \\ 112.264 - 111.068 \end{cases} = 2.607 \text{ N}$$

Percent Difference:

$$\frac{2.607}{112.264} \cdot 100 = 2.322\ \%$$

Total Weight and Load:

$$15.603\ \text{kg} \cdot 9.81\ \text{kgm/s}^2 = 153.065\ \text{N}$$

Load to Arm:

$$153.065\ \text{N} - 112.264\ \text{N} = 40.802\ \text{N}$$

Table 4-2 provides a summary of the load test data.

Table 4-2: Load Test Data Summary

	NO WEIGHT	G1 & G2	ALL WEIGHT
Low Position (N)	112.050	428.234	622.420
Mid Position (N)	113.674	430.602	631.856
High Position (N)	111.068	429.523	630.178
Average (N)	112.264	429.453	628.151
Largest Difference (N)	2.607	2.368	9.436
%Difference (%)	2.322	0.551	1.502
Total Weight (kg)	15.603	47.643	67.778
Total Load (N)	153.065	467.378	664.902
Load to Arm (N)	40.802	37.925	36.751
Average Load to Arm (N)	38.492		

4.3.3 Tachometer Test

The lathe was set to the slowest RPM setting which, according to the machine settings, corresponded to 60 RPM. However, upon validation of this value using a tachometer, the actual recorded value ranged from 84.8-84.9 RPM. Due to the discrepancy between the expected and recorded RPM value, the rotational speed was recorded for every test to

ensure a fixed parameter. Converting this value to a sliding velocity is calculated as follows:

$$85\text{RPM} \cdot 314.16\text{ mm} = 26703.60\text{ mm/min}$$

$$\frac{26703.60\text{ mm}}{\text{min}} \cdot \frac{1\text{ m}}{1000\text{ mm}} \cdot \frac{1\text{ min}}{60\text{ s}} = 0.445\text{ m/s}$$

This speed lies within an acceptable and realistic range as discussed in previous chapters.

4.3.4 Temperature Collection

For the completion of the pilot experiments, precautions were in place to ensure consistencies in temperature. The experiments were completed in a cold room during maintenance shutdown. Installed temperature gauges on the room provided continual readings of the room temperature. The concrete cylinders, ice blocks and ice holding arm were stored in various refrigerators and freezers to maintain consistent temperatures from test to test. Table 4-3 provides a summary of the range and average temperatures collected during the course of testing.

Table 4-3: Temperature Collection Summary

	Minimum	Maximum	Average
Room Temp (°C)	-10.0 & 15.0	26.0	18.6
Concrete Temp (°C)	-2.0	3.6	2.1
Ice Temp (°C)	-15.4	-9.6	-12.6
Arm Temp (°C)	-18.1	-12.9	-15.7

It is important to note that room temperature was not controllable. Typically, the temperature remained within the range of 15-26 °C, however there was one test that was completed while the cold room was functioning, lowering the temperature to -10 °C. The

concrete and ice samples were maintained in a small temperature range that was deemed appropriate from the literature review. Freezer storage of the ice holding arm helped reduce the melting of the ice sample.

4.4 Sample Preparation

4.4.1 Ice Samples

Freshwater ice was decided upon for these experiments. This was chosen as reproducibility was much easier and the ice is stronger than saline ice. This provides worst case scenario interactions between the concrete and ice.

The ice preparation process was based on the methodology detailed by Bruneau et al (2013). Fresh ice was passed through a chipping machine to achieve uniform ice grains before being added to de-aerated, deionized and distilled fresh water. This produced a consistent mix and decreased the required freezing time. Seen in Figure 4-10, the ice chip-water mixture was arranged in a stainless steel bucket that was hung in a freezer using a specially made holder. The mixture was stirred as more ice and water were added to ensure uniformity. The bucket was insulated around the sides, with the exception of the bottom. This setup induced directional freezing from bottom to top allowing any remaining air to escape from the top and reducing the risk of internal cracking of the ice during freezing.

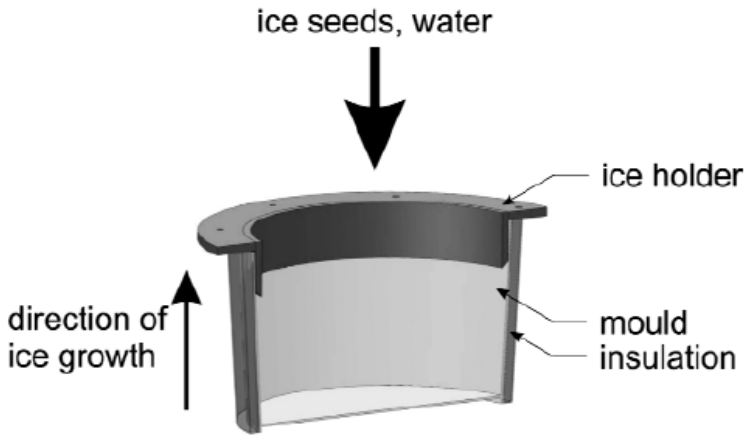

Figure 4-10: Ice Preparation Schematic (Bruneau et al, 2013)

Once completely frozen, the samples were removed from the molds by rubbing a cool, wet cloth over the outer surface of the steel bucket until the ice released itself. The cylinder of ice was then cut to the desired size using a band saw. Ice sample size measured 110 mm x 110 mm to fit in the arm with a height ranging from 110 mm - 130 mm. Figure 4-11 shows some pictures documenting the ice preparation process.

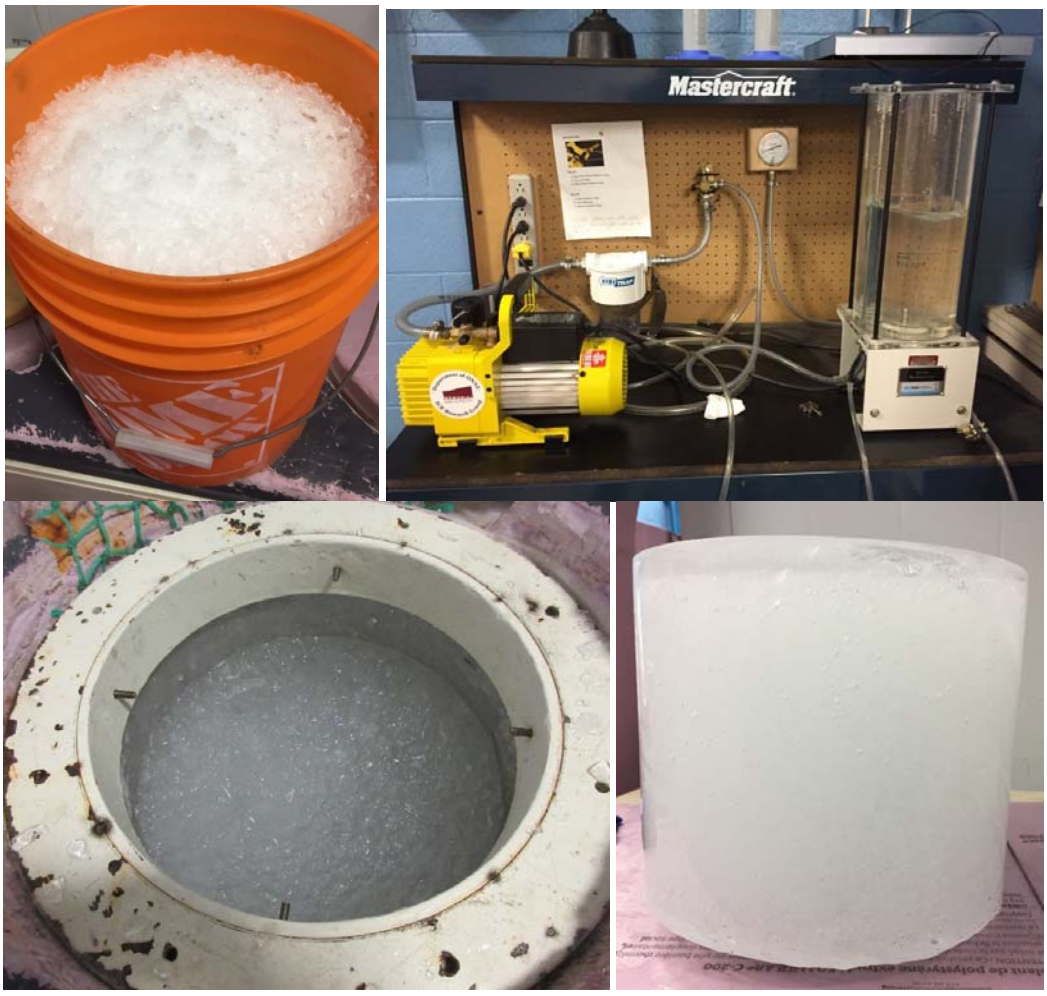

Figure 4-11: Ice Preparation Process

(top left: ice that has passed through the chipper, top right: distilled water in the deaeration process, bottom left: ice chips and water mixed in the bucket, bottom right: a frozen sample removed and ready to be cut)

Polarized images of thin sections taken from the fabricated ice samples provide insight into the internal structure of the ice. Specific attention is paid to orientation, size and distribution of the ice crystals (Bruneau et al, 2015). The thin section of ice is arranged on a glass plate and is placed in a viewer that uses polarizers to show the individual crystals. Figure 4-12 shows the uniform grain size and distribution seen in the sample ice sections.

As well, the range of colours indicates varied orientation of the crystals. These visuals reveal a homogeneous mixture confirming the desired ice type for the pilot experiments.

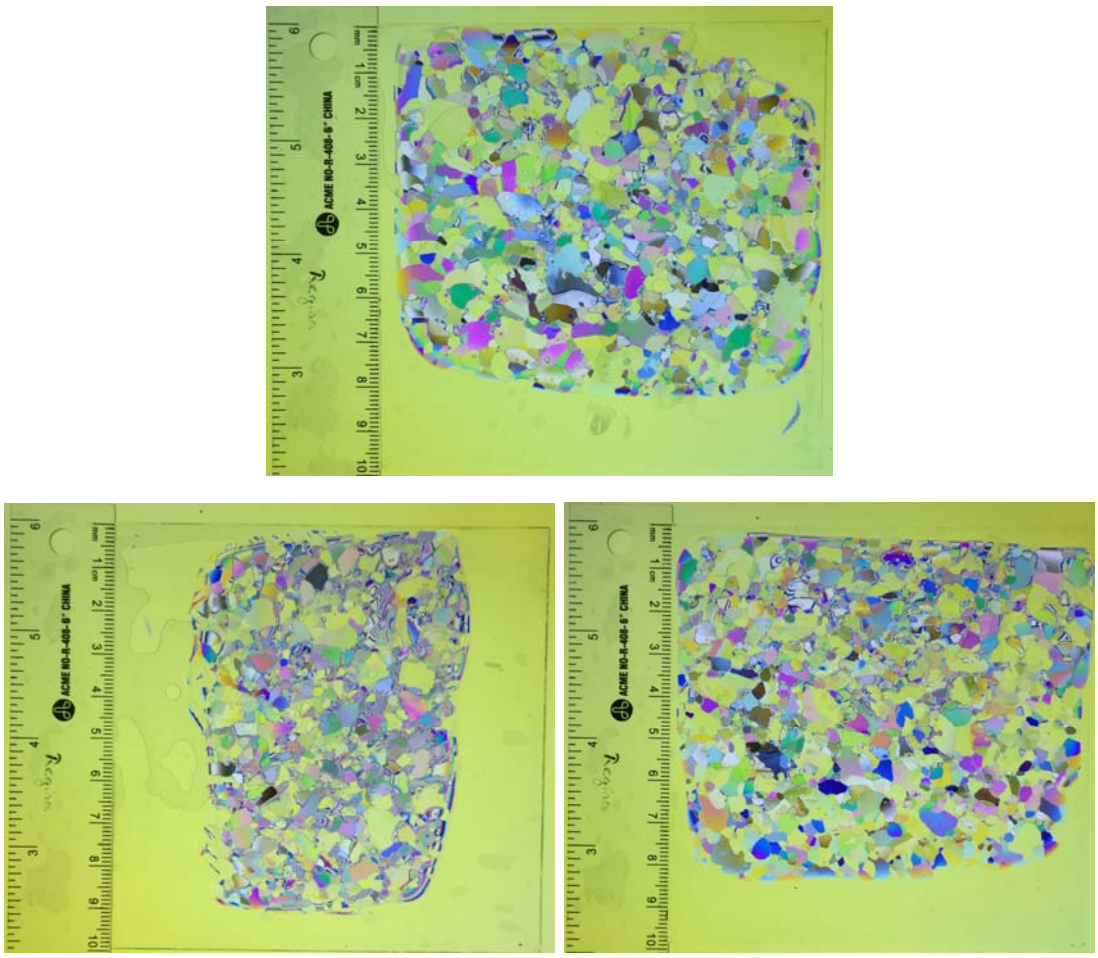

Figure 4-12: Polarized Ice Thin Sections

4.4.2 Concrete Samples

For these experiments, three concrete mix designs were used. This was an easily controlled factor and would provide insight into the interactions of ice with both high and low performance concrete grades.

Two of the mixes, 1 and 2, were designed to mimic concrete mix designs used in previous ice abrasion experiments at Memorial by a former graduate student. This allowed for

comparisons between current and previous abrasion test results, additionally the required materials were readily available. The mix designs for Mix 1 and Mix 2 are based on Mix I and Mix II as summarized in Table 4-4. Mix I is considered high performance due to its high compressive strength, silica fume content and a lower W/B ratio. According to Tijsen (2015), Mix II has higher aggregate content and should reach a stable abrasion rate in less time (Tijsen, 2015). The additional mix seen in Table 4-4 is shown as a reference mix from industry.

Table 4-4: Previously Studied Mix Designs (Tijsen, 2015)

	Mix I (High perform.)	Mix II (Low perform.)	PA-B C60/70 (Kvaerner)
Component			
Air volume	3 – 5%	3 – 5%	4 – 6%
SCM	8%	0%	
Binder	500	300	
C/F	1.2	1.2	
W/B	0.33	0.5	0.37
Absorption	0.01	0.01	
Cement	(460)	(300)	(454)
Portland cement	460	300	-
Norcem standard cement	-	-	227
Norcem Anlegg cement	-	-	227
SF	40	0	5.5%
C.A (8 – 16 mm)	952.09	1070.39	879
F.A (0 – 8 mm)	793.41	891.99	783
W	165	150	
TW	182.46	169.62	

In addition to these two mixes, a third design, Mix 3, representing a very weak, commonly found concrete mix with no additives was tested. This type of mix is frequently used in small coastal projects including slipways, sidewalks, etc. Including this mix in the experiments provided a more complete indication of the effect of concrete mix

and its recommended usages. Table 4-5 provides a complete summary of the concrete mixes used in the pilot experiments.

Table 4-5: Concrete Mix Summary

Component	Mix 1 (High Performance)	Mix 2 (Mid Performance)	Mix 3 (Low Performance)
Air Volume	3-5%	3-5%	-
SCM	8%	0%	0%
Binder	500	300	200
C/F	1.2	1.2	1.2
W/B	0.33	0.5	0.7
Absorption	0.01	0.01	-
Cement	460	300	200
Silica Fume	40	0	0
C. Agg.	952.09	1070.39	1150.1
F. Agg (<10mm)	763.41	891.99	958.4
Water	165.22	150	-
Total Water	182.46	169.62	146.1

Each mix was prepared and formed in standard 100 mm diameter x 200 mm high cylinders. This size was easily replicated and provided appropriate dimensions to fit in the lathe for testing. All materials were weighed, combined and evenly mixed before being poured into the individual cylindrical forms. The preparation process can be seen in Figure 4-13.

Figure 4-13: Concrete Sample Preparation

(top left: weighing the mix ingredients, top right: mixing process, bottom: each mix poured into the cylinder forms)

Six companion cylinders of each mix were poured. This allowed for four cylinders of each mix to be used in abrasion testing. In addition, destructive compression tests, Figure 4-14, were completed to determine the compressive strength and supplement the obtained abrasion test results. The results of the compression strength testing can be seen in Table 4-6.

Figure 4-14: Compressive Strength Testing

Table 4-6: Compressive Strength Results

	Mix 1 (High)	Mix 2 (Mid)	Mix 3 (Low)
Test 1 (MPa)	75.23	36.07	17.77
Test 2 (MPa)	70.04	35.17	16.35
Average f'c	72.64	35.62	17.06

The results were consistent with the compressive strengths obtained by Tijsen (2015), where recorded values of f'_c were 73.0 MPa and 40.7 MPa for MixI and MixII, respectively.

4.5 Measurement Techniques

Various measurement techniques were employed to determine the degree of abrasion for each test. Some of these methods were completed as a trial to see if meaningful and measurable results could be obtained.

4.5.1 Visual Markings and Pictures

For documentation purposes and visual observation, before and after pictures were taken of each cylinder. The samples were marked into quarters along the length of the cylinder, as well as three markings along the central circumference. The three central markings were in the interaction zone with the ice for the duration of each test. The goal of the markings and the pictures was to provide qualitative recordings of the wearing process. Figure 4-15 shows sample markings on the concrete prior to any testing.

Figure 4-15: Cylinder Markings Prior to Testing

4.5.2 Loss of Material

Collection of the abraded concrete material was desired for multiple purposes. From a quantitative perspective, collection of debris would provide measurement of actual amount of material loss from the concrete samples. However, in addition, debris collection would provide insight into the type of material lost, ranging from cement paste up to fine and coarse aggregate. For each round of testing, a pre-weighed tray was placed

below the spinning concrete and collected worn debris and melt water. The trays were then placed in a drying oven and once dry, weighed again. This method allowed measurement of the weight of lost material and visual insight into the progression of concrete abrasion. Figure 4-16 shows the placement of the aluminum tray in below the concrete and ice, as well as sample trays to be weighed after drying in the oven.

Figure 4-16: Debris Collection

(left: tray in place to collect debris and meltwater, right: trays in drying oven)

4.5.3 Diameter Measurements

Across the circumferential markings on each cylinder, three cross-sectional diameter measurements were recorded using a Mitutoyo Digimatic Micrometer. Diameter measurements were taken throughout the course of testing, in an effort to show a decreasing diameter as more abrasion testing continued.

4.5.4 3D Scanning

3D scanning of each cylinder was completed using a FARO Platinum Arm with a Laser Line Probe. Approximately 1 inch thick scans were taken down the length of the cylinder at each marked quarter, thereby providing a detailed surface topography depiction. The scans were completed prior to any abrasion testing and the files can be viewed and analyzed using CAD software. The goal is that upon completion of the testing program; the cylinders will be rescanned and will show measurable loss of material, change in surface elevations and distinct abrasion markings. Figure 4-17 shows the cradle setup that held the cylinder in place as the FARO Platinum Arm was used by a technician to complete the scans.

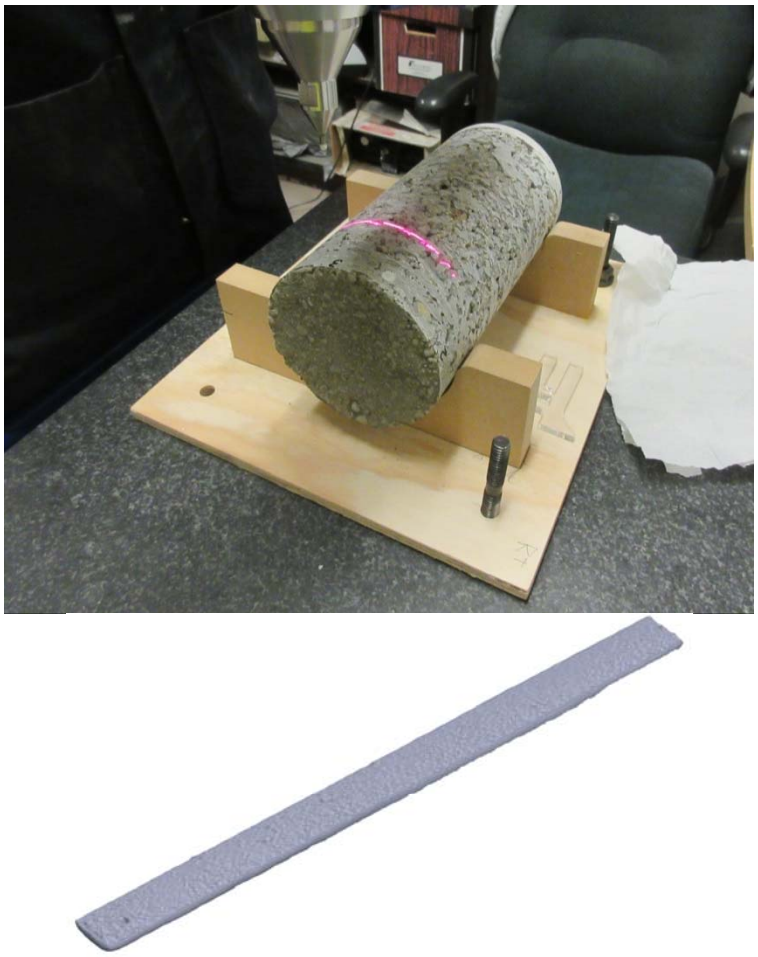

Figure 4-17: 3D Scanning Setup (top) and Sample Scan (bottom)

4.6 Testing Procedure

Testing commenced once all the preparation work was complete. This included parameter validation, sample preparation, pre-testing measurements and apparatus design. Initial tests were completed using one cylinder of each concrete mix, this refined the testing process. The test program was based on time, with each program consisting of 6 hours for each mix type. This resulted in around 9.5 km of testing, which was close to the target distance of 10 km. The testing was broken down into four different test programs and

each test program was further broken down into test rounds. Nomenclature for the concrete cylinders was based on mix type and cylinder number, Sample Mix#-Cylinder#. As an example, the first tested cylinder of Mix1 was named Sample 1-1. Due to time constraints and limited availability of space in the cold room, Test Program 3 and 4 were reduced to only perform tests on the mid performance concrete. The refined and finalized test matrix is shown in Table 4-7.

Table 4-7: Test Matrix

Test Program	Samples	Air Temperature	Applied Load	Duration	Length	Status
1	1-1/2-1/3-1	Room	369 N	6 hrs	9.5 km	Complete
2	1-2/2-2*/3-2	Room	527 N	6 hrs	9.5 km	Complete
3	2-2*	Room	527 N	6 hrs	9.5 km	Complete
4	2-3	Room	626 N	6 hrs	9.5 km	Complete
Standard	1-4/2-4/3-4	Completed as per concrete abrasion standard				Not started

*Sample 2-2 was tested for a total of 12 hrs at 527 N

4.6.1 Test Program 1

A concrete sample from each mix was used in Test Program 1 (TP1), Sample 1-1, 2-1 and 3-1. Half of the available weight was used for the first series of experiments; this included a 16 kg and 10 kg weight, as well as the weight of the arm itself. The exact weights are listed in Table 4-8.

Table 4-8: TP1 Weights

Green Weight 1 (G1)	15.900 kg
Circle Weight 1 (C1)	10.050 kg
Arm Total	15.603 kg

The following calculations detail the applied load to the rotating concrete cylinder, accounting for the load taken by the supporting arm, determined in Table 4-2.

Total Weight:

$$15.900 \text{ k g} + 10.050 \text{ kg} + 15.603 \text{ kg} = 41.553 \text{ kg}$$

Applied Load:

$$41.553 \text{ kg} \cdot 9.81 \text{ kgm/s}^2 = 407.635 \text{ N}$$

Adjusted Load (including loss to arm):

$$407.635 \text{ N} - 38.492 \text{ N} = 369.143 \text{ N}$$

For each cylinder, 1-1, 2-1 and 3-1, this load was held constant through multiple rounds of testing until 6 hours of testing was reached.

4.6.2 Test Program 2

Test Program 2 (TP2) used three untouched samples of each concrete mix, 1-2, 2-2 and 3-2. For this program, another 16 kg weight was added to the arm. The applied weights are listed in Table 4-9, followed by the calculations for adjusted load.

Table 4-9: TP2 Weights

Green Weight 1 (G1)	15.900 kg
Green Weight 2 (G2)	16.140 kg
Circle Weight 1 (C1)	10.050 kg
Arm Total	15.603 kg

Total Weight:

$$15.900 \text{ kg} + 16.140 \text{ kg} + 10.050 \text{ kg} + 15.603 \text{ kg} = 57.693 \text{ kg}$$

Applied Load:

$$57.693 \text{ kg} \cdot 9.81 \text{ kgm/s}^2 = 565.968 \text{ N}$$

Adjusted Load (including loss to arm):

$$565.968 \text{ N} - 38.492 \text{ N} = 527.476 \text{ N}$$

As with TP1, through multiple rounds each sample underwent 6 hours of testing at this load.

4.6.3 Test Program 3

Test Program 3 (TP3) was an extension of TP2, the exact loading was applied as seen above in Table 4-9. After the completion of TP1 and TP2, there was an interest in observing the results of even longer testing. Sample 2-2 was selected, as it was the mid-performance concrete mix, and subjected to another six hours of abrasion testing.

4.6.4 Test Program 4

Mix 2 was again the only mix used in Test Program 4 (TP4) due to it being the middle ground between Mix 1 and 3. Sample 2-3 was tested under the heaviest load of the experiments; the second 10 kg load was added to the arm. Table 4-10 details the list of weights, followed by the calculation for adjusted load.

Table 4-10: TP4 Weights

Green Weight 1 (G1)	15.900 kg
Green Weight 2 (G2)	16.140 kg
Circle Weight 1 (C1)	10.050 kg
Circle Weight 2 (C2)	10.085 kg
Arm Total	15.603 kg

Total Weight:

$$15.900 \text{ kg} + 16.140 \text{ kg} + 10.050 \text{ kg} + 10.085 \text{ kg} + 15.603 \text{ kg} = 67.778 \text{ kg}$$

Applied Load:

$$67.778 \text{ kg} \cdot 9.81 \text{ kgm/s}^2 = 664.902 \text{ N}$$

Adjusted Load (including loss to arm):

$$664.902 \text{ N} - 38.492 \text{ N} = 626.410 \text{ N}$$

Sample 2-3 was tested for six hours under this loading.

4.6.5 Pressure Distribution

The three loads from the various test programs, 369 N, 527 N and 626 N, can be used to determine estimates of applied pressure as the ice sample progressively wears. Pressures here are calculated under idealized wear conditions and do not represent the exact applied pressures during testing. However, it effectively demonstrates how the applied pressure decreases as the ice wears down. The areas used for the pressure distribution shown in Figure 4-18 assumes the ice dimension in one direction remains 110 mm and the other increases from a line load (5 mm) to half the concrete diameter (50 mm). It is clear that as the ice wears away and conforms to the shape of the concrete, the interaction area becomes larger and therefore decreases the pressure.

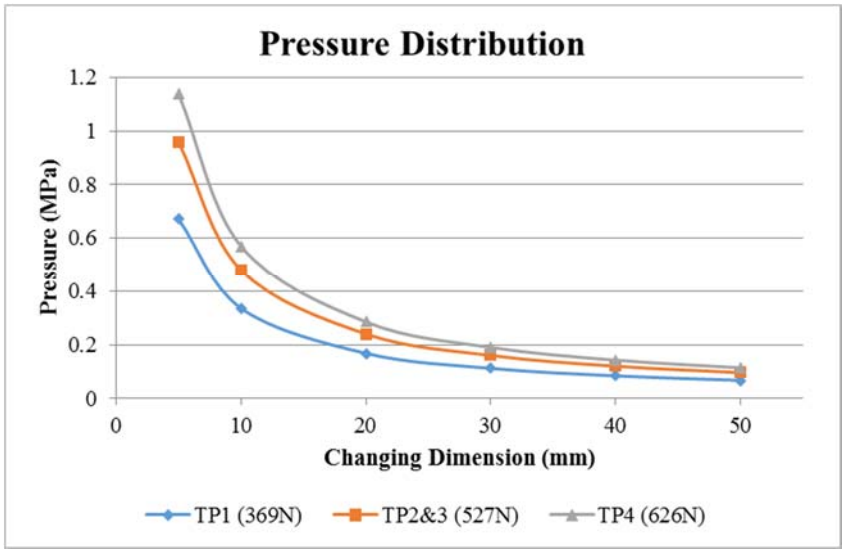

Figure 4-18: Pressure Distribution

4.7 Results

A summary of the results of all completed test programs is provided in Table 4-11. A more detailed analysis of each result is provided in the following sections. The lower average room/air temperature during TP1 test on 1-1 was due to the temperature change noted above in the previous section on temperature collection. Of note, an ice failure during the first testing program shortened the test time by 5 minutes. The test duration distance (km) was based on a nominal cross-sectional diameter of 100 mm for all cylinders.

Table 4-11: Test Results Summary

	TP1			TP2		TP3	TP2	TP4
Sample	1-1	2-1	3-1	1-2	2-2		3-2	2-3
Avg RPM	84.8	84.9	84.8	84.9	84.8	84.9	84.9	84.8
Avg Room Temp (°C)	3.5	20.6	19.3	15.3	16.7	25.3	23.8	24.5
Avg Concrete Temp (°C)	2.3	2.0	3.5	0.7	2.4	1.2	1.2	3.3
Avg Ice Temp (°C)	-12.0	-13.6	-15.4	-11.7	-16.1	-10.2	-11.8	-9.8
Avg Arm Temp (°C)	-16.2	-16.2	-16.2	-16.2	-16.2	-16.2	-16.2	-16.2
Adjusted Load (N)	369.14	369.14	369.14	527.48	527.48	527.48	527.48	626.41
Test Duration (mins)	355	355	355	360	360	360	360	360
Test Duration (km)	9.46	9.46	9.46	9.60	9.59	9.60	9.60	9.59
Total Material Lost (g)	1.4	3.0	8.6	5.0	2.6	2.2	6.5	3.8

4.8 Analysis

Provided in this section is a closer look at the collected data, trends in recordings, results of measurement techniques and an overall summary of the abrasion process. Each section will offer insight into the completed testing and provide lessons learned in moving forward. A complete collection of all raw data is included in Appendix B: Raw Data Sheets.

4.8.1 Sample Duration

One of the goals of the pilot experiments was to gain insight into the duration ability of the ice samples when testing is not being done in a controlled cold room. As addressed, previously completed testing has often been completed at -10 ºC. However, due to the proposed inclusion of a water bath, ambient temperatures around 0 ºC are required. The shaped ice blocks were cut to 110 mm x 110 mm with a hanging height typically ranging

from 85 mm to 105 mm. Hanging height, as shown in the cross-section in Figure 4-19, is defined as the dimension of the ice sample that hangs below the holder.

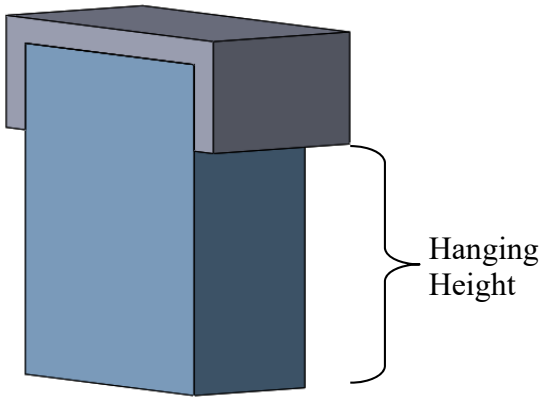

Figure 4-19: Cross-section of Ice Holder and Sample

Completion of the first few rounds of testing in TP1 showed that 2 hours was a reasonable target time to reach for each ice block sample. Surpassing 2 hours proved to have multiple risks, the primary one being interference of the ice holder with the spinning concrete. If the hanging height had been increased to allow more time, there was a risk that the catch tray would overflow and also would have resulted in a more unsteady testing arrangement on the concrete. Table 4-12 provides a summary of collected data from each Test Program including hanging height of the ice sample, test duration of each round and air temperature at the time of testing.

Table 4-12: Sample Duration Summary

TEST PROGRAM 1 LOAD: 369N

	1-1		2-1			3-1			
Hanging (mm)	90	95	105	105	100	40	95	85	100
Duration	1hr55mins	4hrs	1hr55mins	2hrs	2hrs	20mins	1hr35mins	2hrs	2hrs
Minutes	115	240	115	120	120	20	95	120	120
Air Temp (°C)	17	-10	19.1	20.6	22	21.3	17	17	22

TEST PROGRAM 2 LOAD: 527N

	1-2			2-2			3-2			
Hanging (mm)	100	100	100	95	85	95	90	100	100	100
Duration	1hr55mins	2hrs5mins	2hrs	2hrs	2hrs	2hrs	1hr30mins	1hr50mins	1hr30mins	1hr10mins
Minutes	115	125	120	120	120	120	90	110	90	70
Air Temp (°C)	16	15	15	16	19	15	24	24	23	24

TEST PROGRAM 3 LOAD: 527N

	2-2			
Hanging (mm)	100	100	100	100
Duration	1hr45mins	1hr25mins	1hr35mins	1hr15mins
Minutes	105	85	95	75
Air Temp (°C)	26	25	25	25

TEST PROGRAM 4 LOAD: 626N

	2-3			
Hanging (mm)	100	100	100	100
Duration	1hr10mins	1hr40mins	1hr40mins	1hr30mins
Minutes	70	100	100	90
Air Temp (°C)	26	24	24	24

There are two outliers in this series of data; the first can be seen in TP1, Sample 1-1, Round 2. Four hours of testing was able to be completed in one round due to the room temperature being -10 ºC. At this temperature, the ice wear was much less and the testing could have continued on for longer, however 6 hours of testing had already been reached. The second is the small ice block with a hanging height of 40 mm that was used in TP1, Sample 3-1, Round 1 for a short 20-minute test.

The two major factors considered here when comparing sample durations were applied load and room temperature. Mix type would also be a factor as the rougher concrete surfaces can wear the ice down faster. Figure 4-20 provides a compiled graph of all ice sample duration data, minus the two outlying conditions noted above. The line marking

120 minutes represents the target two hours for each round of testing. It can be seen by the circled data points that in higher temperatures, greater than 22 ºC, the ice samples did not reach the target time. The samples wore away and melted before two hours could be reached.

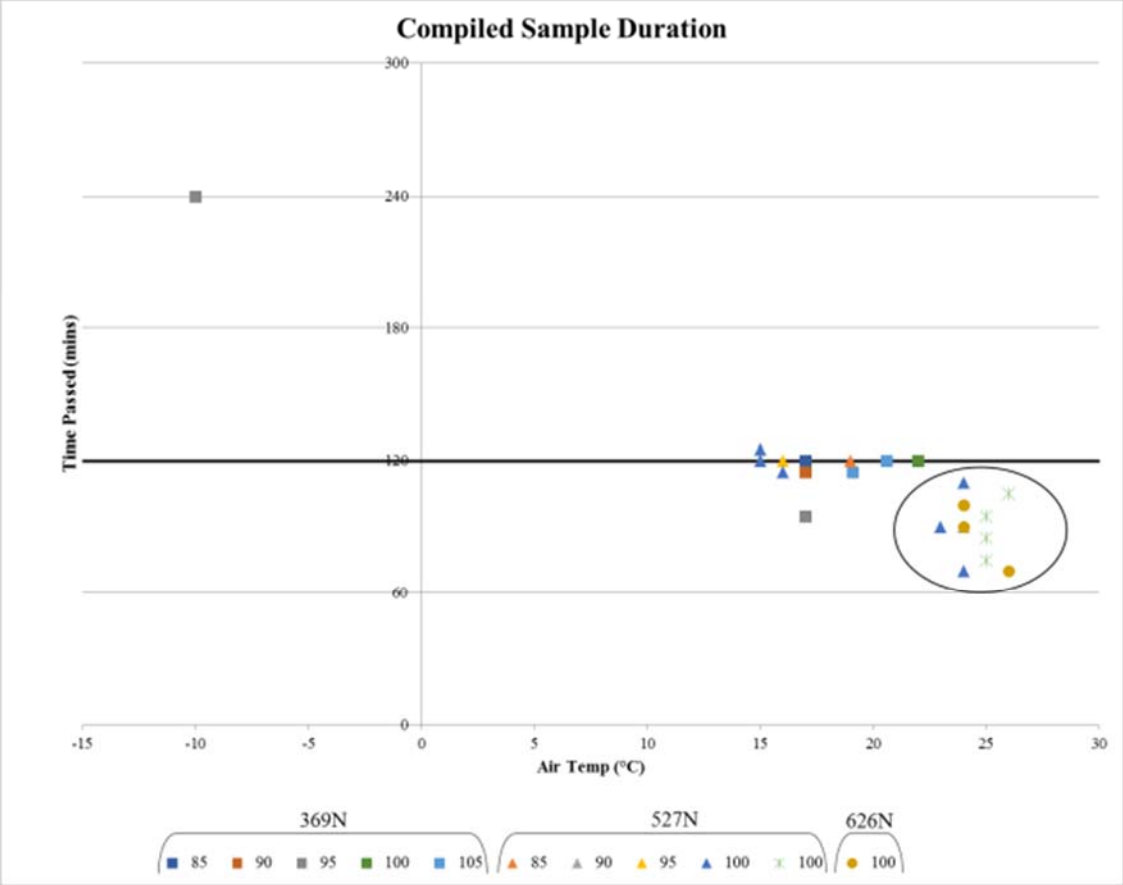

Figure 4-20: Sample Duration Data

In cooler air temperatures, for these small scale experiments, two hours was a feasible target. The conceptual design, as outlined in the previous chapter, will be able to perform experiments in controlled ambient temperatures ranging from 0-5 ºC. At this temperature, larger ice samples will be able to continue testing for more than two hours, thereby further decreasing the need to pause experiments.

4.8.2 Visual Markings and Pictures

The markings on the concrete cylinders provided perspective into the surface wear of the concrete as well as spatial awareness of prominent voids, aggregates and features of the concrete. The ice block remained in contact with the three circumferential markings, thereby creating a consistent interaction area. Additionally, those three markings were reference points for diameter measurements.

Figure 4-21 shows sample before and after pictures of each concrete mix. Comparisons of Mix1 pictures show wear on the markings and enlargement of existing voids in the concrete surface. Worn debris can be seen stuck to the surface of the after pictures of Mix1. Similarly, Mix2 after pictures show a loss of cement paste on the surface, exposing voids in the concrete. As expected, Mix3 had the most significant change in markings, as they are barely visible in the after picture. The pictures and markings show the consistent trend that is loss of cement paste and void enlargement and exposure. More pictures of before and after markings of each cylinder can be seen in Appendix C: Concrete Sample Pictures.

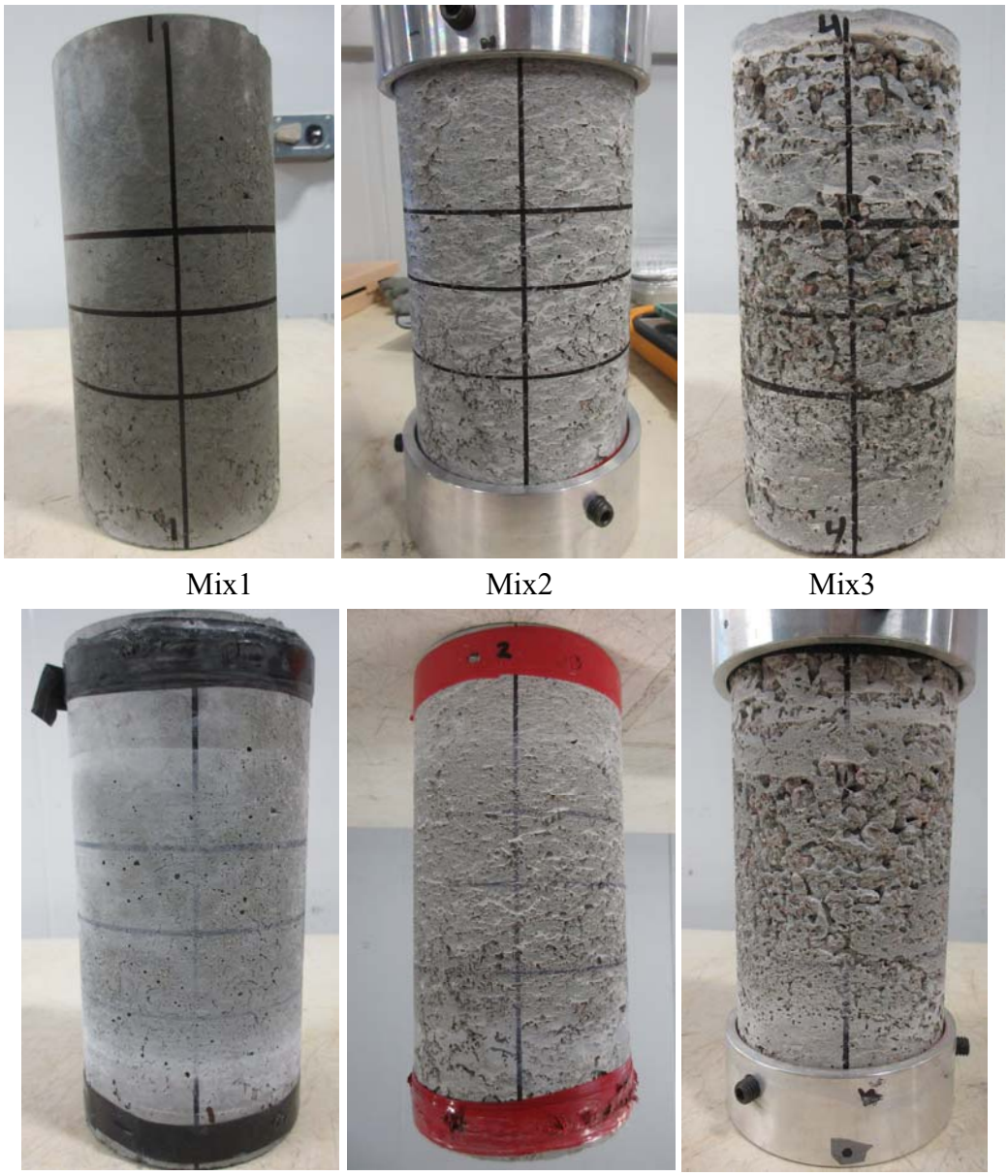

Figure 4-21: Before (top) and After (bottom) Markings

Pictures were also valuable in documenting specific observations that were of interest throughout the experiments. A close look at a sample of Mix3 after testing shows an accumulation of ice within the concrete voids, Figure 4-22. This could potentially serve as protection to the concrete by coating the concrete and smoothing the surface.

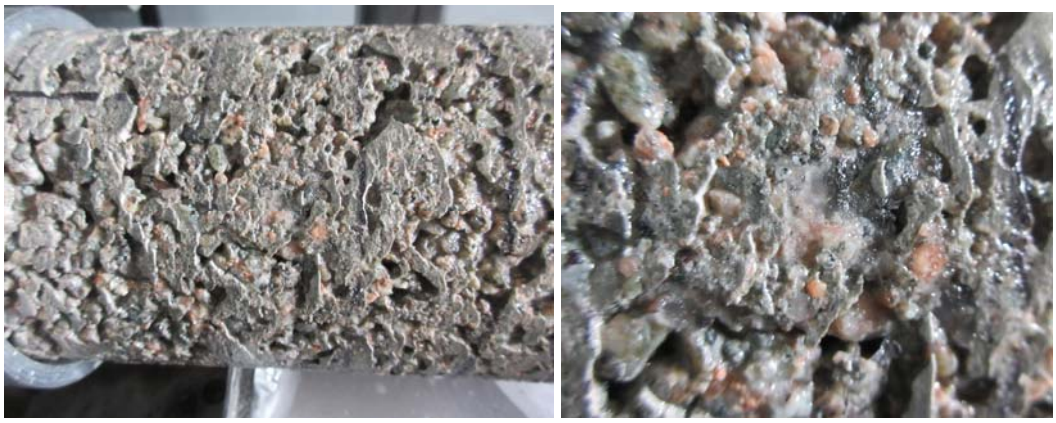

Figure 4-22: Ice Collection in Voids

Figure 4-23 shows a picture of the concrete cylinder that underwent testing in the -10 ºC room condition. Cement paste was worn from the surface as typically seen; however it remained frozen to the concrete cylinder as opposed to melting into the catch tray. Again, this was of interest as it forms a protective layer over the concrete.

Figure 4-23: Frozen Cement Paste

4.8.3 Loss of Material

Quantifying the actual amount of debris loss was an important outcome of the pilot experiments. Additionally, collection allows investigation and observation of the most

vulnerable worn material. Table 4-13 provides a tabulated summary of all the weighed material lost for each round of testing and a combined total. The testing time, given in minutes, is cumulative.

Table 4-13: Summary of Debris Lost

TEST PROGRAM 1 LOAD: 369N

	1-1		2-1			3-1			
Time (mins)	115	355	115	235	355	20	115	235	355
Debris Lost (g)	1.3	0.1	1.6	0.8	0.6	-	6.7	0.9	1.0
Total Lost (g)	1.4		3.0			8.6			

TEST PROGRAM 2 LOAD: 527N

	1-2			2-2			3-2			
Time (mins)	115	240	360	120	240	360	90	200	290	360
Debris Lost (g)	3.1	1.0	0.9	1.2	0.7	0.7	3.2	1.7	1.0	0.6
Total Lost (g)	5.0			2.6			6.5			

TEST PROGRAM 3 LOAD: 527N

	2-2			
Time (mins)	465	550	645	720
Debris Lost (g)	0.9	0.7	0.3	0.3
Total Lost (g)	2.2			

2-2 Total Lost
4.8 g

TEST PROGRAM 4 LOAD: 626N

	2-3			
Time (mins)	70	170	270	360
Debris Lost (g)	1.5	1.1	0.7	0.5
Total Lost (g)	3.8			

Throughout the experiments, it was consistently seen that the highest amount of debris loss occurred during the first two hours of testing. The most vulnerable material that was worn away first was the cement paste. Losing the cement paste resulted in a rougher concrete surface. However, as the rounds of testing continued, the amount of collected material decreased. This is in agreement with previously completed research by Tijsen (2015). The now exposed aggregate has a higher abrasion resistance than the cement

paste and therefore stabilizes the amount of material lost (Tijsen, 2015). Figure 4-24 shows a comparison of the dried debris collected from Sample 1-2 after round 1 (1-2rd1) and round 2 (1-2rd2) of testing. The tray 1-2rd1 contains a larger amount of worn material than seen in 1-2rd2; this is obvious from visual observation. Quantitatively, 3.1 g of material was worn after round 1 whereas only 1 g of material was lost during round 2.

It is important to note, as previously discussed, though the load remains constant throughout each test, the applied pressure decreases due to the increasing interaction area as the ice wears. This decrease in pressure could be a factor in the decreased material loss over time.

Figure 4-24: Round 1 and Round 2 Debris Collections

Further proof of the higher abrasion resistance of aggregate, in comparison to surface cement paste, can be seen by plotting the amount of debris lost over time. Figure 4-25 shows for each tested cylinder the amount of material loss decreases as testing time continues. General wear, as defined by Fiorio et al (2002), occurred during the pilot experiments. It is expected, as with previous research, that as the abrasion process

continues, the aggregates will loosen and eventually become plucked from the concrete, an indication of catastrophic wear.

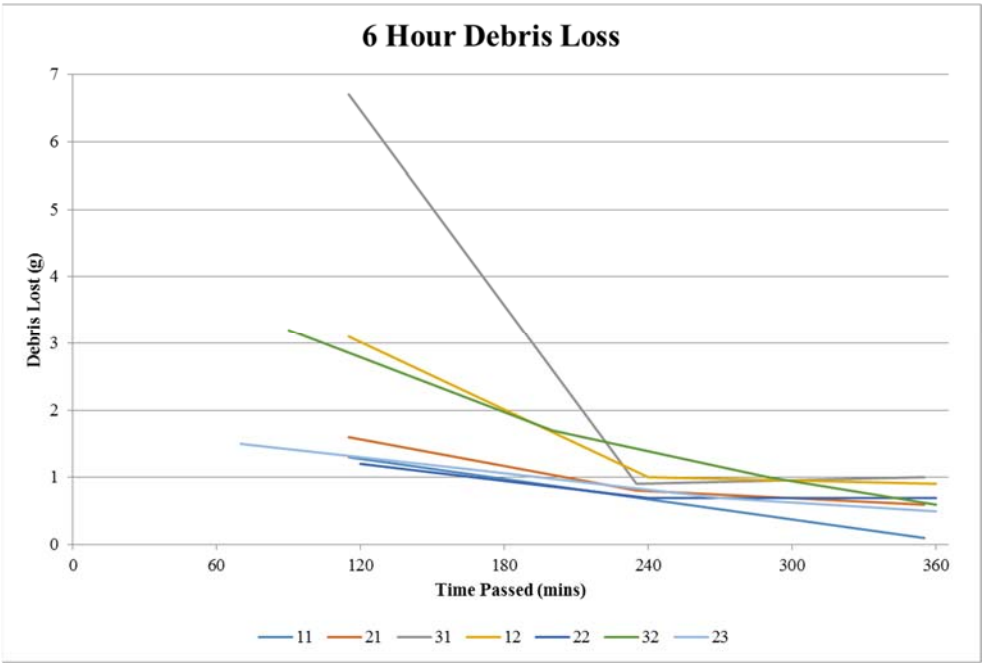

Figure 4-25: Debris Loss over 6 hours of Testing

The graph shown in Figure 4-26 provides a valuable summary and comparison of the material loss in the pilot experiments. Interesting observations can be taken from this data by breaking the graph down by mix type. The numbers shown on the bars indicate total material lost for each test program as seen listed in Table 4-13.

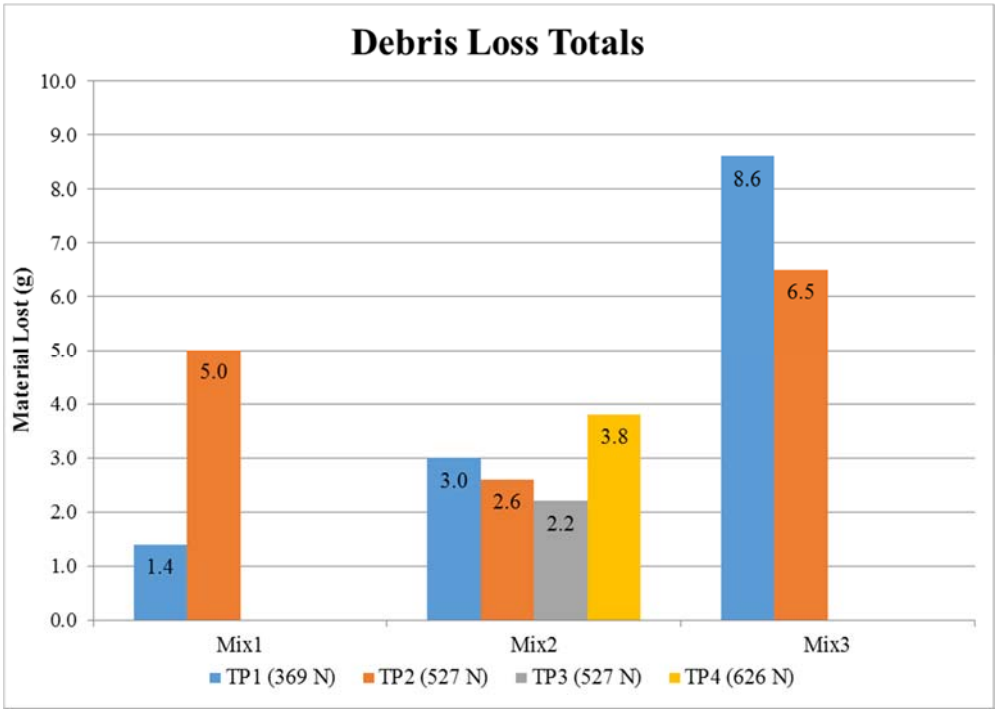

Figure 4-26: Debris Loss Totals

Mix1:

Material lost in TP1 at a load of 369 N is not an indicative measurement that can be compared with the other debris collections from the experiments due to the temperature difference. As with the other tests, the cement paste was the first to wear away, however, due to the -10 ºC room temperature the abraded cement paste froze onto the concrete surface effectively creating a protective barrier between the ice and concrete. As expected, the material loss in TP2 was much higher than seen in TP1, shown in Figure 4-27.

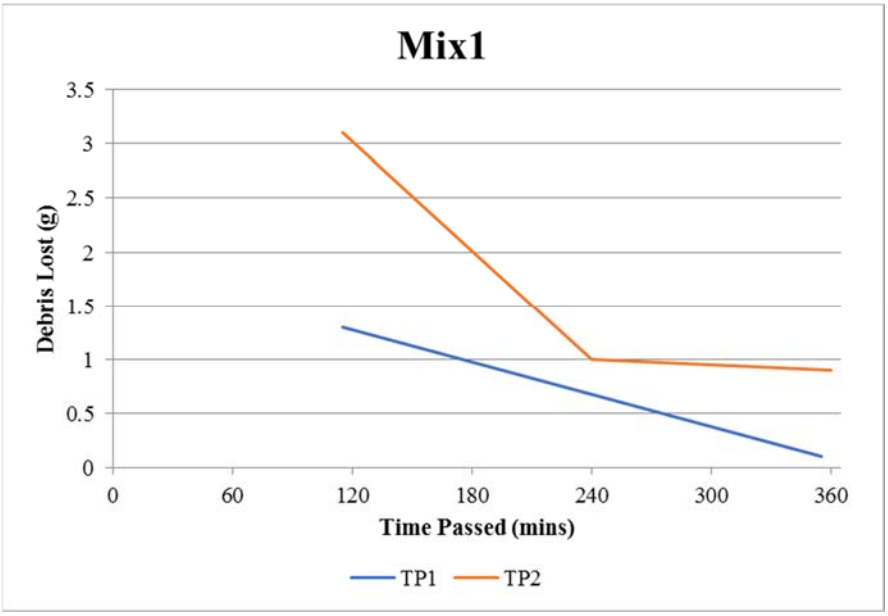

Figure 4-27: Material Loss of Mix1

Mix2:

Mix2, as the mid performance concrete, underwent the most testing of all the mixes and had the most consistent material loss over the various test programs, see Figure 4-28. There were two unexpected results from the testing, the first being that more material was worn away under the 369 N load than from the 527 N load. Further testing would provide more data and confirm these results. The second unexpected result was that more material loss was seen from the high performance Mix1 sample than Mix2 in TP2. A possible explanation for the reduced material loss seen from the Mix2 cylinders is that the mix design had a smoother surface finish, partly due to a higher water-cement ratio. While this reduced the compressive strength of the concrete, the surface of the concrete was much smoother due to the extra water. In terms of expected results, abrasion rate stabilization was seen and the amount of material loss decreased as TP2 continued into TP3 for an

additional 6 hours of testing. TP4, with a load of 626 N, resulted in the largest material loss experienced by a cylinder from Mix2.

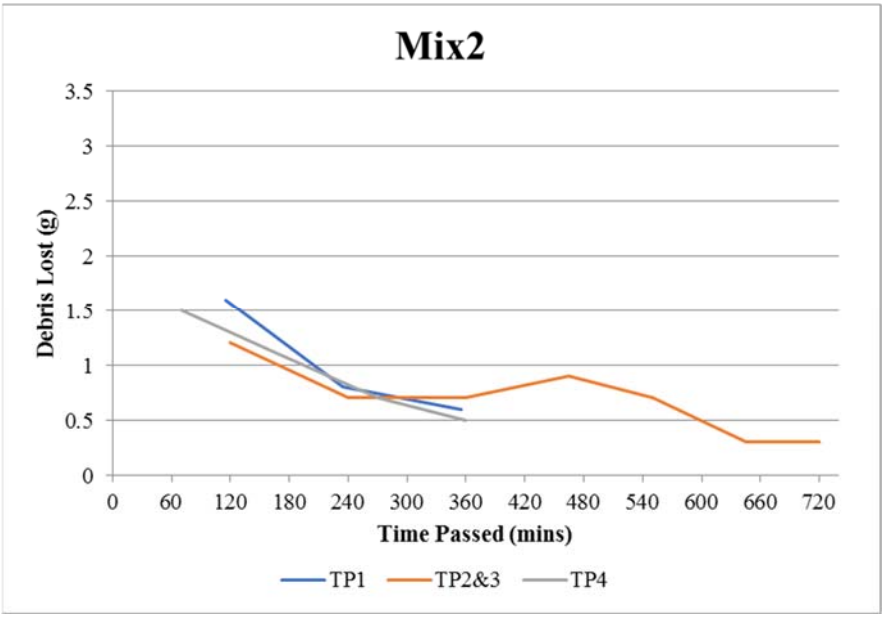

Figure 4-28: Material Loss of Mix2

Mix3:

Figure 4-29 shows that in both TP1 and TP2, Mix3 had the largest collection of debris in comparison to Mix1 and Mix2. As it was the low performance mix, this was an expected result. Again, as seen with Mix2, more material was abraded during TP1 than TP2 which was not an anticipated outcome. More testing and observation of this measurement technique would provide insight into any procedural and experimental errors and the significance of these results.

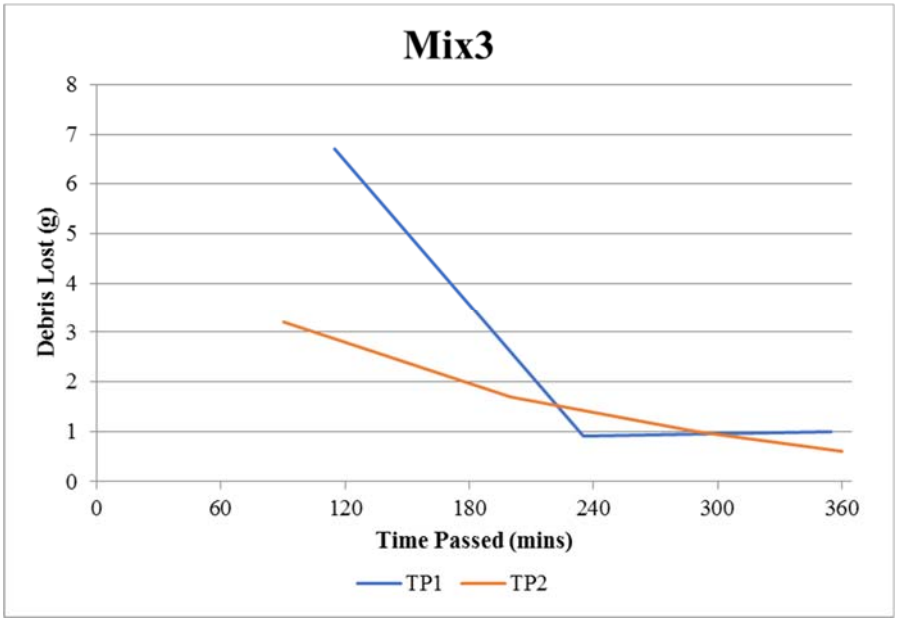

Figure 4-29: Material Loss of Mix3

4.8.4 Diameter Change

Diameters were recorded at three points along each of the samples on the marked gridlines. Recordings were taken before and after each round of testing. As the ice melted during a round of testing, the ice sample would shift in the holder. The ice loaded on the concrete was placed to ensure interaction at the measured points throughout the test; however improvements could be made to hold the ice in a more secure position.

Unfortunately, the outcomes of these measurements were varied and the data was inconclusive to specific and tangible results. There was significant experimental error when taking measurements as it was difficult to place the micrometer on the exact same points each time. The difference in diameter between rounds of testing was so small that any error is very significant. At times, little to no change was seen if the micrometer measurement point was located on the exposed aggregate, acting as a high point. Additionally, some measurements show a larger after diameter, which is not an accurate

result. This could be due to a slightly different micrometer position, or small pieces of abraded debris on the concrete surface which interfere with the readings.

In general, there was a trend indicating a small decrease in diameter, representing the loss of cement paste and some finer aggregate. However, it was not a reliable measurement technique for these experiments.

Cylinders from Mix2 are reviewed in this analysis; Figure 4-30 shows the varying diameter results for each test program. Loss values recorded in red show an increase in diameter after testing. A full summary of the measurements can be found in Appendix D: Diameter Change Graphs.

TP1

2-1	Before	After	Loss
	100.209	100.143	0.066
	100.433	100.290	0.143
	100.607	100.526	0.081

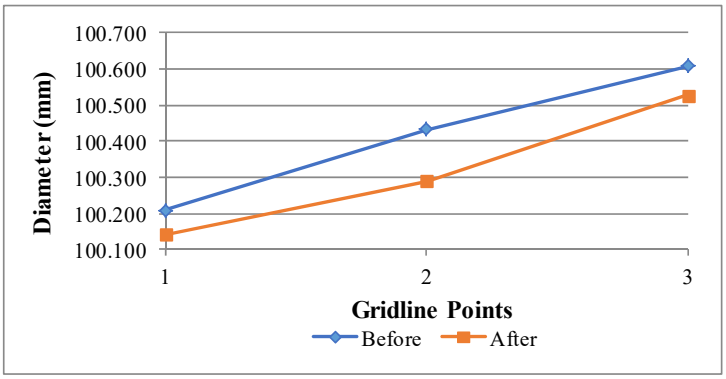

TP2

2-2	Before	After	Loss
	100.105	99.969	0.136
	99.968	99.996	-0.028
	99.986	100.156	-0.170

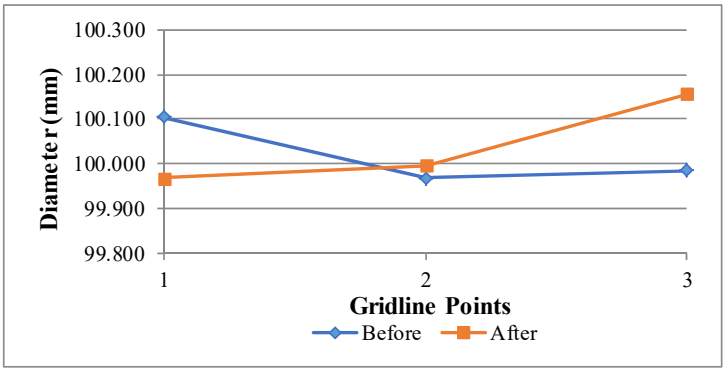

TP3

2-2	Before	After	Loss
	99.969	99.848	0.121
	99.996	99.962	0.034
	100.156	100.107	0.049

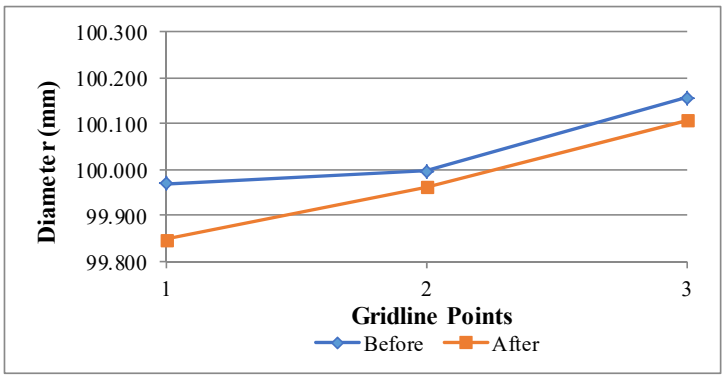

TP4

2-3	Before	After	Loss
	100.206	100.172	0.034
	100.091	100.045	0.046
	99.966	99.898	0.068

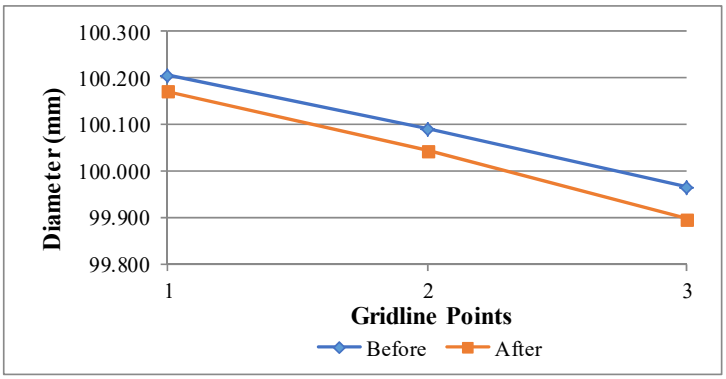

Figure 4-30: Mix2 Changes in Diameter

Taking a look at average decrease in diameter for each mix type, Figure 4-31, shows that Mix2 had the lowest average diameter change. This is consistent with the result seen in debris lost and could be due to the smoother surface finish. Expectedly, Mix3 had the largest average diameter changes. As the rougher surface was abraded quickly fine aggregate became looser much quicker.

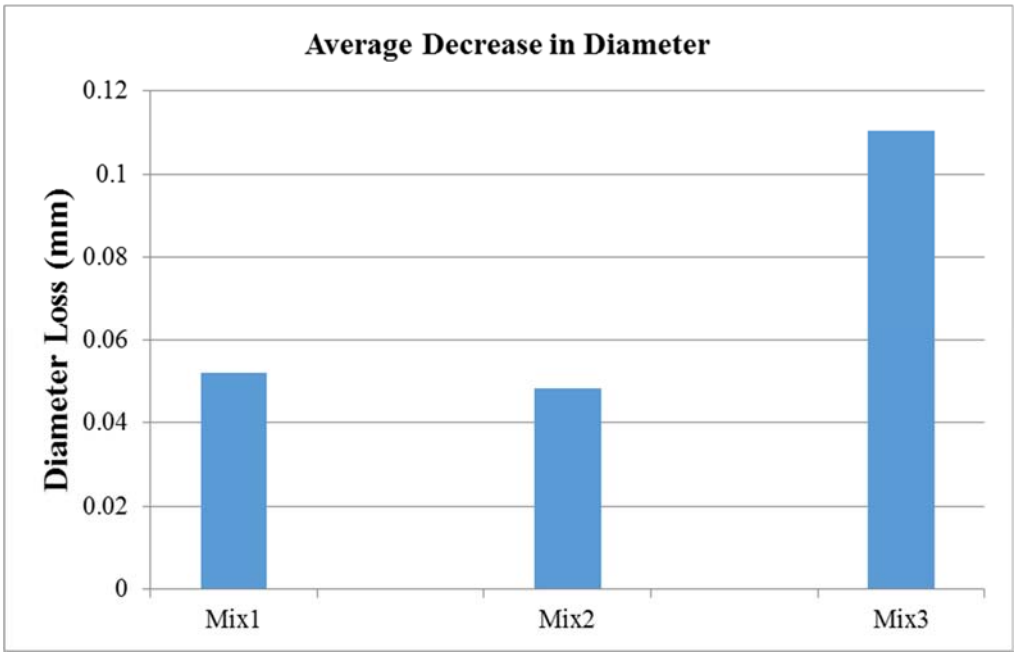

Figure 4-31: Average Decrease in Diameter

4.8.5 3D Scanning

Upon completion of the testing plans, the concrete cylinders were rescanned. Geomagic Design Software was used to superimpose the before and after scans. Figure 4-32 shows a sample of the overlay of the two scans of Mix3 cylinder 3-2. The green strip was taken before and the surrounding blue shows the concrete surface, after testing.

The visible green that is shown in the bottom picture is indicative of material lost during the testing process; thereby providing a qualitative view of ice abrasion effects. In

addition to loss of material, the scans provide a clear view of changes in surface roughness. This is valuable information, as the other abrasion measurement strategies showed the significant impact surface roughness had on the amount of material loss. Quantitatively, it is also possible to analyze the images and the changing elevation points on the surface to provide an estimate of the volume of material loss; however the accuracy of this estimate is unknown. Unfortunately, the FARO Platinum Arm required servicing and further scans and investigation into this measurement method were halted.

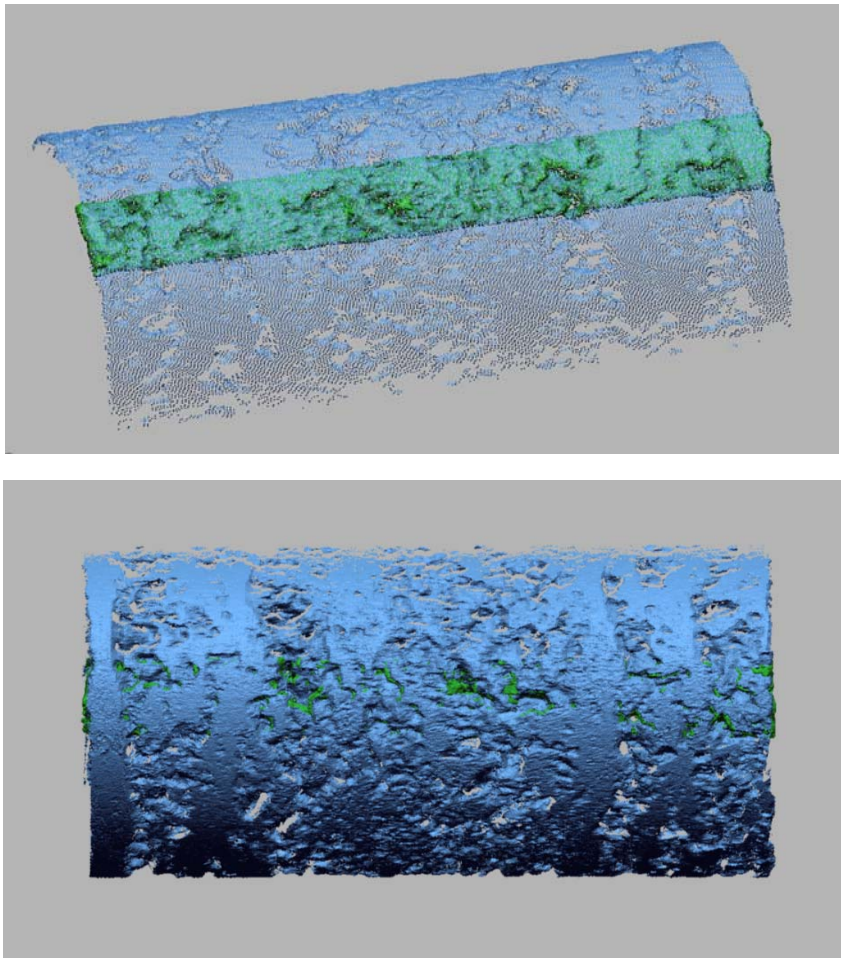

Figure 4-32: Superimposed 3D Scans of Sample 3-2

It is worth noting that there was some difficulty re-aligning the two scans from before and after testing. The surfaces had changed from ice wear and the set screws in the end caps had damaged the end of the cylinders. Additionally, there was no indication to mark one end from the other for alignment. With some manipulation and viewing, alignment was achieved but the uncertainty can be eliminated moving forward with the use of proper surface registration techniques.

Chapter 5 Refined Testing Apparatus Design

Completion of the pilot experiments offered insights and practical knowledge that were applied to the initial conceptual design. Observations on the use of equipment, testing procedures and experimental results confirmed aspects of the conceptual design as well as insight into design and test condition improvements. Importantly, it was seen that a rotating interaction between concrete and ice capably induced measurable concrete wear.

Lessons learned from the pilot experiments required design refinement for temperature control, ice holding capabilities, removal of debris, duration and applied load, and ice-concrete interaction area. Further investigation into concrete surface finish and compressive strength is needed, and stick-slip testing can be explored.

The tests in the lab showed that physical processes can be observed and measured using laboratory scale testing and detailed measuring techniques. These same conditions do not easily lend themselves to long term, high load, field-like conditions for routine sample testing. Where the laboratory approach attempts to simulate field conditions, a field testing approach does so implicitly if it can be executed in a practical way. If rotary motion is used to expedite the wear phenomenon in the lab, then doing the same in the field can reduce the complexity of controlling or modelling all other environmental conditions. Given the vastness of stable natural ice covers in many temperate and northerly environments, an apparatus for this approach has also been conceived.

The lab experiments will continue to focus on the physical wear process and accurate measurement of concrete abrasion, while field testing will allow aggressive wearing and

comparative analysis of various concrete samples under actual in-situ conditions. Splitting into two approaches may relieve the lab scale apparatus from having to approach the extremes of loads and duration that make the design and testing difficult, whereas the field approach covers these ranges but may not capture the details of the processes in play.

The following chart, shown in Figure 5-1, provides the layout from the initial problem and the proposed available testing opportunities based on desired outcomes and results. Most importantly, are the outcomes of standardized laboratory testing and field condition testing. Text in red describes background and research opportunities that were outside the scope of this thesis.

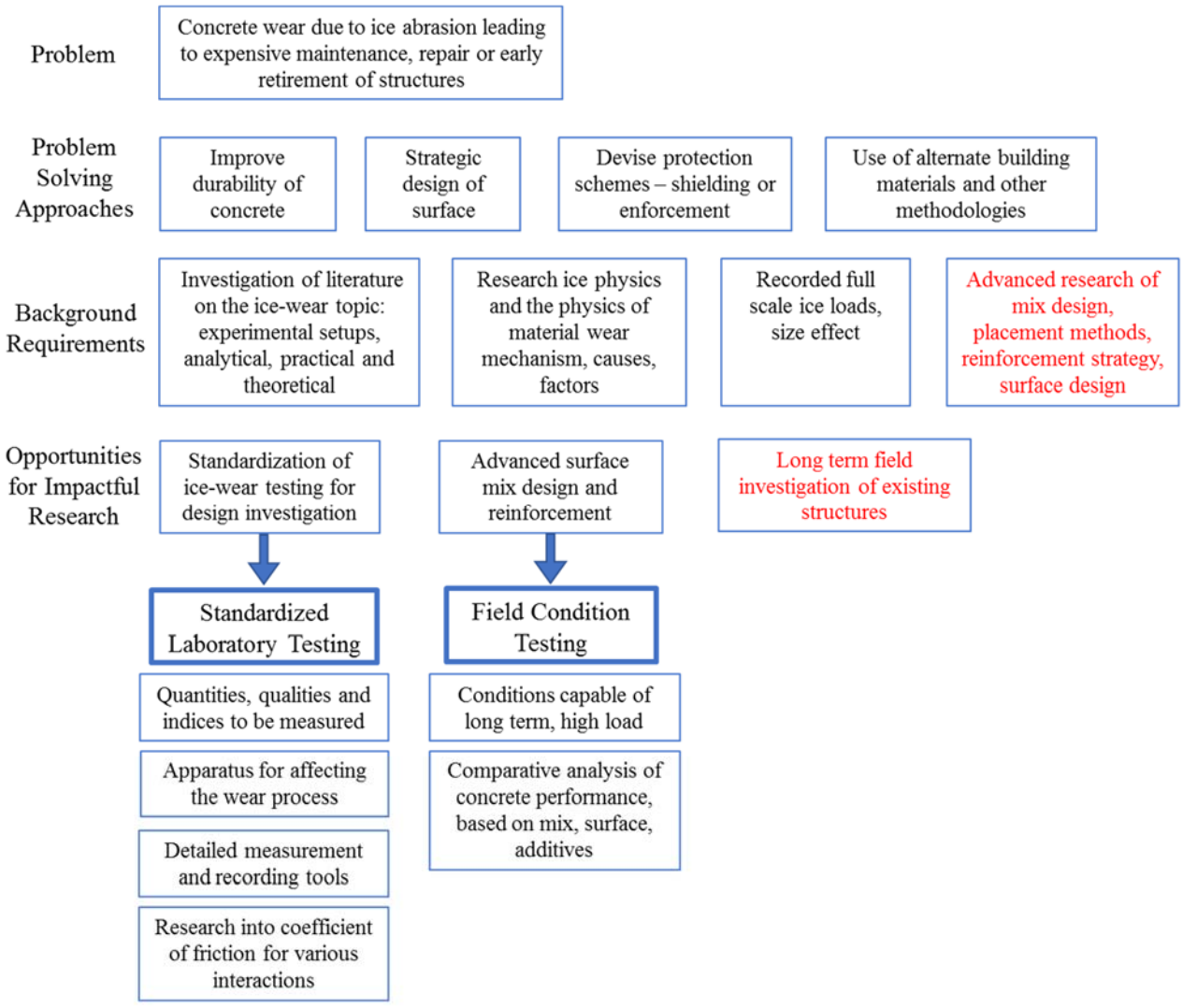

Figure 5-1: Testing Opportunities

5.1 Specific Observations from Pilot Experiments

The pilot experiments provided valuable learnings into ice abrasion testing with concrete. Observations regarding future conceptual apparatus, the performance of concrete and ice samples, and the measurement methods are as follows in this section.

5.1.1 Apparatus and Procedures

The ability to control the temperature in the testing area is essential moving forward as it is such a significant variable that affects the interaction between the ice and concrete, and the removal of debris. As learned from the pilot experiments, maintaining a steady ice sample is difficult in temperatures above freezing. The average room temperature for the pilot tests was 18.6 ºC, this quickly warmed up the metal arm and accelerated ice melting.

During testing, as the ice holder arm rose in temperature, the ice could be seen slipping and unevenly loading the concrete. While the ice always remained within the targeted gridlines, inconsistencies were evident. Moving forward it is important that the ice sample be held firmly in place and a temperature controlled setting will maintain the holder at a colder temperature.

It was observed in the pilot experiments that the applied pressure decreased during testing due to the increasing cross-sectional interaction area as the ice wore away and formed to the 100 mm concrete sample diameter, see Figure 4-18. However, the loads applied were at the upper limit of this specific test apparatus. In future, a larger, and therefore flatter, concrete diameter would provide a better interaction surface with the applied ice sample and the apparatus should be capable of applying and sustaining 2 MPa of pressure.

5.1.2 Sample Performance and Duration

Ice sample blocks were utilized in the pilot experiments and while the ice type formation was consistent and worked well, the production process wasted significant material and required extra effort in cutting and shaping the samples.

As room temperature was not a controlled variable for the pilot experiments, the ice melted faster than would normally be seen if a cold room was in use. That said, samples were generally seen to last two hours which shows that long duration testing using secure and replaceable ice samples is a viable option. Temperature control of the surroundings is an important contributing factor that influences a consistent testing environment. It also has a large effect on ice sample duration and surface wetness.

The concrete did wear appreciably and the loss of the initial paste layer was detected fairly quickly. The completed 9.5 km tests, in this case, were not long enough to appreciably wear into the aggregate but the process worked and could be easily extended for further distances in future work. 10 km should be used as a minimum test distance.

The pilot experiments showed that a smoother surface finish on the concrete resulted in less abrasion than the concrete with a higher compressive strength. Theoretically, if softer aggregates were used in mixes and they wore away with the cement, there could be a reduction in catastrophic plucking that leaves significant voids in the concrete surface. The proposed field test apparatus will be helpful in achieving long duration and robust testing. This can be used to compare concrete performance and can investigate the effect of aggregate hardness on the uniformity of abrasion.

5.1.3 Abrasion Measurement

In terms of abrasion measurement, it could be seen that the debris collection was a better indicator of wear than measuring the diameter; the debris plots are more consistent than the diameter measurement plots.

Though debris collection is not possible for the field setup; the laboratory apparatus will have active debris collection and filtration. The proposed apparatus will provide insight into the effects of water on the removal or retention of grit in the ice concrete interaction area.

3D scanning or another form of optical micrometry measurement is recommended for more precise measurement of before and after surface roughness of the concrete. An important lesson learned from completing 3D scanning during the pilot experiments is marking and surface registration of the concrete so that the before and after scans can be easily aligned. Indication markers of scanned areas on the concrete using a permanent marker can interfere with the concrete surface scanning. Plus, these marking can be worn away during testing. A permanent reference would allow easy match-up between the before and after scans of the concrete. As advised from the scanning technician, the laser better picks up surface bumps rather than holes. Scans are able to be completed on concrete samples from the laboratory and field proposals.

5.2 Laboratory Equipment

Figure 5-2 shows the refined design of the laboratory testing setup. The design features a standalone refrigeration unit, allowing temperature control, and sits on a trolley for easy portability. The top picture shows the apparatus with one wall of the refrigeration unit removed for a view of the inside layout. The bottom picture shows the stripped apparatus main reaction frame.

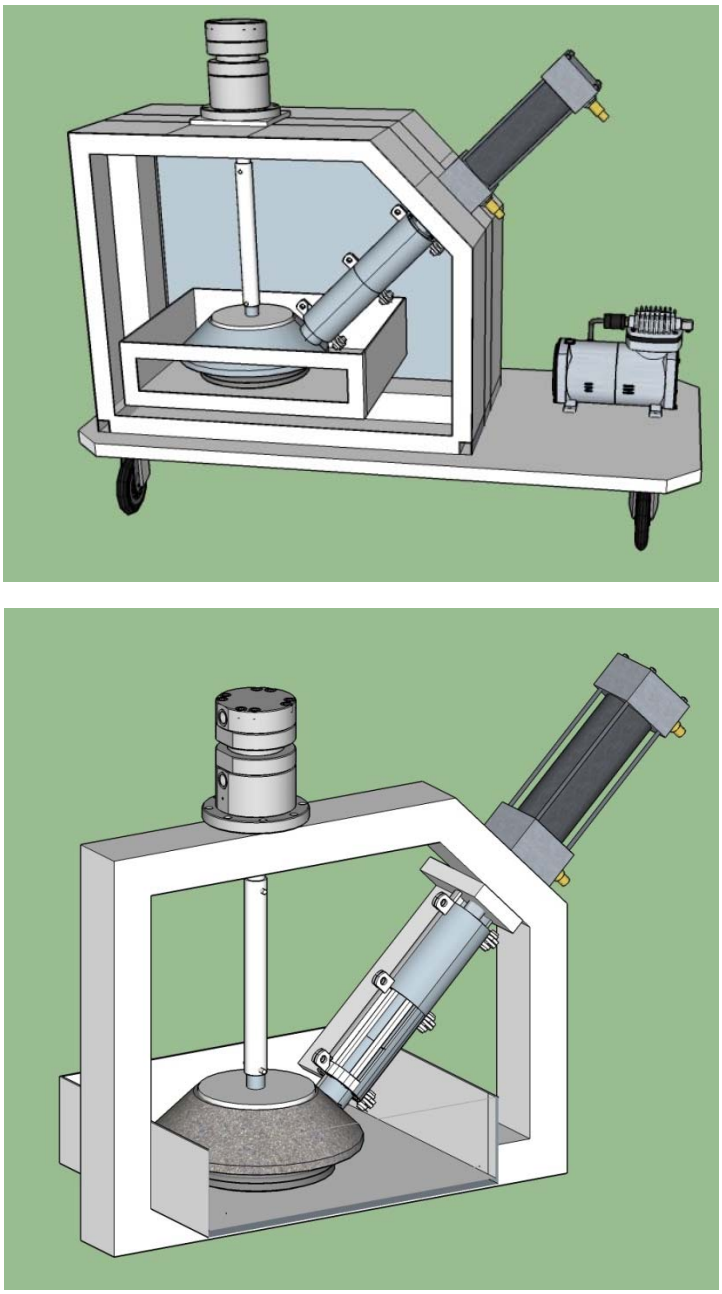

Figure 5-2: Refined Conceptual Laboratory Apparatus

A breakdown of the apparatus and features are shown in Figure 5-3 and are described as follows.

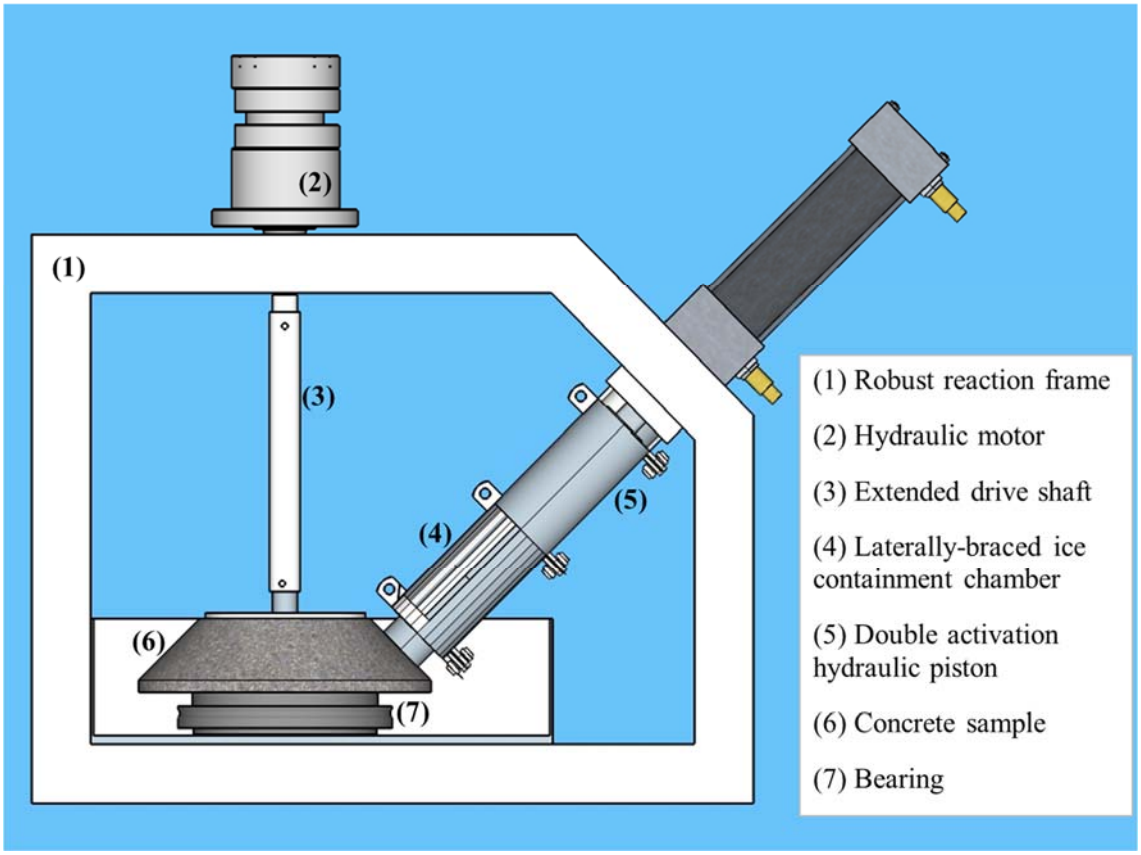

Figure 5-3: Laboratory Equipment Component Breakdown

(1) The first component is a robust reaction frame inside of which all applied and reactionary forces are contained. The application of forces up to the unconfined crushing resistance of ice will be achievable.

(2) A powerful hydraulic motor will be attached to apply the necessary torque and speed control to easily overcome the torsional grinding resistance of ice on concrete for extended periods of time.

(3) The extended drive shaft from the hydraulic motor to the concrete sample is pinned so that it can be easily removed for better access and changing of the concrete samples.

(4) The ice samples will be loaded using a laterally-braced ice containment chamber. Delrin plastic guides within the chamber will allow easy ice cartridge advancement while under considerable lateral shear forces at the point of contact with the concrete.

(5) A double activation hydraulic piston which can advance the ice cartridges down the chamber under steady load or rate – and do so until ice replenishment is required. Retracting the ram and opening the chamber allows new ice cylinders to be fed into the machine for continuation of the testing.

(6) The concrete sample shaped as a truncated cone and placed inside a water tight basin facilitates testing under a full range of submerged, wet and dry conditions – while keeping all primary equipment in the dry without need of any pass-throughs or watertight seals.

(7) The concrete sample sits on a very robust bearing which must resist all normal and shear forces while maintaining low rotational resistance while underwater.

(8) Figure 5-4 provides a side view of the apparatus showing that attached to the water basin is a drain with a valve so that waste water can be removed and will spill through a filter liner into a collection bucket.

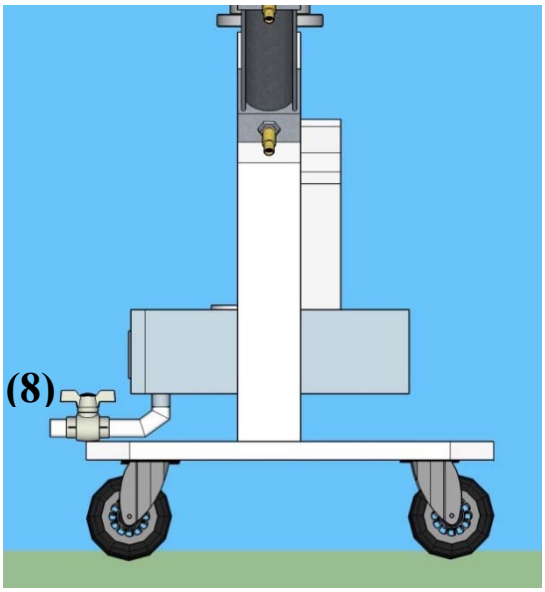

Figure 5-4: Side View of Laboratory Apparatus

5.3 Laboratory Testing Procedure Recommendations

In terms of experimental equipment that can be improved, the most significant consideration is the setting of the testing. However, dependence on an available cold room involves scheduling with other projects and minimal allowance for project delays and extensions. Therefore, it is desirable to develop an independent temperature controlled setting that is large enough to simply house the testing equipment, this leads to the standalone refrigeration unit. The addition of temperature control would eliminate the need to freeze the ice holding device and would keep consistent testing temperatures for the ice and concrete samples. Temperature acclimatization for the ice and concrete would still be necessary prior to testing. Target setting temperatures will range from 0-5 ºC and will enclose the robust and continuous reaction frame that contains all loads and equipment.

The size of the concrete sample has also been considered. While this naturally will be enlarged due to testing scale, it is important that an increased diameter will produce a flatter and more uniform interaction area on the concrete. This is essential in an effort to keep a more uniform pressure applied from the ice sample. The conceptual design, from Chapter 3, proposed a concrete sample in the shape of a truncated cone with a 1m bottom nominal diameter. The refined concrete shape design, Figure 5-5, is slightly smaller with a proposed 0.6 m (2 ft) bottom diameter with a 0.1524 m (6 inch) height. The interaction of concrete samples of this size with the suggested ice sample dimensions will result in a more uniform and consistent interaction area. The concrete forms will be shaped so that unnecessary center material is not required, saving on materials and reducing the weight of the samples. It is proposed that a robust fitting or interaction plate be set into the concrete to fit the bearing and drive shaft that will attach and rotate the sample. A portable lift will be purchased to help with the movement and placement of the concrete sample into the testing setup.

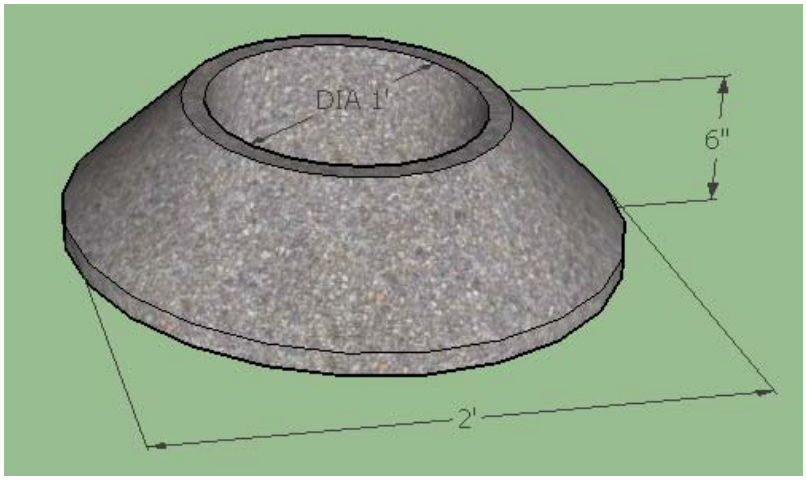

Figure 5-5: Proposed Concrete Sample Dimensions

Ice samples will be made using 100 mm diameter and 200 mm height standardized cylindrical forms that will produce the desired sample size for testing. These forms are used for concrete standard testing and are readily available. Additionally, they will eliminate the need for excessive band saw cutting.

An ice cartridge silo is recommended, for easy replacement of the ice sample, and will contain hard plastic prisms. These prisms are less susceptible to heat conduction to better hold the ice in place. To apply force to the ice sample, a hydraulic piston will be in place and properly supported by the frame applying constant pressure. A hydraulic actuator was chosen over electric for the initial design to easily achieve a slow, constant load application. For consistency, a hydraulic motor was also chosen, however future changes could incorporate electric actuators. A viewing slot in the piston will allow easy observation and recording of ice sample duration and an indication of when to replenish the ice samples. The ice sample duration and rate of degradation can then be compared to surface roughness of the concrete. Higher loads than those achieved in the pilot experiments are important. Keeping with the initial concept, a maximum pressure of 2 MPa would be effective.

As detailed in the conceptual design, a robust water basin will be included to offer varying submergence conditions. A drainage arrangement will allow easy control of the water level. Valuable wear information was obtained by collecting, weighing and observing the worn concrete material during the pilot tests. It is recommended that this practice be used for the future lab experiments. To accomplish this, an active drainage and filtration system is suggested, circled in Figure 5-6. This would remove the water and

any worn material from the basin, and allow collection of the debris. It is important to keep water in the basin clean as any cement paste, debris or aggregate that remains suspended in the water can infiltrate the interaction zone and accelerate the wear process.

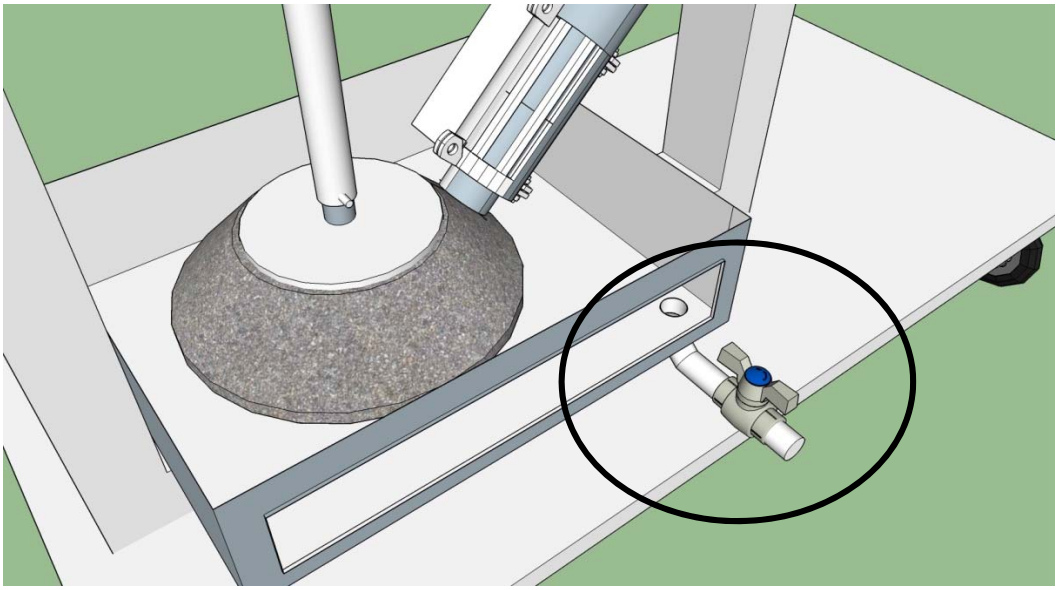

Figure 5-6: Water Basin Drainage System

Under wet testing conditions, the water helped remove abraded debris from the concrete surface. However, under dry conditions, there is a risk that debris will remain on the surface and accelerate the wear process. An addition to the arrangement would be an air blowing device that would blow off any debris into the basin once the rotating concrete passes by the ice sample. This ensures a clean face returns to the ice sample without the risk of causing additional abrasion.

3D scans of the concrete sample can easily be completed with the option to attach a scanning arm to the testing frame. This would allow in-place before and after scans of the concrete sample without the effort of moving and potentially damaging the concrete.

Additionally, the surface scans will be useful in analyzing wear patterns changes in relative surface smoothness. For more accurate comparisons, once the concrete has been cured and removed from the forms, small holes can be drilled and filled with epoxy and small protruding pins. The technician recommends a square or rectangular protrusion for optimal scanning. These pins would be picked up in the initial scans and then can be referenced and aligned to eliminate confusion when completing the post-testing scans.

5.3.1 Additional Considerations

As the focus of the lab testing is the wear process under controlled settings, insight into the coefficient of friction would offer valuable information. This can be determined from data acquisition by using fitted sensors to monitor the hydraulic pressure and the torque of the rotary motor. Equation 4 from Chapter 3 can be rearranged to calculate the friction coefficient as follows:

$$\mu = \frac{\tau}{r_{con} P A_{ice}} \qquad (5)$$

At the end of the testing rounds in the pilot experiments, the ice was found to be stuck to the concrete after the stop in motion. This proves that stick-slip interactions are able to be implemented into the testing process and could provide further insight of specific interaction type.

Future experiments will employ Design of Experiment (DOE) theory to complete a testing program that provides statistically correct procedures and results, as well as significant factor and factor interaction outcomes.

5.4 Field Equipment

The field testing concept, Figure 5-7, eliminates the need to develop and control field conditions in a laboratory setting. The apparatus permits long duration wear tests in which a rotating concrete cylinder is pressed against a stationary natural floating ice cover.

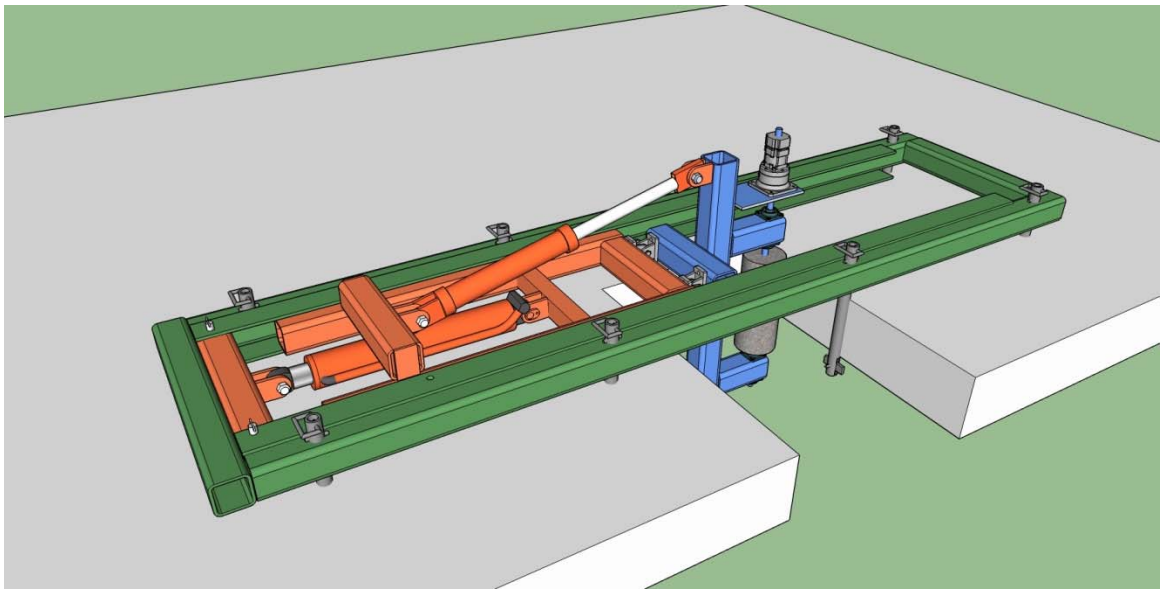

Figure 5-7: Conceptual Field Apparatus

A component breakdown can be seen in Figure 5-8, followed by a brief description of each element.

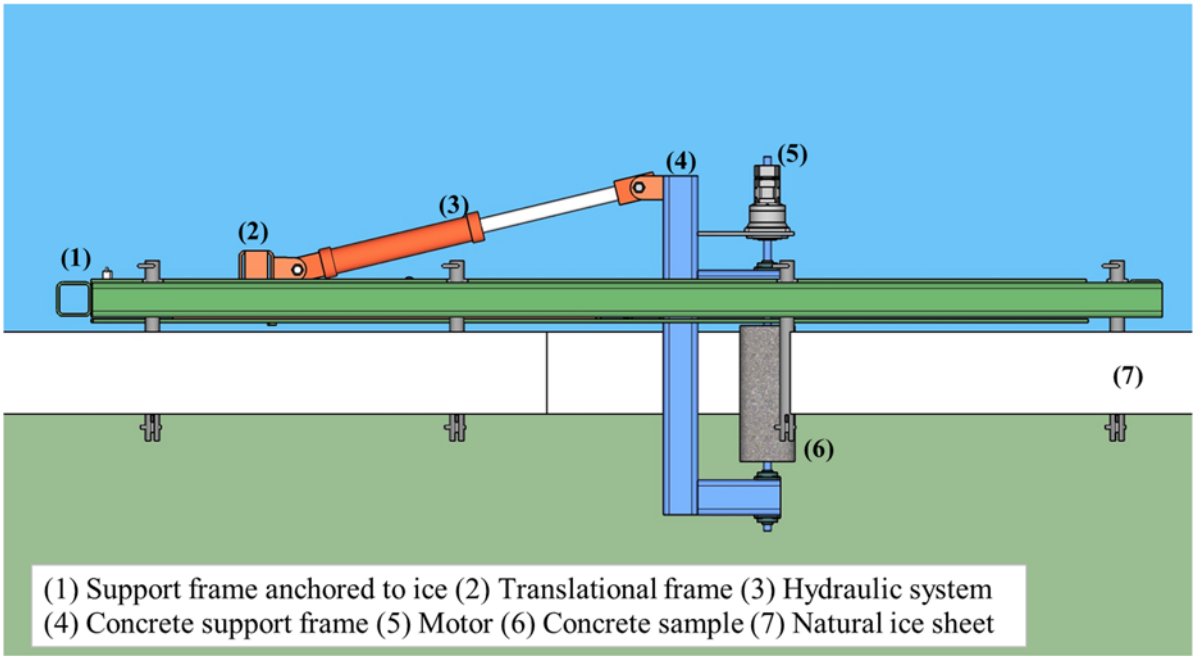

Figure 5-8: Field Equipment Component Breakdown

(1) The first component, shown in green, is the main support frame which will be anchored to the ice cover using typical ice anchors placed through pre-augured holes in the sheet.

(2) Seen in orange, within the support frame, will sit the translational frame that will slide within the guides of the green frame as the concrete wears and pushes through the ice.

(3) The hydraulic ram system will be used to induce ice crushing loads on the attached concrete sample in the apparatus. The tilting mechanism provides the accessibility to change the concrete sample.

(4) The concrete sample support frame, in blue, is supported by the translational orange frame and can be rotated hydraulically, raising and lowering the test sample for inspection or otherwise.

(5) The concrete sample will be driven by a rotary motor, applying sufficient torque to spin the concrete as it is being pushed into the ice sheet.

(6) Cylindrical concrete samples of various mix designs will be used to achieve the rotational testing concept

(7) The concrete will be abraded against a naturally formed ice sheet, which will also be used as the foundation for the entire apparatus and equipment.

5.5 Field Testing Procedure Recommendations

The idea behind the field testing is to reduce the focus on the physical wear process and instead pay attention to the performance of various concrete types in an actual ice wear environment. The concept is similarly derived from the lab testing proposal in that a rotating concrete sample will be interacting with the ice to induce wear.

The hydraulic system and heavy frame permit very high torque and normal stresses in the ice-concrete interactions, reaching up to ice crushing limits. A single hydraulic power pack can operate the entire machine through independent pressure regulators, lines, and actuators. The device can be installed onto a frozen ice surface with a cutout in which the vertical concrete cylinder can be placed. The whole assembly can be transported by sled to a test site.

When the horizontal ram reaches full extension, the orange frame footing, shown in Figure 5-7, can be re-pinned at an advanced position within the green frame. If the orange frame advances to the point where it reaches the end of the guides in the green frame, the

anchors of the green frame can be pulled and the whole assembly can be moved to a new advanced position, with the orange frame once again fully retracted.

There will be less focus on controlled variables as the actual field conditions will be determined by the field setting. As the testing is completed in-situ, temperature cannot be controlled but must be recorded for reference. The type of ice used in the experiments will depend on the environment in which the testing is completed and as the ice will naturally be in place, use of an ice holder is not required. There will be no dry testing completed for these tests. The ice formation at the waterline level will induce wear as seen for all concrete structures in a realistic pack-ice setting.

In order to fully develop the abrasion process and begin removal of the coarse aggregate, a few options should be further explored. Longer testing at a constant pressure would provide better proof of catastrophic wear in the form of coarse aggregate plucked from the concrete. Investigation should also include hardness of aggregates, surface finish, compressive strength and mixture additives. Comparative studies could show if more uniform abrasion maintains a smoother concrete surface for ice interaction.

Collection of debris is not possible for this testing arrangement. Direct comparison of performance for each concrete sample, based on mix design, will be the focus. 3D scanning can also be completed on the concrete samples tested in the field arrangement. As with the lab tests, surface registration protrusions can be embedded into the concrete in order to complete comparisons of the surface finish.

Chapter 6 Conclusions and Recommendations

This thesis presents the development of two new concepts for experimental apparatus and procedures to advance research into ice abrasion of marine concrete structures; including a standardized laboratory apparatus and field scale equipment. There have been numerous previous ice abrasion studies and testing programs completed, however, opportunities for improving the research were highlighted by the literature review of previous experiments, results, and full scale data collection. Long duration testing with minimal stops, as well as the ability to provide wet concrete testing are the primary advancements to improve ice and concrete wear testing.

6.1 Initial Concept for Laboratory Scale Apparatus

The process of development started with the literature review that identified a number of areas of importance in experiments related to ice wear on concrete and led to a list of ten design criteria in which a new apparatus could improve over previous experiments. Following this an initial laboratory apparatus concept and significant features were provided to address the ten issues identified in the initial review. The brainstorming process for the initial concept led to the rotating concrete idea, in order to achieve long duration testing.

Some issues related to the design of the apparatus and the development of testing procedures could not be entirely resolved based on the literature. This included the size and the rate of wear of the ice samples, test setting, removal of worn ice, and abrasion measurement methods. As a result, a series of pilot experiments was conducted to explore

aspects of measurable wear in the concrete, the rate of ice consumption in longer term testing, possible methods of measuring the relatively small wear in the concrete and some practical issues associated with handling ice and concrete samples under high wearing pressures.

6.2 Pilot Experiment Conclusions

The main takeaway from the pilot experiments was that the applied ice load on a continuously rotating concrete sample did induce measurable wear of the concrete. Analysis of the results showed that the smoother surface of the mid-performance Mix2, due to a higher water content ratio, actually showed less abrasion than the high performance Mix1, which is in good agreement with the results of Itoh et al (1994) and Nawwar and Malhotra (1988).

From the pilot experiments, it was seen that as the ice continued to wear and melt, there was some removal of debris from the meltwater, however it was impossible to say for certain if complete removal of all worn material in the interaction area was accomplished. This solidifies the proposal that the ability to control the water level of the concrete and ice interface is crucial for more comprehensive research results.

Another conclusion from the pilot testing was the value in long distance testing. A testing length of 9.5 km was completed in the pilot experiments, 19 km completed on one of the cylinders, and this should be considered a minimum test distance. This is essential in better understanding the progression of the wear process and reducing the amount of data extrapolation from short duration testing.

Collection and examination of the debris proved valuable in quantitatively measuring concrete wear, but also for observing the progression of material wear from initial paste to fine aggregate removal.

The completed pilot experiments resulted in important lessons regarding setup, procedures, and abrasion measurement techniques. These learnings were used to refine the laboratory apparatus, as well as provide a clearer picture of possible outcomes from the laboratory and from the field testing proposal. The primary focus in the laboratory proposed will be on specific abrasion mechanisms and the ice-concrete interaction. The more robust field apparatus will be employed to create in-situ, high pressure tests that evaluate and compare concrete performance. Using these outcomes, a more refined concept design for a laboratory experimental apparatus was developed and a second concept for an in-situ field apparatus was developed.

6.3 Refined Concept for Laboratory Scale Apparatus

The second iteration of the laboratory apparatus incorporated design improvements noted from the pilot experiments. Notably, is the inclusion of a standalone refrigeration unit that will provide a controlled testing environment, eliminating the need to schedule a cold room. A breakdown of the apparatus and equipment components has been provided to describe the design proposal.

Modifications to the concrete and ice sample size will improve the loading application and the interaction between the two surfaces. Abrasion measurement will continue to be monitored by debris collection, based on the valuable information obtained in the pilot

experiments using this method, while opportunities for 3D scanning will continue to be investigated.

It is proposed that the laboratory concept be implemented and operated prior to development of the field concept as it is likely, based on the pilot experiments, that further knowledge will be gained from smaller scale experiments that will influence the larger scale apparatus.

6.4 Full Scale In-situ Apparatus

The initial laboratory apparatus concept and the lessons from the pilot experiments were valuable towards the development of the field apparatus. The use of a rotary device has been further developed to take advantage of naturally occurring settings in cold, ice-prone environments. Experimental controls will be limited as they will be based on given field parameters at the time of testing.

As with the refined concept for the laboratory scale apparatus, a component breakdown of the field apparatus and equipment has been provided. The robust frame will load a rotating concrete sample into the ice sheet, focusing on the in-situ performance of varying concrete mixes as opposed to the detailed physical abrasion mechanisms.

6.5 Summary of Completed Work

These described apparatus and setups provide a foundation to further explore the concrete-ice abrasion interaction. This will develop the knowledge required to better

design and increase the service life of coastal and marine concrete structures in ice prone environments.

Table 3-2, has been updated to account for the lessons learned from the pilot experiments, as well as the inclusion of the field testing opportunity. Table 6-1 summarizes the design criteria and features for both laboratory and field testing arrangements.

Table 6-1: Refined Apparatus Criteria and Design Features

Identified Design Issue	Design Criteria	Laboratory Apparatus Design Features	Field Apparatus Design Features
1. Relative wear rates	Ability to provide ice at relatively high rates. Required rate to be determined by subsequent experimentation	Ice sample refills will be pre-made and readily available. Samples will be made in sufficient lengths (200 mm) to last multiple hours each, allowing long duration testing	Dictated by the extent and quality of natural formed ice
2. Motion mode	Continual movement with minimal start-stop and no reversal of motion	Conical concrete sample on a rotary table and motor with the ability to apply sufficient torque	Cylindrical rotating concrete sample driven by a rotary motor with the ability to supply sufficient torque
3. Applied pressure	Applied loads that are consistent with full scale data with a minimum 2 MPa at nominal sample size and higher pressures available for reduced sample sizes	Hydraulic ram and frame designed to induce 2 MPa pressure Normal F_{Max} = 15.7 kN* Tangential F_{Max} = 1.57 kN* *using 100 mm diameter cylindrical forms for ice samples	Hydraulic ram to induce high loads up to ice crushing. Load to be determined based on final sample size.
4. Wet or Dry testing	Wet and dry testing conditions to be accommodated within the design	Rotating concrete sample to be located in a stainless steel water bath allowing dry, submerged and semi-submerged conditions	Dry testing unavailable. In-situ waterline loading conditions.
5.Ice sample type	Design to be able to accommodate samples of a uniform size/shape but with differing ice types in terms of saline content, grain structure or samples cut from in-situ locations	Ice samples to be grown in 100 mm diameter x 200 mm height standardized cylindrical forms to eliminate band saw cutting	Naturally formed ice cover will provide ice for the testing, record thickness for reference
6. Relative velocity	Control of sliding velocity within the range of 0 to 2 m/s to be translated into a rotary velocity of 0 to 40 RPM	Achieved with off-the-shelf variable speed drive to be sourced as part of detail design	Achieved with off-the-shelf variable speed drive to be sourced as part of detail design
7. Temperature control	Control of atmospheric temperature	Apparatus to be housed in standalone refrigeration unit for temperature control, placed on trolley for portability	Field condition environment controls temperature, record temperature during testing for reference
8. Waste ice interfering with testing	Removal of worn ice from concrete surface to be incorporated into design	Modular system, ability to brush/blow away waste ice	Not required, field submergence creates real setting of water in interface
9. Accurate measurement of abrasion/material loss	Collection of wear material to be incorporated into design	Drainage, collection and filtration system built into water bath, 3D scanning opportunities available	Comparison of wear on various concrete mixes to determine effect of additives, surface finish, and compressive strength
10. Load measurements	Ability to measure normal and tangential forces at the wear interface to be incorporated into the design	Normal and tangential maximum load range determined, load cells can be placed to take measurements. Alternately indirect measurements based on applied feed force for ice sample and resulting motor torque from rotary table drive.	Applied force can be measured directly with instrumentation or indirectly based on applied hydraulic pressure. Tangential force can be measured directly by instrumentation or indirectly by rotary motor torque.

References

Barker, A. (2016). Physical Experimentation Related to Friction and Wear: As Related to Ice-Concrete Studies. *Memorial University.* Term Paper, Unpublished.

Bekker, A., Uvarova, T., Pomnikov, E., Farafonov, A., Prytkov, I., & Tyutrin, R. (2011). Experimental Study of Concrete Resistance to Ice Abrasion. *International Offshore and Polar Engineering Conference*, (pp. 1044-1047). Maui.

Bjerkås, M. (2006). *Ice Actions on Offshore Structures.* Doctoral Thesis - Norwegian University of Science and Technology.

Bjerkås, M. (2007). Review of Measured Full Scale Ice Loads to Fixed Structures. *26th International Conference on Offshore Mechanics and Arctic Engineering*, (pp. 1-10). San Diego.

BlackRockTools. (2016). King Industrial Gearhead Metal Lathe. Retrieved from https://www.blackrocktools.com/king-canada-12-x-36-gearhead-metal-lathe-kc-1236ml.html

Blanchet, D. (1998). Ice Loads from First-year Ice Ridges and Rubble Fields. *Canadian Journal of Civil Engineering, 25*, 206-219.

Brown, T. (1997). The Confederation Bridge - Early Results From Ice Monitoring Program. *Canadian Society of Civil Engineering Annual Conference*, (pp. 177-186). Sherbrook.

Brown, T. (2001). Four Years of Ice Force Observations on the Confederation Bridge. *International Conference on Port and Ocean Engineering Under Arctic Conditions*, (pp. 285-298). Ottawa.

Brown, T., & Määttänen, M. (2009). Comparison of Kemi-I and Confederatio Bridge Cone Ice Load Measurement Results. *Cold Regions Science and Technology, 55(1)*, 3-13.

Brown, T., Jordaan, I., & Croasdale, K. (2001). A Probabilistic Approach to Analysis of the Ice Loads for the Confederation Bridge. *Canadian Journal of Civil Engineering, 28(4)*, 562-573.

Bruneau, S., Dillenburg, A., & Ritter, S. (2013). Ice Sample Production Techniques and Indentation Tests for Laboratory Experiments Simulating Ship Collisions in Ice. *23rd International Offshore and Polar Engineering Conference*, (pp. 1268-1271). Alaska.

Bruneau, S., Sullivan, A., Zhang, Z., & Colbourne, B. (2015). Ice-Microtome Design for Procurement and Crystal Analysis of Ice Thin Sections. *25th CANCAM Conference*. London.

Cheung, M., Tadros, G., Brown, T., Dilger, W., Ghali, A., & Lau, D. (1997). Field Monitoring and Rresearch on Performance of the Confederation Bridge. *Canadian Journal of Civil Engineering, 24(6)*, 951-962.

Fiorio, B. (2005). Wear Characterization and Degradation Mechanisms of a Concrete Surface Under Ice Friction. *Construction and Building Materials, 19*, 366-375.

Fiorio, B., Meyssonnier, J., & Boulon, M. (2002). Experimental Study of the Friction of Ice Over Concrete Under Simplified Ice-structure Interaction Conditions. *Canadian Journal of Civil Engineering, 29*, 347-359.

Fosså, K. (2007). Improvement of the Ice Zone on Concrete Structures for Sub Arctic Areas. *Nordic Concrete Research Workshop Ice Abrasion on Concrete Structures*, (pp. 1-4). Helsingfors.

Fransson, L., & Lundqvist, J.-E. (2006). A Statistical Approach to Extreme Ice Loads on Lighthouse Norströmsgrund. *25th International Conference on Offshore Mechanics and Arctic Engineering*, (pp. 1-6). Hamburg.

Frederking, R., & Barker, A. (2002). Friction of Sea Ice on Various Construction Materials. *16th IAHR International Symposium on Ice.* Dunedin.

Hoff, G. (1989). Evaluation of Ice Abrasion of High-Strength Lightweight Concrete for Arctic Applications. *Offshore Mechanics and Arctic Engineering Conference*, (pp. 583-590). Hague.

Huovinen, S. (1990). Abrasion of Concrete by Ice in Arctic Sea Structures. *Journal of Structural Mechanics*, 23-35.

Itoh, Y., Tanaka, Y., & Saeki, H. (1994). Estimation Method for Abrasion of Concrete Structures Due to Sea Ice Movement. *International Offshore and Polar Engineering Conference*, (pp. 545-552). Osaka.

Itoh, Y., Yoshida, A., Tsuchiya, M., Katoh, K., Sasaki, K., & Saeki, H. (1988). An Experimental Study on Abrasion of Concrete Due to Sea Ice. *Offshore Technology Conference*, (pp. 61-68). Houston.

Jacobsen, S., Scherer, G., & Schulson, E. (2015). Concrete-ice Abrasion Mechanics. *Cement and Concrete Research, 73*, 79-95.

Janson, J. (1988). Long Term Resistance of Concrete Offshore Structures in Ice Environment. *7th International Conference on Offshore Mechanics and Arctic Engineering*, (pp. 7-12). Houston.

Jones, D., Kennedy, F., & Schulson, E. (1991). The Kinetic Friction of Saline Ice Against Itself at Low Sliding Velocities. *Annals of Glaciology, 15*, 242-246.

Møen, E., Høiseth, K., Leira, B., & Høyland, K. (2015). Experimental Study of Concrete Abrasion due to Ice Friction - Part I: Set-up, Ice Abrasion vs. Material Properties and Exposure Conditions. *Cold Regions Science and Technology, 110*, 183-201.

Nawwar, A., & Malhotra, V. (1988). Development of a Test Method to Determine the Resistance of Concrete to Ice Abrasion and/or Impact. *American Concrete Institute, 109*, 401-426.

Newhook, J., & McGuinn, D. (2007). Ice Abrasion Assessment - Piers of Confederation Bridge. *Confedeation Bridge Engineering Summit Canadian Society of Civil Engineering*, (pp. 145-157).

Schulson, E. (2015). Low-speed Friction and Brittle Compressive Failure of Ice: Fundamental Processes in Ice Mechanics. *International Material Reviews, 60(8)*, 451-478.

Sistonen, E., & Jacobsen, S. (2007). Probabilistic Service Life Modeling of Ice Abrasion on Concrete Structures. *Nordic Concrete Research Workshop Ice Abrasion on Concrete Structures*, (pp. 138-145). Helsingfors.

Sodhi, D. (2001). Crushing Failure during Ice-Structure Interaction. *Engineering Fracture Mechanics, 68*, 1889-1921.

Tibbo, J., Obert, K., Shrestha, N., Tripathi, D., Mayne, C., & Brown, T. (2009). Year Twelve of the Confederation Bridge Ice Monitoring Program. *20th International Conference on Port and Ocean Engineering under Arctic Conditions.* Lulea.

Tijsen, J. (2015). *Experimental Study on the Development of Abrasion at Offshore Concrete Structures in Ice Conditions.* Master's Thesis - Delft University of Technology.

Tijsen, J., Bruneau, S., & Colbourne, B. (2015). Laboratory Examination of Ice Loads and Effects on Concrete Surfaces from Bi-axial Collision and Adhesion Events. *Port and Ocean Engieering Under Arctic Conditions International Conference.* Trondheim.

Appendices

Appendix A: Parameter Validation Data

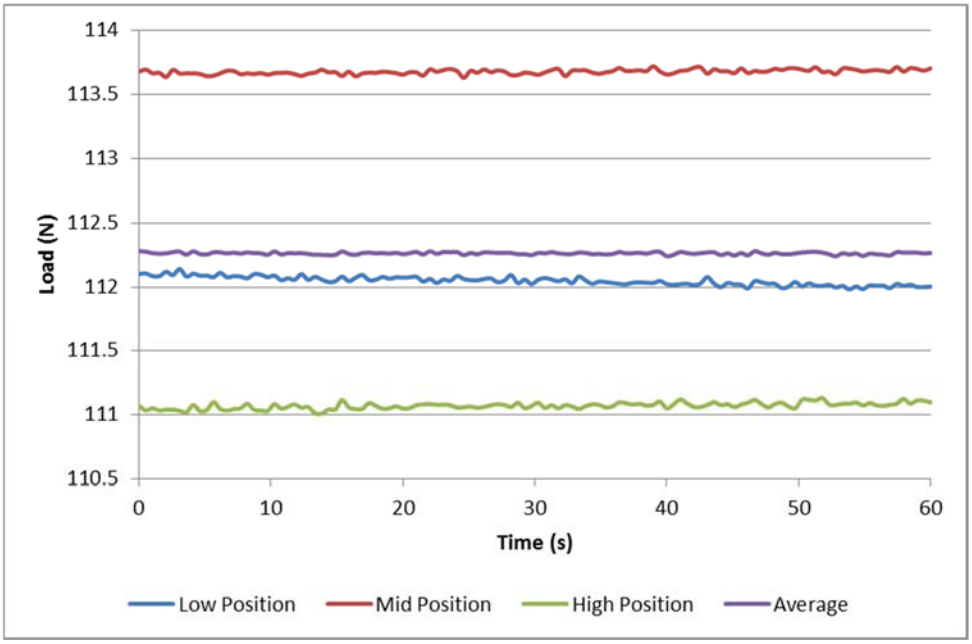

No Weight Condition

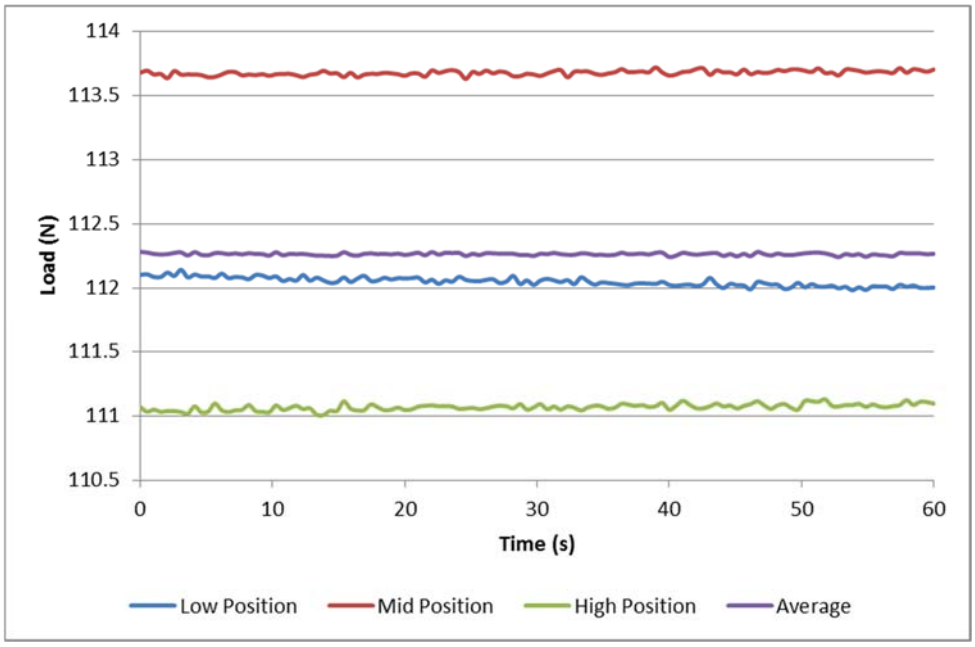

2 Green Weight Condition

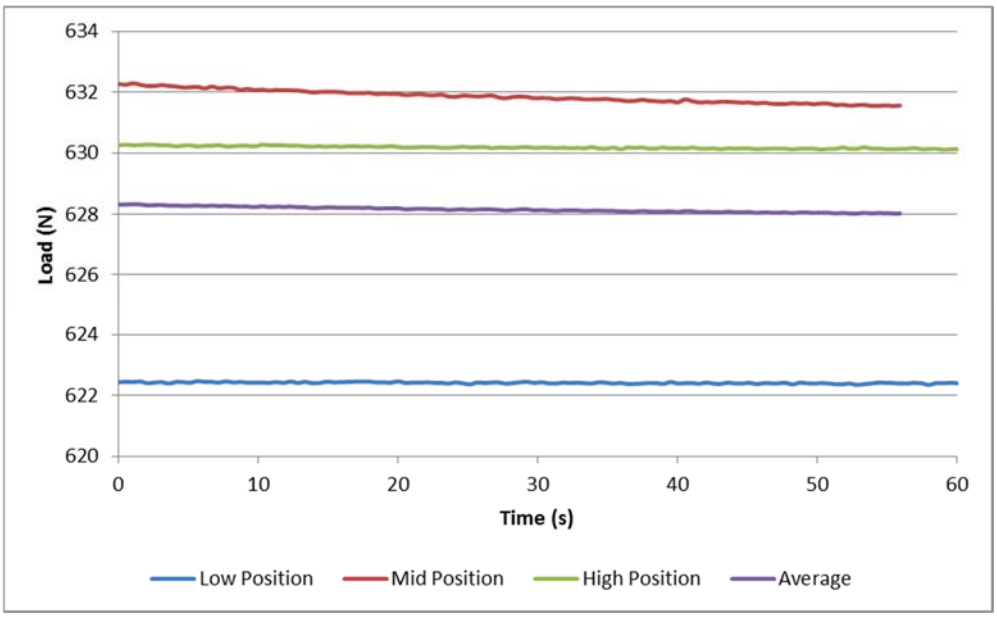

All Weight Condition

Appendix B: Raw Data Sheets

Cylinder	1-1	1-1
Round	1	2
Test Number	1	5
Mix	High	High
Date	May30/17	June7/17
Tachometer Test (RPM)	84.8	84.8
Air Temperature (°C)	17	-10
Ice Temperature (°C)	-12	
Concrete Temperature (°C)	2.3	
Arm Temperature (°C)		
Applied Load (kg)	41.55	41.55
Adjusted Load (N)	369.14	369.14
Ice Sample Hanging Length (mm)	90	95

Ice Duration (hrs)	1hr55mins	4hrs
Cumulative Minutes	115	355
Empty Tray (g)	16.8	16.7
Dried Tray (g)	18.1	16.8
Total Debris (g)	1.3	0.1

Before Cross Sections (mm)		
Centre	100.346	100.24
Mid	100.106	100.064
Chuck	100.008	99.943
After Cross Sections (mm)		
Centre	100.24	100.233
Mid	100.064	100.002
Chuck	99.943	99.992

Cylinder	2-1	2-1	2-1
Round	1	2	3
Test Number	2	4	7
Mix	Mid	Mid	Mid
Date	May31/17	June5/17	June12/17
Tachometer Test (RPM)	84.9	84.9	84.8
Air Temperature (°C)	19.1	20.6	22
Ice Temperature (°C)	-14.3	-12.9	
Concrete Temperature (°C)	3.5	1.2	1.3
Arm Temperature (°C)			
Applied Load (kg)	41.55	41.55	41.55
Adjusted Load (N)	369.14	369.14	369.14
Ice Sample Hanging Length (mm)	105	105	100

Ice Duration (hrs)	1hr55mins	2hrs	2hrs
Cumulative Minutes	115	235	355
Empty Tray (g)	16.9	16.9	16.9
Dried Tray (g)	18.5	17.7	17.5
Total Debris (g)	1.6	0.8	0.6

Before Cross Sections (mm)			
Centre	100.209	100.258	100.146
Mid	100.433	100.453	100.305
Chuck	100.607	100.575	100.527
After Cross Sections (mm)			
Centre	100.258	100.146	100.143
Mid	100.453	100.305	100.29
Chuck	100.575	100.527	100.526

Cylinder	3-1	3-1	3-1	3-1
Round	1	1	2	3
Test Number	3	3	6	8
Mix	Low	Low	Low	Low
Date	May31/2017	June1/2017	June8/2017	June13/2017
Tachometer Test (RPM)	84.8	84.9	84.8	84.8
Air Temperature (°C)	21.3	17	17	22
Ice Temperature (°C)	-15.4			
Concrete Temperature (°C)	3.5			
Arm Temperature (°C)				
Applied Load (kg)	41.55	41.55	41.55	41.55
Adjusted Load (N)	369.14	369.14	369.14	369.14
Ice Sample Hanging Length (mm)	40	95	85	100

Ice Duration (hrs)	20mins	1hr35mins	2hrs	2hrs
Cumulative Minutes	20	115	235	355
Empty Tray (g)		16.7	16.8	16.8
Dried Tray (g)		23.4	17.7	17.8
Total Debris (g)		6.7	0.9	1

Before Cross Sections (mm)				
Centre		99.841	99.841	99.716
Mid		99.785	99.447	99.066
Chuck		99.659	99.578	99.392
After Cross Sections (mm)				
Centre		99.841	99.716	99.63
Mid		99.447	99.066	99.34
Chuck		99.578	99.392	99.651

Cylinder	1-2	1-2	1-2
Round	1	2	3
Test Number	12	13	14
Mix	High	High	High
Date	July12/2017	July13/2017	July13/2017
Tachometer Test (RPM)	84.9	84.9	84.8
Air Temperature (°C)	16	15	15
Ice Temperature (°C)		-11.7	-11.7
Concrete Temperature (°C)		-2	3.3
Arm Temperature (°C)			
Applied Load (kg)	57.69	57.69	57.69
Adjusted Load (N)	527.48	527.48	527.48
Ice Sample Hanging Length (mm)	100	100	100

Ice Duration (hrs)	1hr55mins	2hrs5mins	2hrs
Cumulative Minutes	115	240	360
Empty Tray (g)	16.8	16.9	16.9
Dried Tray (g)	19.9	17.9	17.8
Total Debris (g)	3.1	1	0.9

Before Cross Sections (mm)			
Centre	99.54	99.522	99.483
Mid	99.348	99.382	99.398
Chuck	99.28	99.28	99.279
After Cross Sections (mm)			
Centre	99.522	99.483	99.467
Mid	99.382	99.398	99.341
Chuck	99.28	99.279	99.281

Cylinder	2-2	2-2	2-2
Round	1	2	3
Test Number	9	10	11
Mix	Mid	Mid	Mid
Date	June15/2017	June16/2017	July12/2017
Tachometer Test (RPM)	84.7	84.8	84.8
Air Temperature (°C)	16	19	15
Ice Temperature (°C)		-16.1	
Concrete Temperature (°C)	2.4		
Arm Temperature (°C)			
Applied Load (kg)	57.69	57.69	57.69
Adjusted Load (N)	527.48	527.48	527.48
Ice Sample Hanging Length (mm)	95	85	95

Ice Duration (hrs)	2hrs	2hrs	2hrs
Cumulative Minutes	120	240	360
Empty Tray (g)	16.9	16.8	16.9
Dried Tray (g)	18.1	17.5	17.6
Total Debris (g)	1.2	0.7	0.7

Before Cross Sections (mm)			
Centre	100.105	99.966	99.875
Mid	99.968	100.075	100.007
Chuck	99.986	100.165	100.159
After Cross Sections (mm)			
Centre	99.966	99.875	99.969
Mid	100.075	100.007	99.996
Chuck	100.165	100.159	100.156

Cylinder	2-2	2-2	2-2	2-2
Round	4	5	6	7
Test Number	19	20	21	22
Mix	Mid	Mid	Mid	Mid
Date	July19/2017	July19/2017	July20/2017	July20/2017
Tachometer Test (RPM)	84.9	84.9	84.9	84.9
Air Temperature (°C)	26	25	25	25
Ice Temperature (°C)	-11.8	-9.6	-9.6	-9.6
Concrete Temperature (°C)	1.2	1.2	1.2	1.2
Arm Temperature (°C)				
Applied Load (kg)	57.69	57.69	57.69	57.69
Adjusted Load (N)	527.48	527.48	527.48	527.48
Ice Sample Hanging Length (mm)	100	100	100	100

Ice Duration (hrs)	1hr45mins	1hr25mins	1hr35mins	1hr15mins
Cumulative Minutes	465	550	645	720
Empty Tray (g)	17	16.7	16.8	16.8
Dried Tray (g)	17.9	17.4	17.1	17.1
Total Debris (g)	0.9	0.7	0.3	0.3

Before Cross Sections (mm)				
Centre	99.969	99.908	99.908	99.833
Mid	99.996	99.993	99.993	99.966
Chuck	100.156	100.118	100.118	100.117
After Cross Sections (mm)				
Centre	99.908		99.833	99.848
Mid	99.993		99.966	99.962
Chuck	100.118		100.117	100.107

Cylinder	3-2	3-2	3-2	3-2
Round	1	2	3	4
Test Number	15	16	17	18
Mix	Low	Low	Low	Low
Date	July17/2017	July17/2017	July18/2017	July18/2017
Tachometer Test (RPM)	84.9	84.9	84.9	84.8
Air Temperature (°C)	24	24	23	24
Ice Temperature (°C)				-11.8
Concrete Temperature (°C)				1.2
Arm Temperature (°C)				
Applied Load (kg)	57.69	57.69	57.69	57.69
Adjusted Load (N)	527.48	527.48	527.48	527.48
Ice Sample Hanging Length (mm)	90	100	100	100

Ice Duration (hrs)	1hr30mins	1hr50mins	1hr30mins	1hr10mins
Cumulative Minutes	90	200	290	360
Empty Tray (g)	16.9	16.9	16.9	16.8
Dried Tray (g)	20.1	18.6	17.9	17.4
Total Debris (g)	3.2	1.7	1	0.6

Before Cross Sections (mm)				
Centre	100.196	100.158	100.146	100.146
Mid	100.017	99.994	99.974	99.974
Chuck	99.909	99.93	99.929	99.929
After Cross Sections (mm)				
Centre	100.158	100.146		100.235
Mid	99.994	99.974		99.97
Chuck	99.93	99.929		99.919

Cylinder	2-3	2-3	2-3	2-3
Round	1	2	3	4
Test Number	23	24	25	26
Mix	Mid	Mid	Mid	Mid
Date	July20/2017	July21/2017	July21/2017	July21/2017
Tachometer Test (RPM)	84.9	84.8	84.8	84.8
Air Temperature (°C)	26	24	24	24
Ice Temperature (°C)		-9.8	-9.8	-9.8
Concrete Temperature (°C)		3.1	3.1	3.6
Arm Temperature (°C)				
Applied Load (kg)	67.78	67.78	67.78	67.78
Adjusted Load (N)	626.41	626.41	626.41	626.41
Ice Sample Hanging Length (mm)	100	100	100	100

Ice Duration (hrs)	1hr10mins	1hr40mins	1hr40mins	1hr30mins
Cumulative Minutes	70	170	270	360
Empty Tray (g)	17	17	17	17.3
Dried Tray (g)	18.5	18.1	17.7	17.8
Total Debris (g)	1.5	1.1	0.7	0.5

Before Cross Sections (mm)				
Centre	100.206	100.206	100.191	100.144
Mid	100.091	100.091	100.058	99.993
Chuck	99.966	99.966	99.914	99.897
After Cross Sections (mm)				
Centre		100.191	100.144	100.172
Mid		100.058	99.993	100.045
Chuck		99.914	99.897	99.898

Appendix C: Concrete Sample Pictures

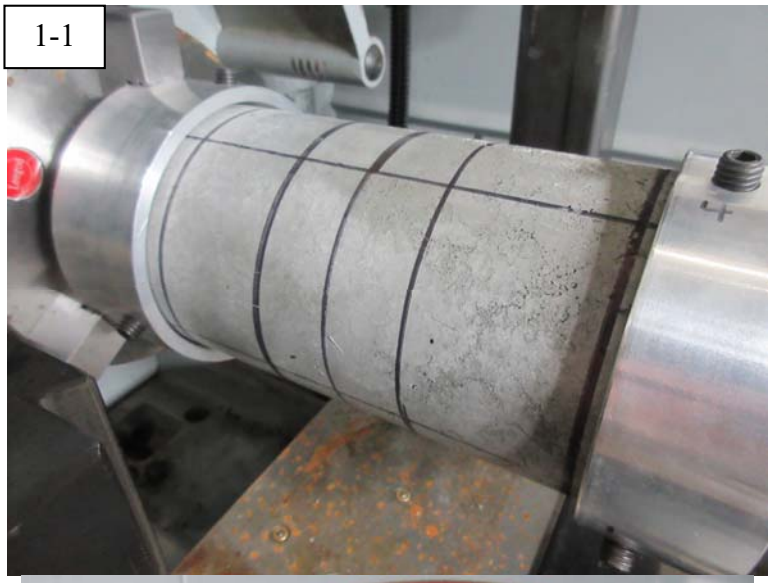


1-2
3
3
3


2-1


2-2

2-3


3-1


3-2

Appendix D: Diameter Change Graphs

TEST PROGRAM 1

	Before	After	Loss
1-1	100.346	100.233	0.113
	100.106	100.002	0.104
	100.008	99.992	0.016

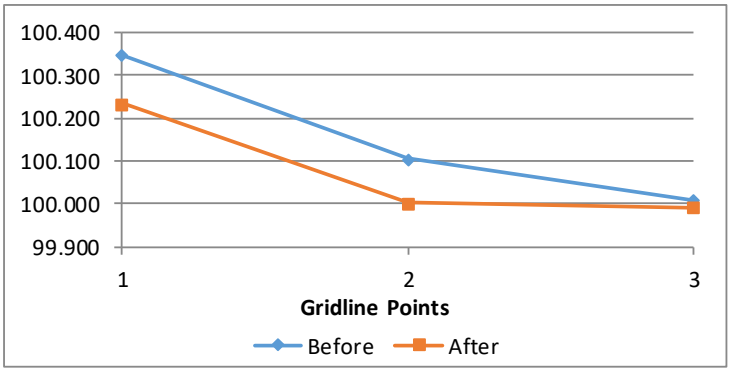

	Before	After	Loss
2-1	100.209	100.143	0.066
	100.433	100.290	0.143
	100.607	100.526	0.081

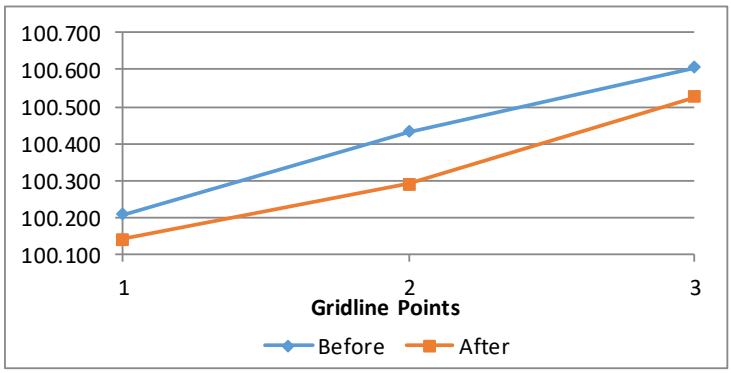

	99.841	99.630	0.211
3-1	99.785	99.340	0.445
	99.659	99.651	0.008

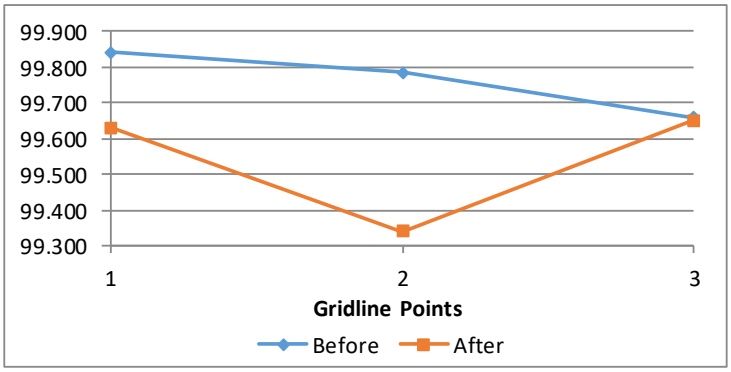

TEST PROGRAM 2

	Before	After	Loss
1-2	99.540	99.467	0.073
	99.348	99.341	0.007
	99.280	99.281	-0.001

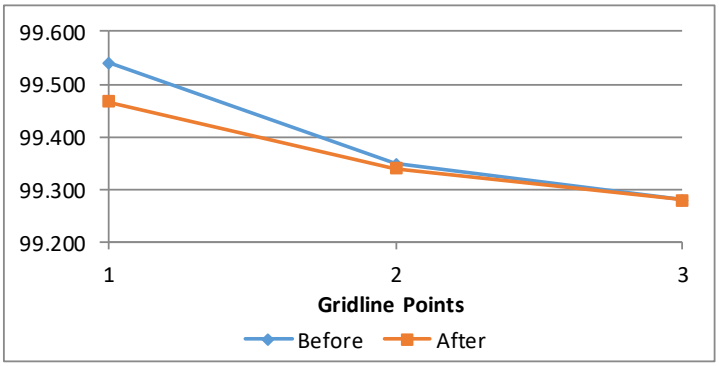

	Before	After	Loss
2-2	100.105	99.969	0.136
	99.968	99.996	-0.028
	99.986	100.156	-0.170

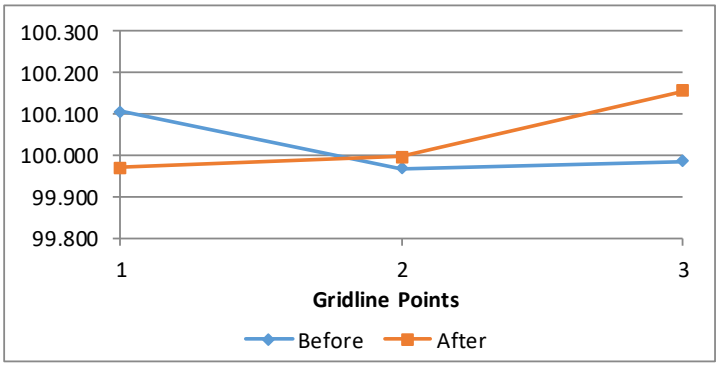

	100.196	100.235	-0.039
3-2	100.017	99.970	0.047
	99.909	99.919	-0.010

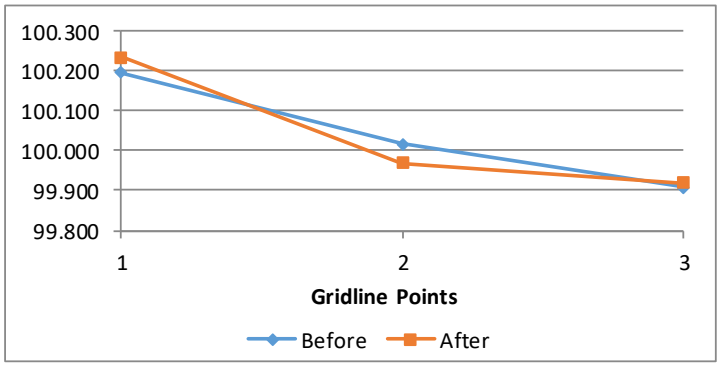

TEST PROGRAM 3

	Before	After	Loss
2-2	99.969	99.848	0.121
	99.996	99.962	0.034
	100.156	100.107	0.049

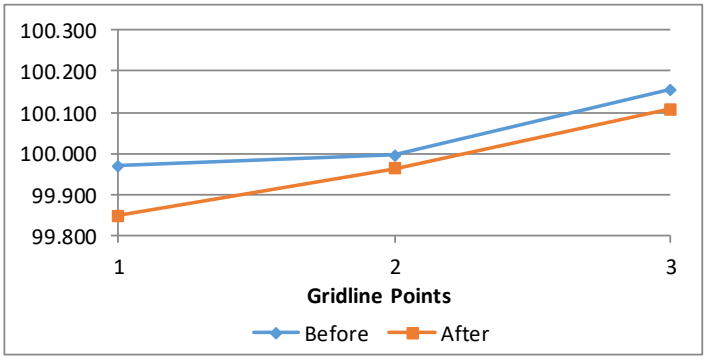

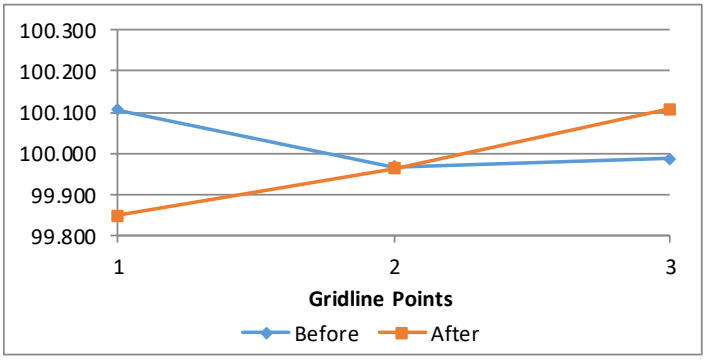

* Shows change over 12 hours of testing

TEST PROGRAM 4

	Before	After	Loss
2-3	100.206	100.172	0.034
	100.091	100.045	0.046
	99.966	99.898	0.068